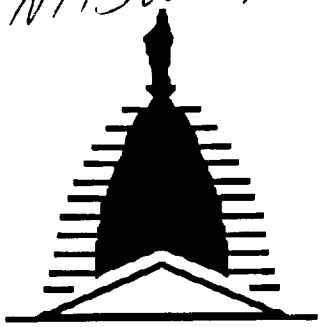

UNIVERSITY of
NOTRE DAME

NASA/USRA UNIVERSITY ADVANCED DESIGN PROGRAM 1991-1992

UNIVERSITY SPONSOR
BOEING COMMERCIAL AIRPLANE COMPANY

FINAL DESIGN PROPOSAL

JEFF

Air Transport System Design Simulation

May 1992

Department of Aerospace and Mechanical Engineering
University of Notre Dame
Notre Dame, IN 46556

JEFF

Remotely Piloted Cargo Aircraft for Service in AeroWorld

Design Proposal

Group B
Oliver Atassi
Douglas Fries
Mark Mahovlich
Edward Nash
Marcia Powell
Charles Smith
Jennifer Sorice

A number of problems beyond the control of Design Group B were encountered during the development of the Final Design Proposal. Therefore the following proposal should be considered in "draft" form and unfortunately a number of figures are missing or incomplete and certain segments of the text do not comply with standard proposal quality requirements.

-Management AE441, Inc.

Table of Contents

Executive Summary

Jeff is a remotely piloted vehicle designed by the Blue Team, a division of AE441, Inc., to fulfill the mission proposed by G-Dome Enterprises: to build a cost efficient aircraft to service Aeroworld with overnight cargo delivery. The design of Jeff was most significantly influenced by the need to minimize costs. This objective was pursued by building fewer large planes as opposed to many small planes. Thus, by building an aircraft with a large payload capacity, G-Dome Enterprises will be able to minimize the large costs and the large number of cycles that are associated with a large fleet. Another factor which had a significant influence on our design was the constraint that our design had to fit into a 2'x2'x5' storage container. This constraint meant that unless we wanted to build foldable wings that Jeff's span would be limited to 10 feet. Since this was not enough lifting surface to suit our needs a canard configuration was chosen to get the needed lifting surface and avoid the structural dilemma of foldable wings.

The aircraft was designed to fly at a maximum altitude of 25 ft, and at low speeds (less than 30 ft/s). To carry large amounts of payload, Jeff consists primarily of a 1408 in^3 fuselage (44"x8"x4"). A rear-mounted pusher propeller was chosen because it acts as a stabilizing force for canard configurations at takeoff. The FX63-137B airfoil was selected for both the wing and canard because of its high lift characteristics and moderate thickness. Both lifting surfaces are rectangular, with aspect ratios of 10. Sized to provide static stability as well as lift, wing planform area is 10 ft^2 and canard planform area is 3.0 ft^2. The two vertical stabilizers have an area of 0.75 ft^2 each and are mounted above and below the wing at a location of 3 feet from the wing tips.

The aircraft is constructed mainly of balsa, with spruce wing and canard spars and a monokote covering. It was designed to support a maximum payload weight of 35 oz. (total aircraft weight of 108 oz.) and withstand a maximum load factor of 2.5. Tricycle landing gear support the plane up to a load factor of 4.0 during landing, and ensure propeller clearance during take-off rotation.

The propulsion system consists of an Astro 15 motor, which was chosen because it can provide the power required for our large aircraft to take off and fly at a cruise velocity of 28 ft/s. Twelve 1.2 volt batteries are required to power the system and to ensure take-off in a distance of 60 ft, a maximum range of 9770 ft, and a maximum endurance of 11.50 min.

Because of the canard configuration, stability of the aircraft became a main design concern. To achieve acceptable static margins, the interior of the aircraft was carefully configured and wing and canard carefully sized and placed. The aircraft achieves good static margins (10-20%) at full payload, and also at a decreased payload with the addition of ballast. Control surfaces were sized accordingly. Ground control is achieved with a moveable nose wheel, and elevons on the main wing provide pitch and roll control.

Economically, the aircraft is very cost efficient. A fleet of nineteen aircraft is sufficient to service our target market--the upper hemisphere of Aeroworld.

The lower hemisphere of Aeroworld was left out because it was thought that the long distances between cities in this hemisphere outweighed the benefits of the limited cargo that existed in this market. At $287,000 per plane, fleet life cost is $33,841,582. This figure translates to a unit volume cost of $3.72/in^3 of cargo. Thus G-Dome Enterprises can charge a competitive price of approximately $4/in^3 and maintain a profit of $12,261,388 per year.

Some areas of concern still remain. Among these are the stability of the aircraft. Since canard configurations are destabilizing, static stability, although achieved, was difficult. The stability will depend largely on payload weight and payload distribution within the fuselage because the center of gravity of the plane empty differs greatly from that full. Also, propeller ground clearance may be a concern as the plane rotates on take-off. Finally, because the aircraft is so large, and because the airfoil chosen has a cusped trailing edge, the manufacturing process may be somewhat time-consuming and difficult.

Despite these technical challenges, Jeff provides the Aeroworld market with a large cargo carrying capacity which will ensure that all cargo can be delivered to its target cities efficiently overnight. It provides G-Dome enterprises with a low-cost small fleet of aircraft that will operate at a profit over the life span of the structure, and it can fully accomplish the specified mission .

For more specific data, see the Critical Data Summary in Appendix B. Also Primary Data Items are listed in Appendix A.

2. Mission Study

2.1 Mission and Market Analysis

The goal of the original mission study was to develop an effective and efficient air route network. This network would be capable of transporting the greatest amount of cargo in the fewest number of planes and cycles for the lowest cost. In order to accomplish this goal, it was decided to develop a large cargo volume capacity that would always fly close to capacity and would be able to meet all of the flight requirements in Aero World. By examining past airplane designs and power plant capabilities, a preliminary guess as to the planes maximum weight was made to be no more than 7 lb. or 112 oz. A plane of any more weight would fail to takeoff under the given maximum velocity of 30 ft/sec. Although the option of going to a larger engine might have alleviated this problem the weight penalty for a larger engine was deemed as too large. The percent weight of cargo compared to the actual weight of the plane was estimated at 33%. Furthermore, the average weight per volume of each piece of cargo was assumed to be 0.025 oz./cu in. This was chosen because it represented the average weight per volume of the cargo transport. Thus, the design volume of the cargo bay was chosen to be 1400 cu. in. The question which still remained was whether there was an efficient route system which would be able to be developed for a cargo hold of 1400 cu. in. at a low cost?

A simultaneous study was done to compare the different possibilities in the distribution network. The concept which was chosen was developed from knowledge of current air delivery networks. A city would be chosen as a central location were all transports would converge, this city would thus be known as the Hub. At 6:00 P.M., all transports would leave their designated cities and fly to the Hub. Upon landing, the plane's cargo would be unloaded and sorted according to

the cargo's designated destination city. When the last plane has had its cargo sorted, the cargo would be loaded back on to the plane whose origin matches the cargo. Finally, in the early morning hours, the fleet would leave the hub and return to their respective cities fully loaded with cargo. The whole process would guarantee cargo delivery by 10:00 A.M.

The choice for the hub location was based on the economic impact and geographic location that the city would have on the mission. City H was computed to be located at the serviceable center of the world by the analysis of a computer program which computed the distances between all the cities. A Hub location at this city will reduce the total flight time and thus reduce the total cost of fuel used each night. However, city H only has 1650 cu. in. of cargo originating from it. This factor was weighed heavily for the final selection of the Hub. If the amount of cargo originating at the Hub is large, then the amount of planes needed for the fleet will be reduced, as well as the number of cycles and total amount of fuel used each day. This factor amounted to a larger economic savings for each fleet life. Thus city K was chosen to be the Hub location. City K's 4,300 cu. in. of cargo is the largest amount of any city, furthermore it is very much geographically centered in Aero World.

With a rough estimate of the cargo size capability and an idea for a mission concept completed, the last step in finalizing the route structure was to determine which cities should be serviced. The Northern Hemisphere of Aero World (11 cities) accounts for 84.7% of the total amount of cargo possible. This was seen as the most economical route system. The other four cities have such a low amount of cargo volume, that in order to service them, it would be required to operate four more planes at only 30% full capacity. This would result in an increase in the price per unit volume. Figure 2.1 is the service route system that was chosen.

Figure 2.1 AeroWorld Route System

However, before finalizing the cargo capacity of the plane that would service this system, a trade off study on cargo size was done to see which size generated the lowest cost per volume. Table 2.1 compares the cargo size of the plane and how well it would accomplish the mission given the above prescribed route system (FCPVOL, fleet cost per volume, FFPD, flights flown per day, NFLEET, Number of planes in the fleet). Furthermore it explores the volume of a 1400 cu. in. cargo hold applied to the whole world.

Cargo Size (cu. in.)	FCPVOL ($)	FFPD	NFLEET
2000	3.59	36	14
1400	3.69	43	19
1400 whole world	4.84	56	24
1200	4.33	50	22
1000	5.01	58	27

Table 2.1 Cargo Volume and Mission Effectiveness

As is shown the cargo size of 2000 cu. in. produces the lowest FCPVOL, however, the size of such a plane is not within the current technology to develop at a low cost. Table 2-2 and Figure 2-1 gives the finalized route structure for a 1400 cu. in. plane that will be designed and used for the overnight delivery service. This table is useful in determining the capacity of each flight, and the exact flight time. Furthermore, several planes make more than one stop, thus the cycles of takeoffs and landings must be kept track of for the determination of when the plane will experience fatigue. The cost to build each aircraft will be $287,000 based upon the estimation of material costs, production time, fuel costs and several other economic parameters which will be discused in Section 12.

Flight (city to city)	Total Distance (ft)	Time (min)	Percent full
A-K	6390	3.80	100
A-H-J-K	6412	3.81	99
B-K	4903	2.92	100
B-K	4903	2.92	82
F-K	2952	1.75	100
F-K	2952	1.75	100
G-K	2800	1.66	100
G-K	2800	1.66	86.6
H-K	2236	1.33	100
I-K	2009	1.19	100
I-K	2009	1.19	75
J-K	894	0.53	100
J-K	894	0.53	100
L-K	2236	1.33	100
L-K	2236	1.33	100
M-K	3255	1.93	100
M-K	3255	1.93	65
N-K	3310	1.97	100
N-K	3310	1.97	77

Table 2.2 City to City Flights

2.2 Design Requirements and Objectives

Mission:

•Design a cargo-carrying aircraft to service the upper hemisphere of AeroWorld with an overnight package delivery service.

•Provide the greatest potential return on investment by minimizing fleet size, flight cycles per aircraft, fuel consumption, weight, and production costs for the aircraft while simultaneously maximizing cargo-carrying capability.

•Deliver all cargo within a maximum of 18.75 minutes delivery time.

External Configuration:

•Hold 1400 in^3 of cargo in a rectangular fuselage.

•Maintain a lightweight (<110 oz), cost-efficient, fairly aerodynamic structure.

•Minimize time required for loading and unloading by easy access to cargo through top doors in front and rear of aircraft.

•Simplify design through use of rectangular components to minimize production time and costs.

•Provide high lift (110 oz) at low speeds (<30 ft/s).

•Ensure roll control and stability through use of dihedral **or** control surfaces on main wing.

•Store in a 2'x2'x5' container.

Internal Configuration:

•Carry 1400 in^3 of cargo. **Note that this volume is a change from the original DR&O. The previous figure (2000 in^3) was too large for practical design and construction purposes.

•House all servos, motor, and battery assemblies in nose and fuselage.

•Place internal and external components for aircraft stability with minimal center of gravity travel.

Structure and Materials:

•Minimize weight to approximately 90-110 ounces (5.6-6.9 lbs).

•Design rectangular fuselage and wing planform for ease in stress analysis and manufacturing.

•Route flight paths to ensure structural life of the aircraft between 200 and 350 days.

•Construct technology demonstrator with balsa, spruce, glue, and monokote.

Propulsion System:

•Provide ample power for take-off and cruise at maximum payload weight condition.

•Contribute 15-20% of overall weight of aircraft.

Control Systems:

•Use servos to move nose wheel (ground control), ailerons and elevators. **Note that this is a change from the original DR&O. These controls proved to be more effective for the present configuration.

•Remove and install radio control system and instrumentation package within thirty minutes.

Performance:

•High lift at low speed (less than 30 ft/s). Target cruise speed is 28 ft/s.**

•High lift to drag ratio (>15).

•Take-off roll less than 60 ft. Target take-off speed is 25 ft/s.**

•Low altitude flight (less than 25 ft).

•Turn radius of 60 ft. in level flight.

•Range between 10,000 and 12,000 ft.

•Endurance between 10 and 12 minutes. **Note that these two figure have changed from the original DR&O due to airfoil selection and size of the aircraft.

Cost:

•Total cost per volume per flight cycle is minimized.

•Total unit cost of the aircraft less than $500.

•Scaled total unit cost of $194,000.

•Scaled production costs of $150,000 with 150 production man-hours.

•Total overall aircraft cost of $344,000.

•Fleet cost (14 aircraft) of $4,816,000.

•Average operation costs of $3.35 per flight.

•Maintenance costs of $100 per flight; two minutes for battery exchange.

•Fuel costs minimized by minimizing current draw.

•Consumer price per unit volume competitive with other designs while yielding a profit.

•For target cost data see section 12.

3. Concept Selection Studies

The main factor in defining our concept was to minimize the number of planes by carrying the maximum amount of cargo per plane. A large plane transporting 1400 cu. in. of cargo in each flight was decided upon to meet this objective. The main challenge was to build a plane with a cargo volume of 1400 cu. in. in under 7 lbs. Figure 3.1 shows a conventional concept which was studied as a possible choice for Aero World. This plane incorporated several good ideas for a successful cargo plane. The large cargo bay with dimensions 8"x 4"x 43.75" allows for 1400 cu. in. of cargo to be transported. The high wing placement on the fuselage will provide greater roll stability and on the wings the ailerons would eliminate the need for a wing dihedral for roll control. Thus, simplifying the construction process. The conventional tail configuration has a rudder for yaw control and a set of elevators for pitch control.

This concept was given consideration as a production prototype. However, some insightful ideas radically altered this concept to the present concept in Figure 3.2. As the weight estimate for the conventional plane was developed, it was found that the weight would be between 6.5 and 7.5 lb. In order to match the lift to weight, a very large wing with a high aspect ratio must be designed. A limit of 10 ft. was placed initially on the span of the wing to accommodate the 5 ft. box constraint because making wings that folded over seemed impractical from a construction perspective and would also result in additional weight to our already heavy design. Also the conventional aircraft tail in Figure 3.1 produces negative lift in order to be a stabilizing surface. Thus, in order to produce enough lift for flight of a 1400cu. in. cargo bay , in under 30 ft/sec, the conventional aircraft became too heavy and too big to adequately meet our mission constraints. Table 3.1 illustrates the strengths and weaknesses of such a design.

Figure 3.1 Conventional Aircraft

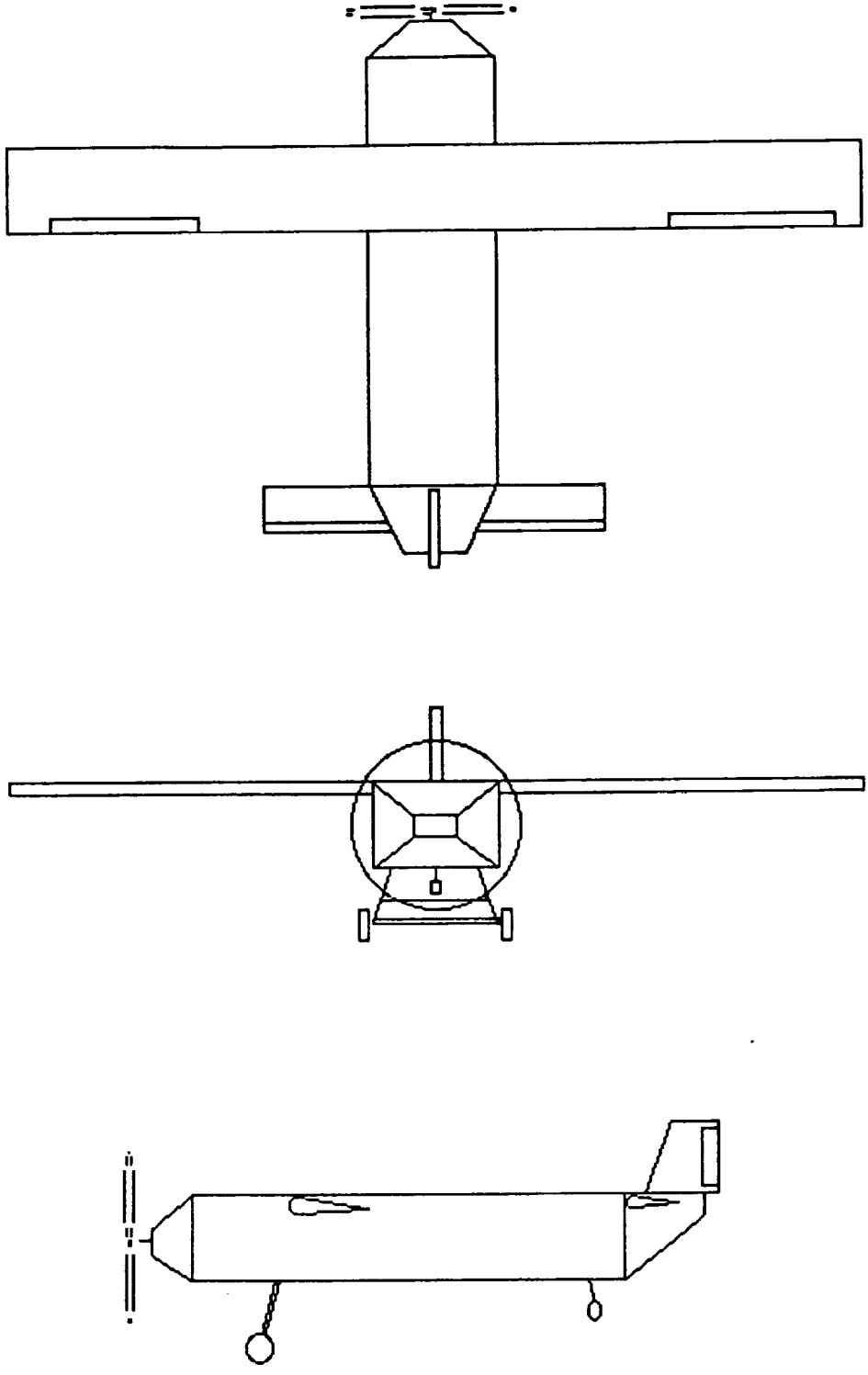

Figure 3.2 Canard Configuration

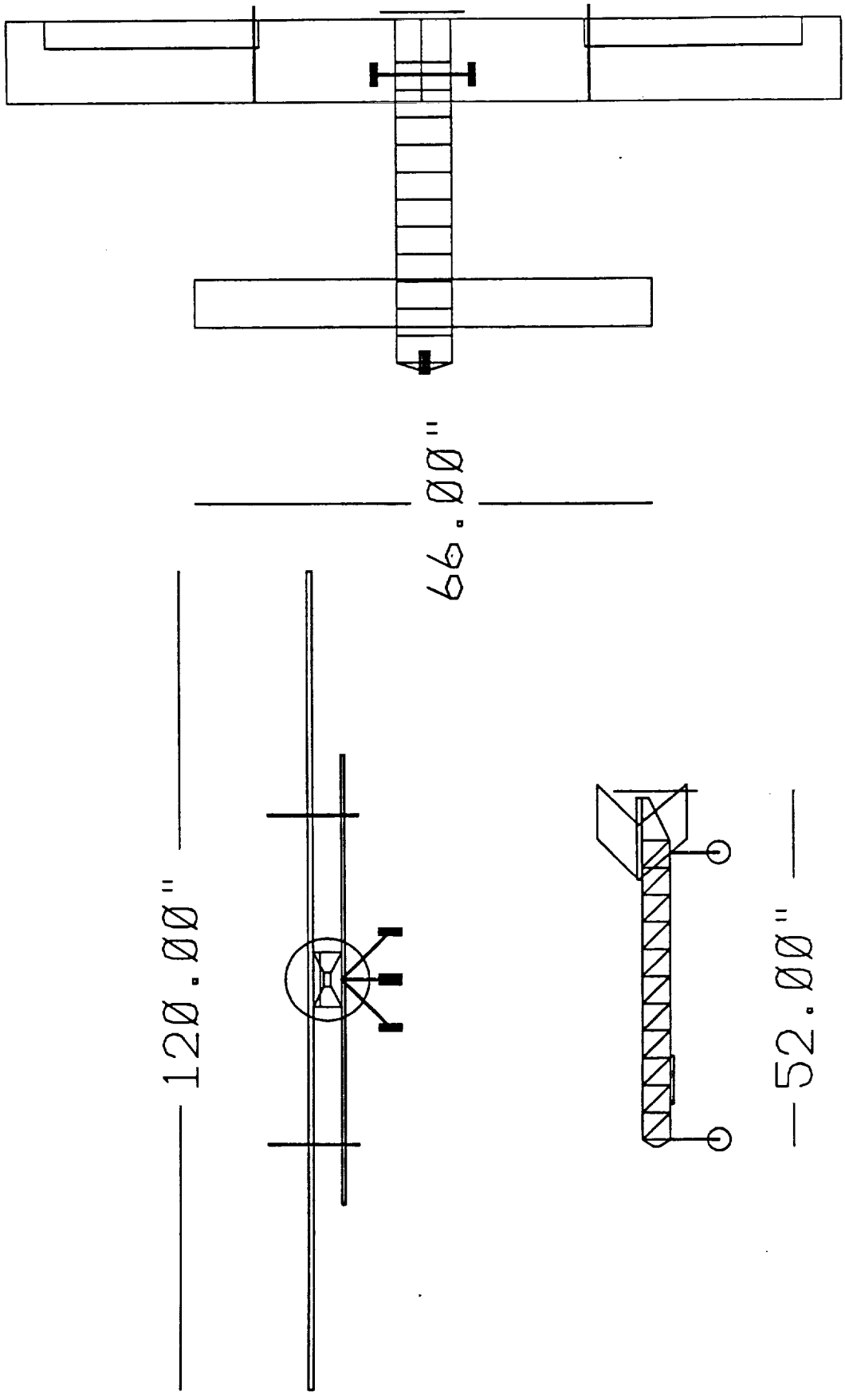

STRENGTH	WEAKNESS
LARGE CARGO HOLD	WEIGHT TOO HIGH
EASY TO CONSTRUCT	NO CARGO ACCESSIBILITY
LARGE DATA BASE	FOLDABLE WINGS NEEDED

Table 3.1 Conventional Plane

By using the canard concept, it enables the placement of two lifting surfaces on the fuselage. This eliminates the negative lift contribution that results from the horizontal tail in a standard configuration and also allows Jeff to meet the storage box constraint without having to go to foldable wings. Furthermore, the total fuselage length is reduced by eliminating the end empennage section from the plane. This can be done because with a canard configuration there is no need for the horizontal tail. This further reduces the weight of the plane. This removal of the empennage allows for the propeller to be placed in the rear of the plane. There are several benefits for this placement.

This plane is a cargo transporter, and as such, the accessibility and ease with which the cargo can be loaded and unloaded is very important. With the engine in the back of the plane the nose of the plane is accessible to cargo loading. Thus, when a plane lands at the airport, it will pull into the gate, the nose door will open and the cargo can be either driven on or off the plane. This will reduce the labor and cost for the ground crew. The plane further has a pair of elevons located on the rear lifting surface for roll and pitch control. It was decided to keep the control surfaces on the rear wing in order to keep the complexity and production cost down. By choosing elevons, it eliminates the production problems of designing a wing to accommodate both elevators and ailerons.

The canard, push-prop configuration must have a tricycle landing gear so the propeller will not hit the ground. The need for ground control is satisfied by installing a steerable nose wheel. Thus, the plane will be easy to taxi to the gate and will hopefully meet the take-off handling tests that will be tested in the taxi tests that our company is having in the next week. Table 3.2 gives a better understanding of the strength and weaknesses of the canard plane.

STRENGTH	WEAKNESS
LARGE, EFFICIENT FUSELAGE	LARGE LANDING GEAR
13.0 FT^2 OF LIFTING SURFACE	DIFFICULT TO CONSTRUCT
EASY CARGO ACCESS	WEIGHT
NEW, COMPETITIVE LOOK	UNPROVEN RELIABLE CONTROLS

Table 3.2 Canard Plane

The strengths and weaknesses for both designs have good arguments for choosing either one. However, it was important for the plane to be able to meet the mission as a cargo transport. The conventional design might have been less risky but the canard plane, based on the aforementioned qualitative arguments, will be a better design to meet our mission constraints and build such a large cargo carrying plane. The canard design was mainly chosen for the reasons stated above. However, the desire to create a product that is new and innovative and at the same time better than the conventional product was also a factor in the final concept of Jeff.

4. Aerodynamic Design Detail

4.1 Airfoil Selection

The aerodynamics of any flying vehicle are highly dependent on the lifting surfaces which are chosen. The airfoil sections for both the canard and wing provide the foundations for the lifting surfaces of *Jeff*.

The airfoil selection process for the wing involved consideration of several main factors. First, due to the high cargo volume which the aircraft will be carrying, an airfoil with a high maximum lift coefficient is necessary. Of the airfoils we considered, the Wortmann FX63-137 exhibited the highest maximum lift coefficient, $C_{l\ max}$=1.6. As with any aircraft, low drag is also desirable, so an airfoil exhibiting low drag characteristics is also necessary. Third, a high lift-to-drag ratio (L/D) is necessary to lessen the power required and enhance the endurance and range characteristics of the aircraft. The fourth consideration is the thickness of the airfoil. This is primarily a weight consideration. The airfoil needs to be thick enough that structural weight does not have to be added to the wing in order to provide structural integrity, but thin enough that it does not add unnecessary weight to the wing structure. Lastly, the airfoil needs to be relatively easy to manufacture.

After consulting previous RPV design data, three main airfoils were compared: the NACA 4415, the CLARK Y, and the WORTMANN FX63-137. The NACA 4415 offers a comparable lift-to-drag ratio to that which was selected, and also appears to be easy to construct due to its relatively flat lower surface. On the other hand, the NACA 4415 does not offer as high a maximum lift coefficient as the airfoil chosen. The CLARK Y seems to have the best drag characteristics and also has a flat lower surface adding to its ease of construction, but it does not have the L/D or lift coefficient characteristics comparable to the Wortmann airfoil. The WORTMANN FX63-137 offers high lift coefficient characteristics, high lift-to-drag

characteristics, and a moderate thickness. The one downfall to the WORTMANN airfoil is that it may not be as easy to construct due to a cusp at the trailing edge, but we feel confident that we can manufacture this airfoil without adding significantly to the manufacturing time and cost. Figure 4.1 illustrates the Cl versus angle of attack for the airfoil.

This graph is taken from A Catalog of Low Reynolds Number Airfoil Data for Wind Turbine Applications, Department of Aerospace Engineering, College Station, Texas, 1982, p.A-104.

Figure 4.1: Cl vs. Alpha and l/d vs. Alpha for WORTMANN FX63-137

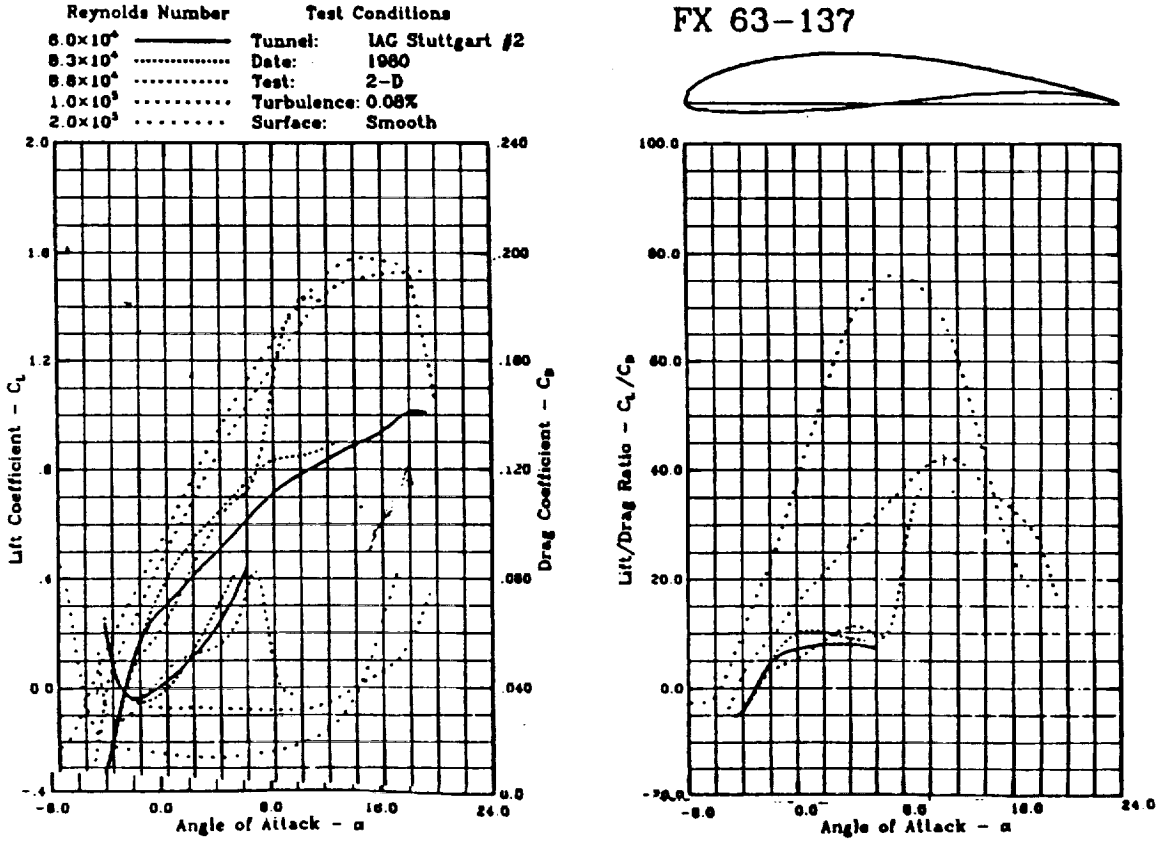

The airfoil selection for the canard is governed by two main factors. First, for stability reasons the canard must stall prior to the wing stalling. If the main wing airfoil stalls first, the result will be uncontrolled pitch-up, the canard will also stall, resulting in a strong possibility of spin or crash. Second, the canard must be able to provide the necessary lift to cruise with the canard mounted on the fuselage at moderate angles of attack. Moderate angles of attack are necessary to limit drag and to allow enough rotation of the nose at take-off before stalling occurs over the canard. For these reasons, the WORTMANN FX63-137 was also chosen. Figures 4.2 and 4.3 illustrate the C_L and L/D versus angle of attack characteristics for the aircraft. The data for these graphs was determined via AIRPLANE DESIGN, Part VI: Preliminary Calculation of Aerodynamic, Thrust and Power Characteristics, Dr. Jan Roskam, Roskam Aviation and Engineering Corporation, Ottawa, Kansas, 1987.

Figure 4.2
CL of the aircraft vs. Angle of Attack

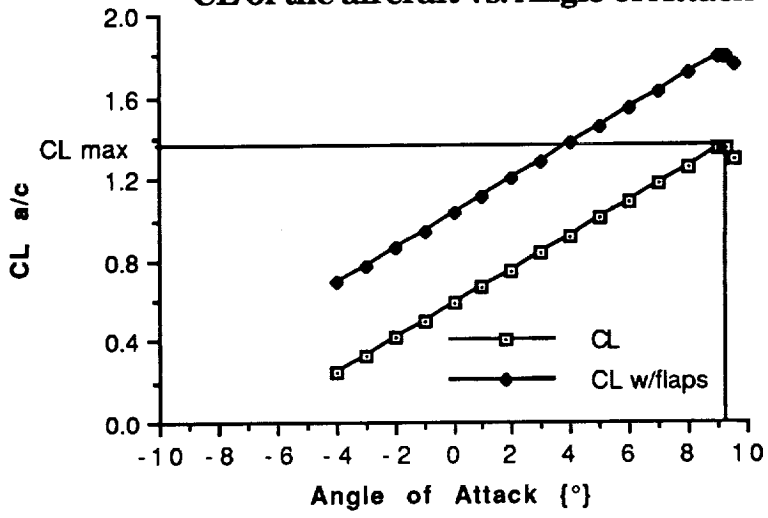

Figure 4.3
L/D for the Aircraft vs. Angle of Attack

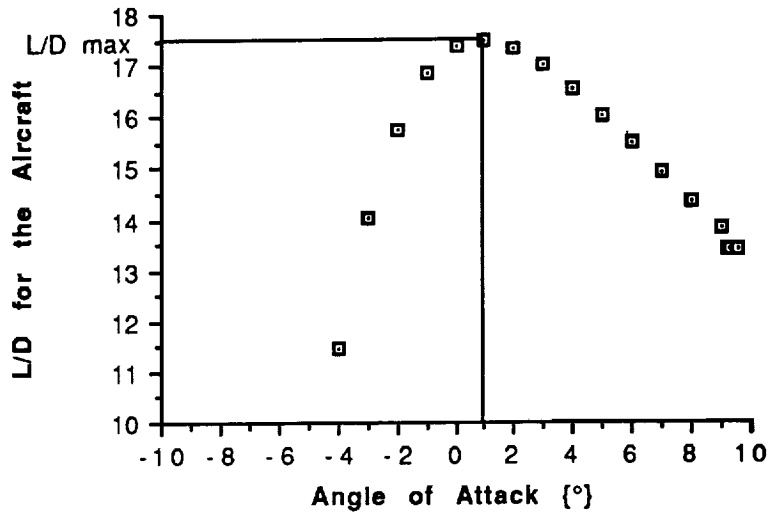

As shown in Figure 4.3, the point of maximum L/D occurs near the cruise condition, i.e., where the angle of attack of the aircraft is 0°. This is beneficial for increasing range and endurance, and decreasing power required in cruise. Figure 4.2 shows the variation in lift coefficient for the aircraft with angle of attack. As the aircraft approaches the stall angle of attack, the lift coefficient was interpolated to give the illustrated curve.

4.2 Drag

Drag is an important parameter in the design of any aircraft. It is directly proportional to the amount of power required to operate the aircraft. Therefore, it has a very important influence on the selection of the propulsion system. The drag also has great influence on the range and endurance of the aircraft---higher drag decreases both of these parameters. This is due to the increased current draw needed to overcome the drag. For these reasons, it was imperative for our design team to minimize the drag, if possible, on all components. This led to repeated compilations of updated, more accurate drag estimates throughout the design process.

4.2.1 Drag Predictions:

Drag prediction for "Jeff" was compiled using the outline provided in Jensen's *Low Reynolds Number Drag Analysis*. A drag polar was constructed using the following formula:

$$C_D = C_{D,0} + C_L^2/\pi eAR,$$

where $C_{D,0}$ is the parasite drag, e is the Oswald efficiency factor, AR is the aspect ratio, C_L is the coefficient of lift, and $C_L^2/\pi eAR$ is the induced drag.

The drag polar was constructed using estimations of the parasite drag, $C_{D,0}$, and the Oswald efficiency factor, e. This data was used in conjunction with the total wetted area of the aircraft to estimate the parasite drag,

$$C_{D,0} = 0.0055(S_{wet}/S_{ref}),$$

where S_{wet} is the summation of each component's wetted surface area, and S_{ref} is the surface area of the wings. The area of the wings is employed as a reference area because it is a major component of the total drag of the aircraft.

A value of 0.005 was added to the resulting number to account for the landing gear of the aircraft which did not seem to be included in this estimation. This produced a value of 0.0185 for the parasite drag coefficient of "Jeff." This method provided an induced drag coefficient of $0.0449C_L^2$ where e was determined using the method described below. This portion of the drag coefficient is strongly related to the C_L at each particular point in flight.

Another method employed was found in a handout from Dr. R. Nelson, entitled *Subsonic Drag Breakdown Method*. This method entailed the estimation of the drag resulting from each component of the aircraft in reference to the planform area of the wing. Parasite drag, using this method, was determined using the following equation:

$$C_{D,0} = \Sigma\,(C_{D\pi}\,A_\pi) / S_{wing},$$

where $C_{D,\pi}$ is the component drag coefficient, A_π is the reference area for each corresponding component, and S_{wing} is the surface area of the wings.

Estimates for $C_{D\pi}$ values were provided in the handout for various components. These values, combined with the particular areas of each component in "Jeff" produced the value of $C_{D,0} = 0.0175$ for the entire aircraft. These values are presented in Table 4.1 below.

Component	$C_{D\pi}$	A_π (ft^2)	% of Total Drag
Fuselage	.110	0.22	14.26
Wing	.007	10.0	40.93
Landing Gear	.017	0.06	5.96
Canard	.008	2.00	10.52
Vertical Tail	.008	1.50	7.01
Elevons (deflected)	.03	1.50	26.31

Table 4.1 Component Drag Breakdown

This value of $C_{D,0}$ was not the one used for calculations and analysis though. As Dr. Nelson suggests, 10% was added to this total to account for interference and roughness in the flow field around the aircraft. This produces a final value of $C_{D,0} = 0.0188$.

The Oswald efficiency factor was calculated using the following formula:

$$1/e = 1/e_{wing} + 1/e_{fuselage} + 1/e_{other},$$

which was also found in Dr. R. Nelson's handout and uses the efficiency of particular components to produce the efficiency factor of the entire aircraft. Values of e_{wing} and $E_{fuselage}$ were estimated to be 0.78 and 0.61 respectively from Figures 4.4 and 4.5. These numbers were obtained using aspect ratios of 10.0 and 6.25 for the wing and fuselage respectively.

Figure 4.4

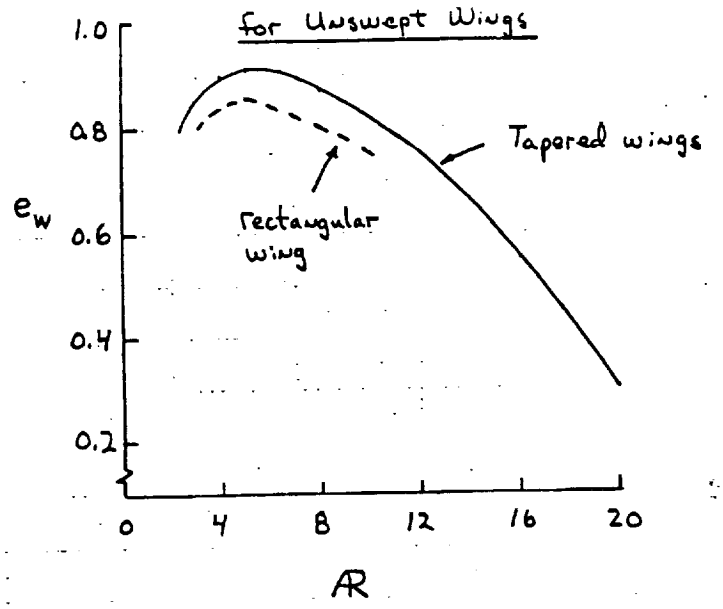

Figure 4.5

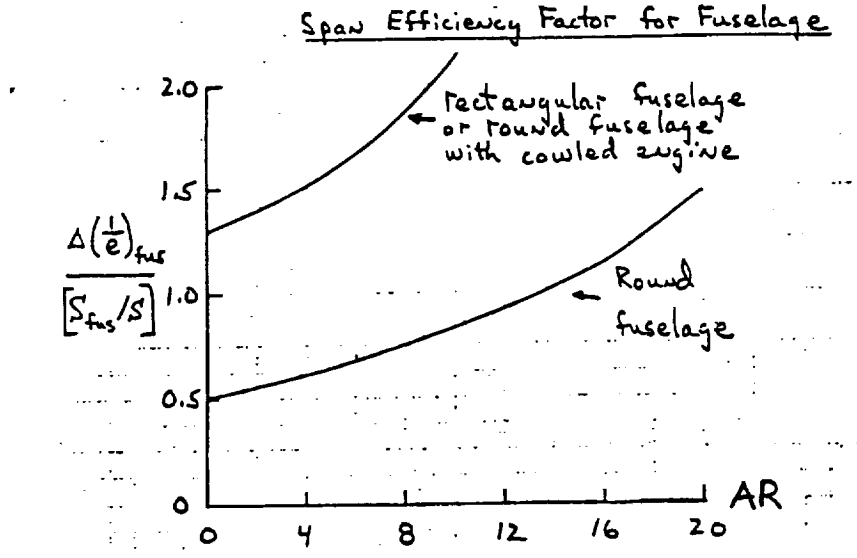

This value of $E_{fuselage}$ was used in conjunction with the following formula:

$$e_{fuselage} = (E_{fuselage})(S_{wing}) / S_{fuselage}$$

to determine $e_{fuselage}$ as 27.45 as Dr. Nelson's handout suggests. A value of 20.0 was employed for e_{other}, also as recommended in the handout, thus producing a final efficiency of 0.731. A computer application, Lin Air, was also consulted to

obtain this value, but it produced what seemed to be a rather high efficiency factor. It was determined that it would be better to design for the lower efficiency factor for safety reasons.

With these values known, it was possible to calculate the drag polar, which turned out to be $C_D = 0.0188 + .0435C_L^2$.

From this equation a drag polar for "Jeff" was constructed, and is displayed in Figure 4.6.

Figure 4.6

Drag Polar

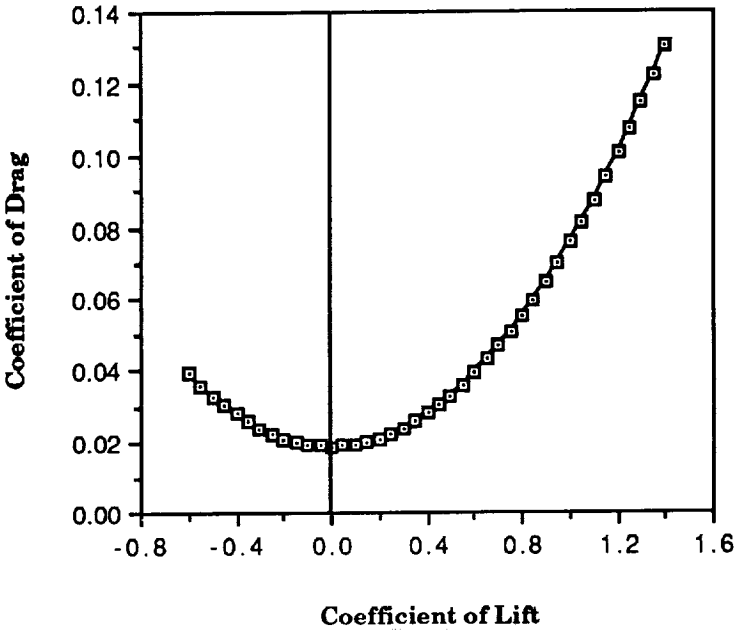

For the design cruise velocity of 28 ft/s, a lift coefficient of 0.571 is required. L/D_{max} turned out to be 17.5 and occurs at an angle of attack of 0.0 degrees, our cruise condition, as designed. When cruising at 28 ft/s and no angle of attack, the drag coefficient is 0.033, 57.0% parasite drag and 43.0% induced drag. With parasite drag significantly higher than induced drag, it became apparent that to decrease drag most effectively, parasite drag would have to be limited.

As shown in Table 4.1, a large portion of the drag, 40.93 %, resulted from the wings. The wings of "Jeff" were designed to accommodate the large size of "Jeff" in that they were required to have enough lifting surface to allow the aircraft to leave the ground. Therefore, the wings must remain at their current size to achieve the design objective of carrying as much cargo as possible as cheaply as possible.

Another large portion of the drag was a result of the elevons. This portion of parasite drag corresponds to the elevons when they are deflected to δ_{max}. This deflection increases lift with the penalty of increased drag. Elevons were selected over elevators and ailerons for their relative ease in construction. Their current size must be maintained for controllability of the aircraft, and is approaching the minimum allowable size that will ensure adequate controllability. Therefore, their size will also not be reduced.

As calculations showed, "Jeff" will fly with the drag due to its current configuration without imposing too many penalties on parameters such as current draw, range, and endurance. Thus, no changes will be made to decrease parasite drag.

5. Propulsion

5.1 Governing Requirements:

G-Dome Enterprises set several mission requirements in their Request for Proposals that governed the selection of a propulsion system. The propulsion system must:

1. Employ one or more electric powered engines
2. Provide enough power for take-off within 60 ft
3. Accomplish take-off and maintain cruise at less than 30 ft/s
4. Provide enough power to sustain flight for 9770 ft
5. Minimize current draw to keep fuel costs low

Attempting to meet these requirements led to a series of trade-offs which will be detailed hereafter. They led to the propulsion system detailed in table 5.1.

Motor Type	Astro 15
Propeller	Top Flight 12-6
Number of Cells	12
Cell Capacity	14.4 volts
Total Power Pack Voltage	1000 mAH

Table 5.1 Characteristics of Propulsion System

5.2 Engine Selection:

The Request for Proposals declared that an electric powered engined was required. It was evident that an engine with the smallest volume and weight that provided enough thrust for the mission was needed. The use of an Astro engine appeared to be appropriate. It was determined that a single engine configuration would be a better choice than a multi-engine system. For equal power output, one larger engine would take up less volume and weigh less than several smaller models.

At this point, five Astro engines were selected as candidates to be employed in "Jeff," the Astro 035, 05, 05FAI, 15, and 25. Table 5.2 provides some useful information for the selection of which motor is best suited for this mission.

Motor	Size	Motor Weight	Suggested Battery Pack	Power Output
Astro 035	1.25 x 1.75 in.	4.5 oz	5 x 800 mA	90 watts
Astro 05	1.25 x 2.00 in.	6.5 oz	7 x 900 mA	125 watts
Astro 05FAI	1.25 x 2.25 in.	6.5 oz	7 x 1200 mA	200 watts
Astro 15	1.25 x 2.25 in.	7.5 oz	12 x 900 mA	200 watts
Astro 25	1.31 x 2.25 in.	11.0 oz	14 x 1200 mA	300 watts

Table 5.2 Motor Specifications

All five motors analyzed have approximately the same volume. All are small relative to the size of the entire aircraft, so size was not a decisive factor in this selection. The weight of the Astro 25 is quite high in comparison to the other motors. This weight combined with the size, weight, and cost of the suggested power pack eliminated this engine from the list of possibilities. Also, the Astro 25 would produce a wealth of excess power. This power would be a luxury to have, but the excess weight makes it unfeasible.

The Astro 035 proved not to produce enough power for take-off within the allowed 60 ft, so it was also eliminated from the list of choices. The Astro 05FAI had efficiencies that ranged from 75.5 to 78.8% over the projected range of cruise rpm. These low efficiency values, in comparison to the range of 87.5 to 90.0% for the Astro 15, eliminated it as a possibility.

This left the Astro 05 and the Astro 15. Both engines produce enough power for take-off and cruise. However, the 15 has a maximum power output 75 watts higher than the output of the Astro 05, while the engine itself weighs only one ounce more. The 75 extra watts of power obtained from carrying only one extra ounce of weight (in an aircraft weighing over 100 ounces) makes the Astro 15 the

wisest choice for the engine in "Jeff." Also, the Astro 05 produces enough power for take-off, but further analysis shows that take-off will not occur within the allotted 60 feet if the actual aircraft weighs more than the projected weight of 108 ounces.

5.3 Propeller Selection:

While the analysis of the engines was underway, the examination of what propeller would most efficiently complete the design requirements began. A propeller that produced high T (thrust), low P_{req} (power required), high η (efficiency), and low Q (torque) for various advance ratios, velocities, or rpm was sought. This would result in high thrust and efficiency with only limited torque produced and power required. Obviously, one propeller will not produce the highest values of T and η, and the lowest values of P_{req} and Q over the flight regime. Therefore, this design team searched for the propeller that best maximizes the effective thrust and efficiency of the aircraft while, at the same time, limits the torque produced and corresponding power required to drive the propeller.

To begin with, several different propellers, including the Zinger 10-6 (Z10-6), Tornado 10-6 (T10-6), Zinger 8-6 (Z8-6), Top Flight 10-4 (TF10-4), and Top Flight 12-6 (TF12-6) were examined using a code entitled "Notre Dame Propeller Program" on the Apple IIe. Propeller data already entered in the program was assumed to be correct. References to check this data were searched for, but not found. A number of other assumptions, just as vital as this first one, were made as well. First of all, C_l/C_d (coefficient of lift / coefficient of drag) coefficient adjustments had to be made. Adjustments due to Mach number, Reynolds number, or both could be made. Due to the low Reynolds number associated with this mission, it seemed appropriate to choose the Reynolds number adjustment. Also, all data

used for the graphs relating power, thrust, efficiency, and torque to advance ratio and propeller rpm was compiled at a constant velocity (v_{cruise} = 28 ft/s). Investigation of C_T's (C_T = coefficient of thrust), C_P's (C_P = coefficient of power), and η's could also have been accomplished at constant advance ratio and various velocities, but this was determined not to provide the exact data that was sought. As a result of these assumptions made, the data collected was tested with hand point calculations for validity. Values of thrust and power produced by hand proved to be within 7.0% of the data obtained from the Apple IIe computer code, as so was accepted as accurate.

The data obtained from the Apple IIe program was combined with information obtained from a fortran code, PAVAILmod, to analyze the propellers selected as possible choices for use in conjunction with "Jeff." Analysis of the propellers was completed using the Astro 15 engine, so data is quite realistic.

An examination of the efficiencies of the five propellers analyzed in figure 5.1 displays the inadequacies of the lower diameter propellers. Thus a choice is left between a 10, 11, or 12 inch diameter propeller. A 10 inch diameter does produce enough power, but not by much. This fact combined with the relatively low efficiencies of the Zinger 10-6 and the high torque and low thrust of the Tornado 10-6 led to the elimination of the 10 inch propellers from consideration.

As a result, a 11 or 12 inch propeller will be employed. A 12 inch propeller, the Top Flight 12-6, in particular, has more thrust and power available than an 11 inch diameter propeller with all other values held constant as shown in the base power and thrust equations:

$$T = C_T \rho N^2 D^4, \text{ and}$$

$$P = C_P \rho N^3 D^5,$$

where T is thrust, C_T is coefficient of thrust, ρ is density, N is propeller revolutions per second, D is diameter, P is power, and C_P is coefficient of power.

Figure 5.1

Efficiencies of Various Propellers versus Advance Ratio

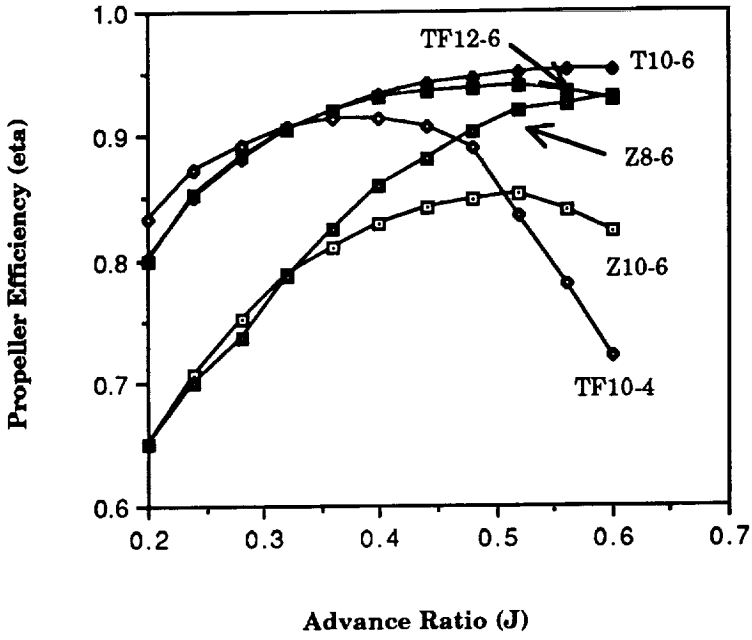

However, it does require a higher torque and thus requires more power to drive it. These values are only slightly higher for the 12 inch diameter though. This fact, combined with the the high efficiency of the TF12-6 led to it's selection as the propeller of "Jeff".

5.4 Battery Selection:

The selection of the power pack for "Jeff" was governed by several factors. The pack had to be a lightweight, as small as possible, and powerful enough to provide for take-off in less than 60 ft, and extended steady, level flight to meet a range requirement of 9767 ft.

Figure 5.2 displays the power available for the Astro 15 motor and the Top Flight 12-6 propeller at various voltage settings. It shows that greater than 8 volts are required to operate the aircraft in cruise. Therefore, at least 7 cells of 1.2 volts apiece are necessary.

Figure 5.2

Power Available and Required for Various Voltage Settings for the Top Flight 12-6

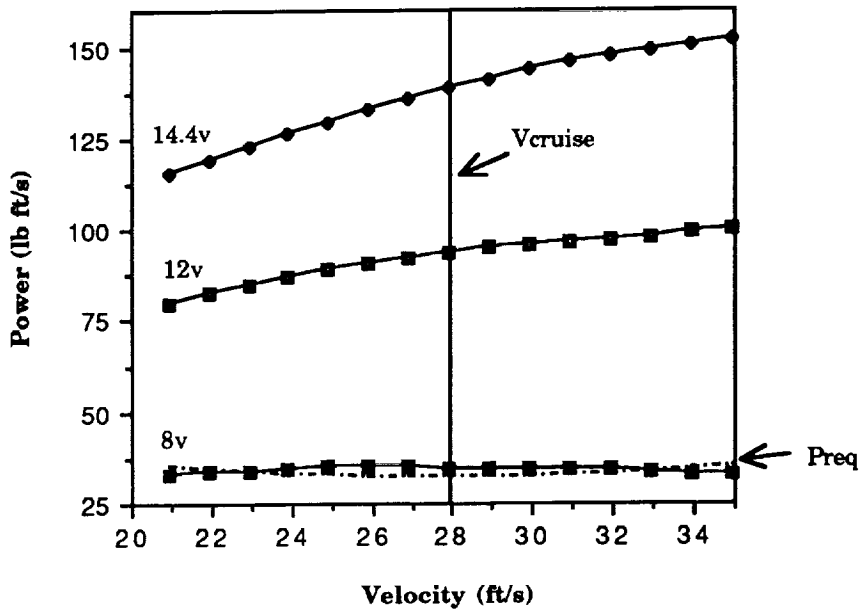

However, as previously mentioned, "Jeff" will not be operating at maximum power due to the corresponding decrease in motor efficiency associated with full throttle as shown in Figure 5.3. To operate at optimum motor efficiency, it is necessary to maintain between 11 and 13 cells. A twelve cell battery pack was selected for the extra voltage over the 11 cell pack. For an additional 1.2 oz, an extra 1.2 volts was added to the system. This will aid in meeting range and take-off distance requirements for only a small weight penalty.

With a current draw of 5.2 amps, as obtained from TK Solver program ELECTRIC PROP, a weight of 108.1 oz, and a required range of 9770 ft, it was necessary to have a relatively large capacity battery. From these requirements, it was determined that a 900 to 1000 mAH capacity battery would be necessary for the propulsion system of "Jeff." A 1000 mAH battery was discovered that provided the higher capacity for a weight within 5% of the 900 mAH cell. For this reason, 12 cells with capacities of 1000 mAH will be employed.

Figure 5.3

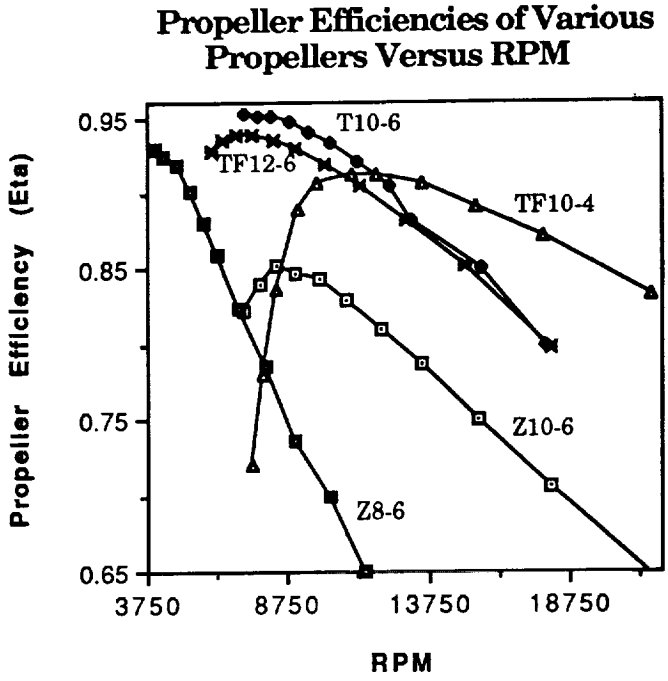

5.5 Speed Controller:

One final instrument that is necessary for the propulsion system of this aircraft is a speed controller to allow the pilot to operate at idle, full throttle, or in between. This is necessary as full throttle, and correspondingly, full power, is required at take-off and climbing while this throttle setting is inefficient in cruise. The lower power required for cruise allows the motor to be operated at less than full power, thus operating more efficiently and saving power and current draw. Examination of previous aircraft design proposals suggests that the pilot may be able to throttle back 40 - 45% in cruise. Calculations of power validate this estimate.

6. Preliminary Weight Estimation Detail

6.1 Weight Estimation

One of the most important tasks which had to be accomplished early on in the design process was the preliminary estimation of the total weight of the aircraft. This estimation was necessary to determine the aerodynamic aspects (airfoil selection, etc.) of the aircraft as well as the propulsion system required.

Once the mission was determined and the need for a large aircraft was established it was necessary to approximate the weight of the structure which would be needed to support the avionics, propulsion system, and payload. Initial estimations were based on accumulated RPV data, and on preliminary fuselage, wing, and canard size estimations. Because these component sizes in turn depended on the lift required for the aircraft, which depended on the overall weight, this cycle proved to be circular, and thus initial estimations were only somewhat accurate. However, as the aircraft design was continually updated, weight estimations were refined as well. The sizes of the fuselage, wing, and canard were also refined according to lift and stability requirements so that a more accurate structural weight estimation could be made.

Initial weight estimates, along with the percentage of total weight for each aircraft component are given in Table 6.1. Note that the weight of the empty aircraft is 73 oz (4.56 lb). This value is typical of many RPV's. However, when fully loaded, the weight increases to 108 oz (6.75 lb) which is rather heavy. For this reason the plane was designed to be as structurally efficient as possible. That is, fuselage and wing design were optimized to support the maximum stresses incurred with the lightest possible structural design. (See Section 9: Structural Design Detail.)

The aircraft structural weights listed in the table were estimated based on data collected from previous years' proposals. Size of our complete structure as

Component	Weight (oz)	Weight Percentage
Fuselage	8.50	7.89
Wing	16.00	14.85
Canard	5.00	4.64
Vertical Tail	3.00	2.78
Batteries (12 @ 1.23 oz)	14.40	13.37
Servos (3 @ .6 oz)	1.80	1.67
Receiver	0.95	0.88
Receiver Battery	2.00	1.86
Speed Controller	1.77	1.64
Nose Wheel	3.00	2.78
Main Landing Gear	4.00	3.71
Engine and Mount	10.30	9.56
Propeller	2.00	1.86
Payload	35.00	32.49
Total	107.72	100

Table 6.1 Aircraft Component Weights

well as size and type of materials to be used in construction were taken into account. Our estimates were then adjusted based on the fact that our structure was somewhat lighter than most previous RPV structures, as a result of the optimization process. The weights of the avionics and propulsion system were obtained from manufacturer information (Group B Design Notebook). The weight of the propeller was estimated based on its size and material composition. The landing gear (nose wheel and main gear) weights were also estimated based on

past data, as actual landing gear type was unspecified at the time of the preliminary weight estimation.

6.2 Center of Gravity Location and Travel

Because of Jeff's canard configuration, placement of the center of gravity was extremely important in ensuring the stability of the aircraft. This task proved to be somewhat difficult as not only did the canard provide a destabilizing effect on overall stability, but Jeff's rear-mounted propeller required placement of the propulsion system and avionics in the rear of the aircraft. Hence the center of gravity of the aircraft, both empty and fully loaded, tended to be fairly far from the nose of the aircraft, and, for many configurations, behind the neutral point (which is unacceptable).

For this reason it was necessary to carefully configure the interior of the aircraft, as well as the the external components (wing and canard) so that the center of gravity position would be forward enough to provide an adequate static margin. Ideal static margins fall in the 10-20% range for canard configured aircraft. External component placement and size were thoroughly investigated by means of a trade study. This study analyzed the effects of varying canard and wing sizes and positions on the neutral point and center of gravity locations and thus on the static margin of the aircraft. As a result, acceptable size and placement of the components were determined. Internal component placement was continually updated until an optimal configuration was found. This configuration can be seen in Figure 6.1.

The neutral point of the aircraft was determined using moment equations of equilibrium which were rederived for a canard configuration. For this aircraft it is located at approximately 31.0 in from the nose of the aircraft.

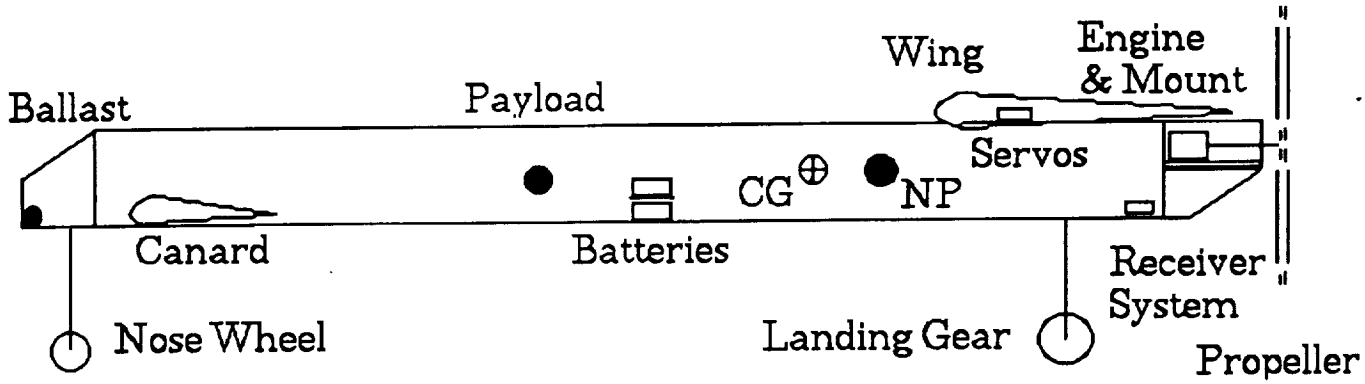

Figure 6.1 Aircraft Internal Configuration

The center of gravity shown is that for the symmetrically loaded, maximum payload condition, where the payload center of gravity is located at the midpoint of the fuselage cargo hold and where three ounces of ballast have been added in the nose of the aircraft for increased stability. This position is 29.4 in from the nose, for a static margin of approximately 13%. When the aircraft is empty, however, the center of gravity travels towards the rear of the aircraft due to the lack of payload in the front of the center of gravity. The empty center of gravity position is 32.8 in from the nose, for a total center of gravity travel of 3.4 in. This distance is important as the center of gravity travel should be minimized for optimal stability. Figures for the static margin and related values may change depending upon the amount of ballast and payload weight carried. See Section 7.3 for a more detailed analysis of the aircraft static stability.

Table 6.2 gives all component center of gravity locations. Overall center of gravity was found using the formula

$$X_{cg}=\frac{\Sigma X_{component} W_{component}}{W_{total}}.$$

The center of gravity in the vertical direction is located along the aircraft's centerline at approximately 1.66 in from the base of the fuselage. The interior configuration is symmetric to align the roll axis with the fuselage centerline as well.

Component	Weight (oz)	CG Location (in from nose)
Fuselage	8.50	32.0
Wing (MAC)	16.00	39.7
Canard (MAC)	5.00	15.0
Vertical Tail	3.00	47.0
Batteries (2 packs @ 7.38 oz)	14.40	25.0
Servos (3 @ 0.6 oz)	1.80	39.7
Receiver	0.95	45.0
Receiver Battery	2.00	45.0
Speed Controller	1.77	45.0
Nose Wheel	3.00	2.0
Main Landing Gear	4.00	42.0
Engine and Mount	10.30	48.0
Propeller	2.00	51.0
Payload	35.00	25.0
Ballast	2.00	1.0
Total (Overall CG)	109.72	31.66

Table 6.2 Component Center of Gravity Location

7. Stability and Control Systems Design

7.1 Surface Location and Sizing

The elevons were designed to produce an aircraft that was statically stable throughout the aircraft's angle of attack range. The initial process for the development of Jeff's control system and stability characteristics was to rederive the longitudinal pitching moment equation for a canard configured aircraft. The development of this equation was achieved by the methods outlined in Reference 7.1. Several simplifying assumptions were made concerning the aircraft's aerodynamic characteristics, they are detailed below.

1. Drag effects on the longitudinal pitching moment were assumed to be negligible.

2. The effects of vertical center of gravity placement, non-symmetric placement in the y axis, were assumed to be minimal.

3. The downwash effects of the canard- wing surfaces were ignored.

4. The destabilizing effect of the fuselage was considered negligible.

5. The small angles assumption was deemed to be valid.

6. The nose down moment of the aircraft was designated as negative.

Using the following assumptions the governing equations for the longitudinal pitching moment of the Jeff aircraft configuration were obtained:

$$L_c = q\, S_c\, Cl_{ac}\, (i_c + \alpha) \quad (7.1)$$

$$L_w = q\, S_w\, [\, Cl_{aw}\, (i_w + \alpha) + Cl_{de}\, de] \quad (7.2)$$

$$Mac_w = q\, S_w\, c_w\, Cmac_w \quad (7.3)$$

$$Mac_c = q\, S_c\, c_c\, Cmac_c \quad (7.4)$$

$$C_{macw} = C_{macwo} + C_{m\delta e}\, \delta e \quad (7.5)$$

$$L_w + L_c = W \quad (7.6)$$

$$L_c\, X_c + Mac_c + Mac_w - L_w\, X_w = M_{cg} \quad (7.7)$$

The next step in Jeff was to determine the stability of Jeff as modeled by the governing equations. As can be seen in equations in the above equations the mathematical calculation of the lift and drag produced by Jeff during flight conditions required implicit knowledge of lifting surface sizing and their location in regards to the aircraft's center of gravity. The lifting surface sizing was set at 10 square feet for the wing and 3 square feet for the canard. The sizing of the lifting surfaces was determined in order to produce the required amount of lift as well as several other considerations outlined by the performance and aerodynamics departments in sections 4 and 8. The center of gravity placement was the main controlling factor in the design of Jeff's established configuration. The canard distance to the center of gravity had to be varied along with the position of various internal components in order to produce an aircraft with a workable static margin (a static margin of 10- 25 % is considered appropriate for canard configured aircraft).

The governing equations were then used with the established quantities for lifting surface area and location to determine the amount of lift and the coefficient of moment produced by the aircraft over a given angle of attack range. Initial calculations involving assumed that Jeff would be cruising in a steady level condition without the aid of elevator flap deflection. This assumption negates the effect of the $Cl_{\delta e}$ δe term in the second equation. The limiting conditions imposed on the last two governing equations were that lift must equal the weight of the aircraft and that the moment must reduce to zero. These conditions were satisfied by varying the incidence angles of both the wing and canard. The incidence angles were referenced to the mean chord line of the established fuselage. Subsequent calculations determined that Jeff would be required to operate with a canard incidence of -.75 and a main wing incidence of 6.2 degrees.

This situation produces the necessary lift of 6.875 pounds and a coefficient of moment of -.015583 .

The calculation of the coefficient of moment also established that Jeff was a statically stable airplane in the fully loaded condition. That is, the slope of the C_{mcg} vs. α curve was seen to be negative (see Figure 7.1).

Figure 7.1
Effect Of Cargo Loading Condition On Moment Coefficient

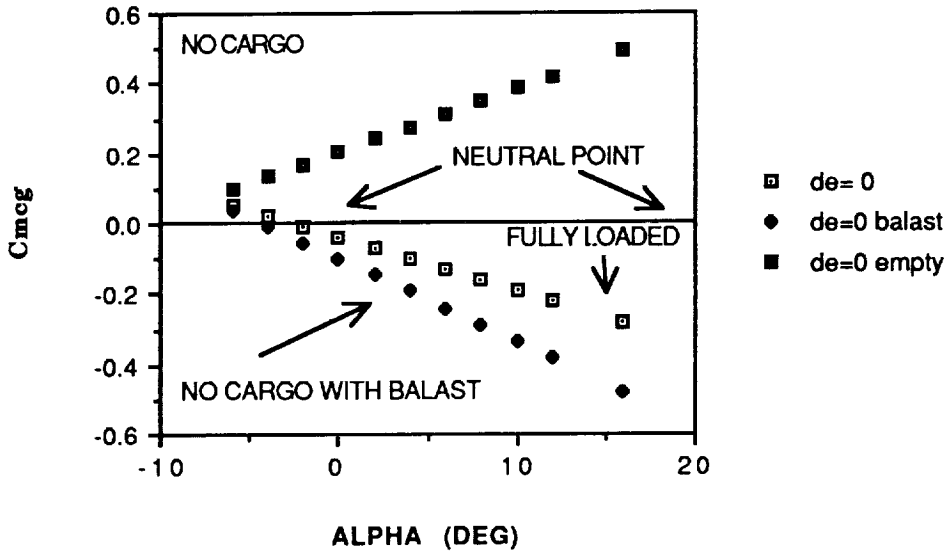

However, it was also determined that Jeff became statically unstable when flying with an empty cargo hold. This condition is to be corrected through the ballasting of the nose during unloaded flight operation. As is seen in Figure 7.1, 8.8 ounces of nose ballast will create a Cm_{cg} vs. α slope comparable to that of the fully loaded cargo hold condition. Besides producing a statically stable aircraft, the addition of ballast produces an aircraft that will maintain its handling characteristics despite cargo loss. The similar handling characteristics of the airplane in various cargo conditions will aid the pilots of Aeroworld. Canard configured aircraft often respond differently than standard aircraft to pilot input. Therefore, piloting a canard configured aircraft requires experience with its handling

characteristics. Obviously, a canard configured aircraft with constantly changing handling characteristics would be unsettling to fly because of its inconsistency. Although a dynamic analysis is necessary to get a better feeling for the handling qualities of the plane consistent response to control deflections (as seen is consistent static margins) seemed like a good place to start. Therefore, it would be advisable to add slight amounts of ballast for the complete range of loading conditions. The amount of ballast to be added for various loading conditions have been determined and are presented in Table 7.1.

Cargo Load (Ounces)	Ballast (ounces)	Static Margin (%)
0	8.8	16.57
5	7.5	16.44
10	6.2	16.32
15	5.0	16.55
20	3.7	16.44
25	2.4	16.34
30	1.3	16.64
35	0	16.73

Table 7.1 Ballast Weight Addition Various Cargo Loads

These ballast additions will produce a coefficient of moment curve comparable to that of the fully loaded condition, thus preserving Jeff's handling characteristics. However, to get a better understanding of the handling qualities of Jeff a dynamic analysis is recommended as a future study.

The inherent difficulty with the development of the canard design is apparent from examining Figure 7.1. The canard configuration's stability is extremely susceptible to slight changes in center of gravity placement. A small

rearward change in the center of gravity can produce an airplane that is statically unstable and thus unflyable. The canard configuration is also suspect to construction flaws. For example, poor estimations of the component weights could lead to an inaccurate calculation of the center of gravity location). Another possible construction flaw is in the placing of the canard and wing at their respective incidence angles of attack. The canard configuration's stability and lift capabilities will change drastically with small shifts in incidence angle (ie. the lift changes by 2% and the coefficient of moment by 30% for shifts in angle of .1 degree).

FIGURE 7.2
EFFECT OF CONTROL SURFACE RATIO (TAU) ON ELEVATOR DEFLECTION ANGLE

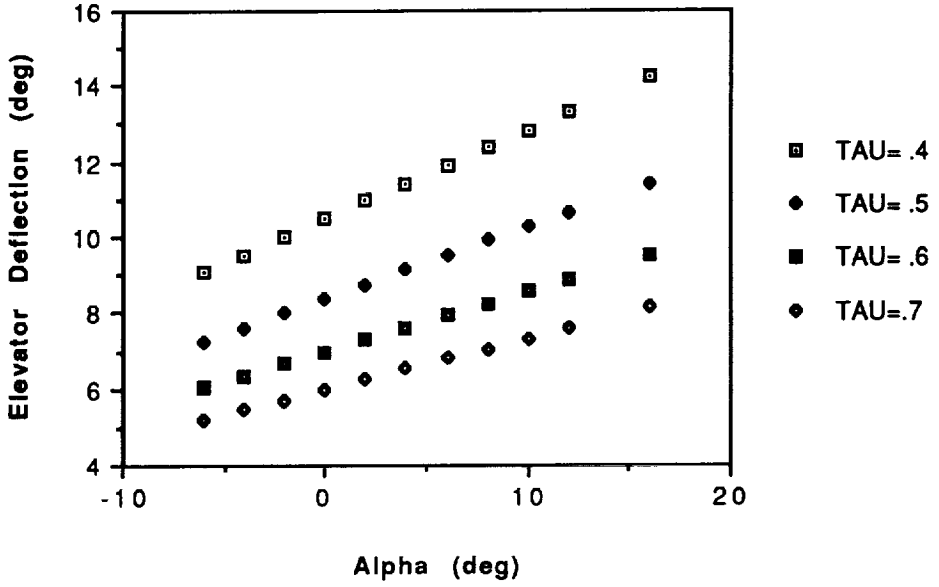

The trim conditions for the aircraft were calculated using equation 7.7 with the subsequent addition of the $Cl_{\delta e}\delta e$ term in equation 7.2. The control effectiveness was established for the Wortman FX 63- 137 using a mathematical approximation found in Reference 7.1:

$$Cl_{\delta e} = Cl_{\alpha surface}\,\tau$$

The value of τ corresponds to a control surface to lifting surface area ratio. An established curve for these values can be found in Reference 7.1. As seen in Figure 7.2, a slight increase in the control surface area corresponds to a noticeable decrease in elevator deflection angle at large aircraft angles of attack. Intuitively, the system design should minimize both the surface area and the deflection angle to reasonable values. These values were established from the Design Data Library to be $\delta e < 15^{o}$ and control surface area of under 25 %. The final design of the elevator surface airfoil was a choice between using a Wortman Fx 63-137 flap or a FXLV- 132R25 25% flap. The required elevator angle to trim for various angles of attack for both cases was calculated and plotted in Figure 7.3 for the aircraft in the fully loaded cargo condition.

FIGURE 7.3
EFFECT OF CONTROL SURFACE
AIRFOIL SELECTION ON ELEVATOR PERFORMANCE

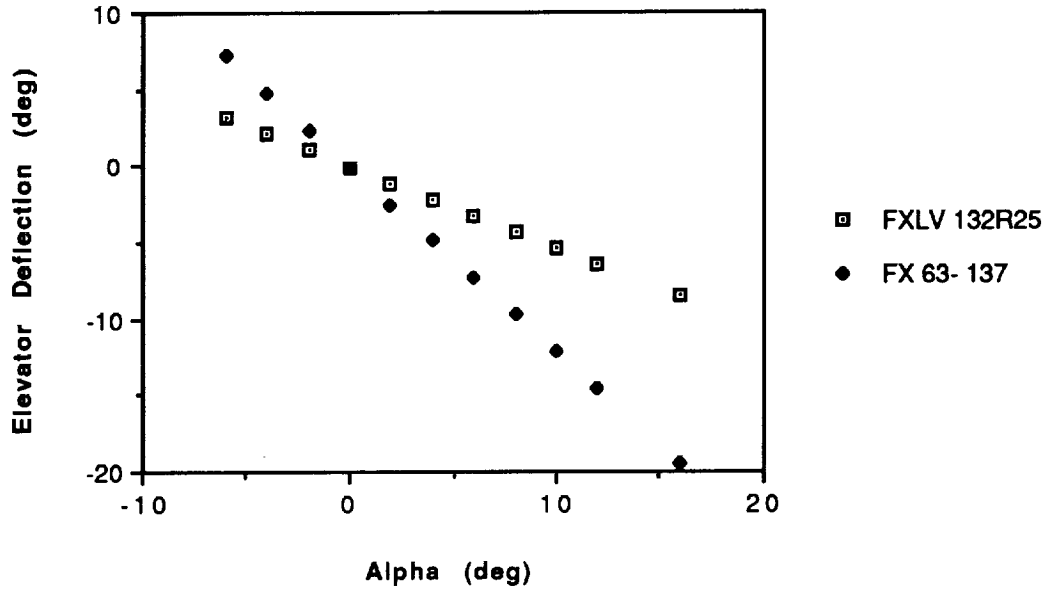

From this graph one can see that the FXLV-132R25 has better performance to the FX 63-137. However, the decision was made to manufacture the elevator surface using the FX 63- 137. This decision was made for two reasons. First, due to the

high incidence angle of the canard the angle of attack range is limited to positive 7° - curtailing the high angle of attack advantages of the FXLV- 1232R25.

Having established the elevator airfoil and sizing, the trim conditions for Jeff could be established. A decision was made to place the elevator surface on the main wing. The obvious disadvantage is that trim conditions for any nose down moment on the aircraft involve an upward (-) deflection of the control surface. Despite this disadvantage, the placement of the surface on the main wing creates many advantages. First, the effect of the induced wake created over the main lifting surface due to canard elevator deflection is negated. Second, the area of the elevator is a smaller fraction of the lifting surface on the main wing. This will help aerodynamic performance and improve the structural stability of the aircraft.

Figure 7.4
Elevator Deflection Required To Trim Aircrat In Fully Loaded Condition

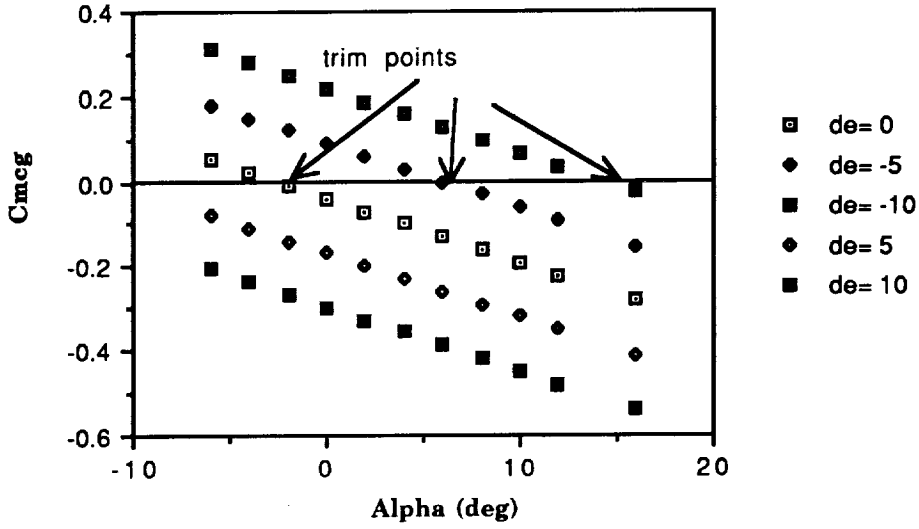

Figure 7.5
Elevator Deflection Required To Trim Aircraft In Ballasted Condition (No Cargo)

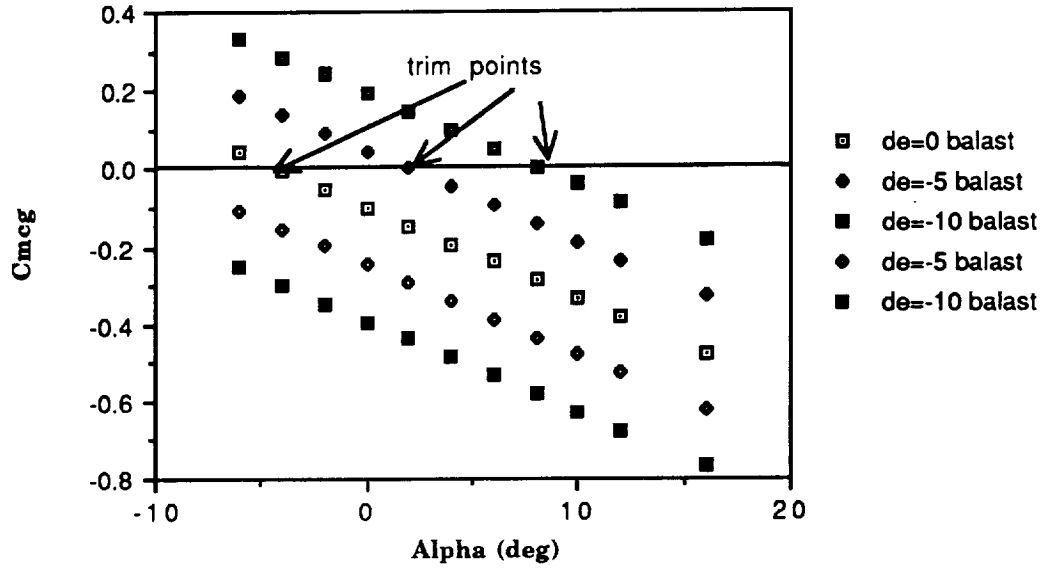

A fully movable canard would require additional bulkheads with the canard structure to support the bending moment created at the tip due the lifting load. A control surface on the main wing would require less of the over all surface area allowing the control surface to be placed between existing rib sections. Thus, the flap surface will be structurally supported on two ends instead of one in the canard flap design. The main wing flaps will be constructed with a four inch chord and 1.25 foot semi-span running from 3.25 feet from the wing root to six inches from the wing tip. The effects of the deflection of this surface on the C_{mcg} versus α curve for the fully loaded and unloaded ballasted conditions can be seen in Figures 7.4 and 7.5.

The placement of the elevator flap in its previously established lateral position serves two important purposes. First, the position from the wing tip allows the flap to be placed directly near an already existing rib in the wing structure. This will allow the flap to be constructed onto the main wing without the addition of much added structure. Secondly, the placement of the elevators

outboard of the wing root will aid in the development of the roll moment produced by the elevon control surface. The elevon control is a dual action surface that can both deflect for pitch stability as well as roll control. The desicion to use elevons came as a result of the large amount of surface area required for the elevators. In order to minimize the amount of lifting surface used for flaps the elevators and ailerons were combined into a single surface. This combination of surfaces also removes extra structure and control devices that would be needed to operate separate surfaces.

FIGURE 7.6
EFFECT OF RESPONSE TIME AND AILERON DEFLECTION ANGLE ON CONTROL SURFACE AREA

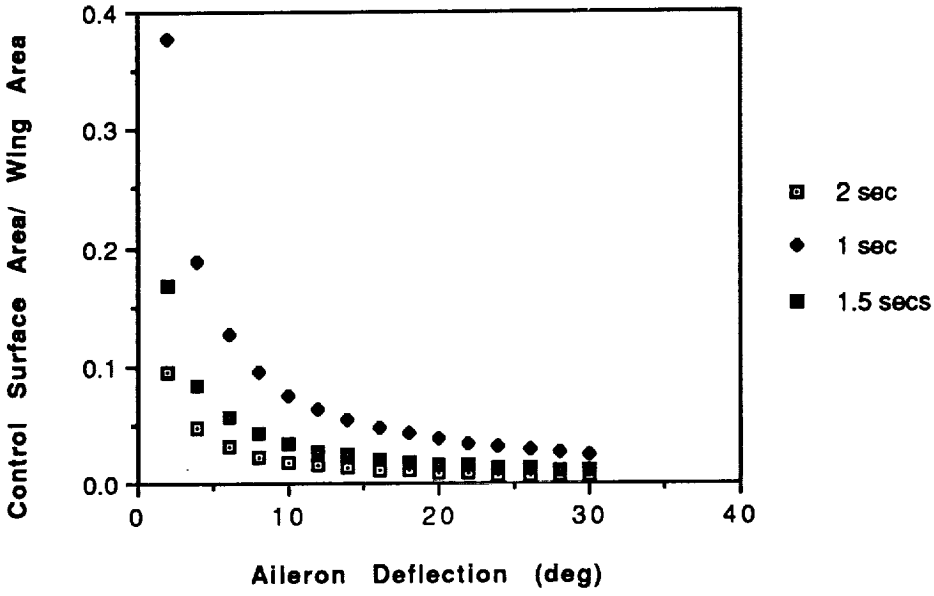

Ailerons were chosen for roll control due to their superior turn performance in comparison to a rudder for canard configured aircraft. Development of the aileron sizing was established by using a simplified lateral equation of motion (Reference 7.1):

$$I_x \varnothing = L_{\delta a}\delta a \text{ (eqn 7.8)}$$

$$L_{\delta a} = 2Cl_{\alpha w} Q \tau \int c\, y\, dy \text{ (eqn 7.9)}$$

The values of y correspond to the integration along the established semi- span. The value of $\varnothing$ was calculated through the approximation $\varnothing = 2\theta/t^2$ (eqn 7-9) in Reference 7.1. The time value in the denominator has a significant effect on aileron deflection angle as is evident in Figure 7.6.

A value of two seconds was established from the Design Data Library (Reference 7.2). The time to turn would allow the Jeff to traverse 56 aerial feet before reaching its full bank angle. However, viewing the performance tapes of a previously designed AE 441 Inc. aircraft, the Valykyre, this value was deemed to be a very conservative estimate. The mass moment of inertia and maximum bank angle were calculated using the equations Reference 7.1:

$$\mathbf{I_x = \int (y^2 + z^2)dm \ (eqn\ 7.10)}$$

$$\mathbf{L \cos \theta = W \quad (eqn\ 7.11)}$$

The values for the mass moment of Inertia for Jeff's main components were determined and tabulated in Table 7.3.

Element	Ix	Parameter	Value
wing	.749	δe_{cruise}	-.052 deg
canard	.322	δe_{max}	+/_ 10 deg
nose wheel	.003	flap dimensions	.33 x 4.5 ft
Landing gear	.002	C_{mo}	-.0523
Vertical tail	.023	$C_{m\alpha}$	-.3856

Table 7.3 Mass Moment of Inertia and Selected Important Values

From Figure 7.6 it is evident that Jeff will be able to obtain the maximum bank angle with little deflection angle and control surface area.

REFERENCES

7.1 Nelson, R. C., Automatic Stability and Control.
7.2 Group Valyklre, Design Proposal Report.

7.2 Control Surface Mechanism

The control surfaces for Jeff will be deployed in an elevon configuration. An elevon is a dual function single surface control that will allow the elevator surface to also serve as the aileron surface. The elevon is implemented through use of a special servo attachment called a mixer. The addition of the mixer will allow the elevator and aileron servos to be connected into a single unit that actuates the elevator motion and the aileron motion. The elevon servo will then be connected directly to the mixer unit which will actuate atop the aileron servo. The aileron servo will be connected through control rods, bell cranks and horns to the control surfaces (see Figure 7.7) The main control rods will run between to bell crank assemblies, and all units will be attached through stationary parts of the main wing. Actuation control rods will run from both the aileron servo and the control surface. The actuation rods will be attached to the control surface via a control horn on the flap surface and a clip.

7.3 Static Stability Analysis

The static stability of the aircraft was analyzed based on calculation of the static margin. The equation used was

$$\text{Static Margin}=\left(\frac{X_{np}}{\bar{c}}-\frac{X_{cg}}{\bar{c}}\right)x100\%$$

As noted in Section 6.2 (CG Location), the neutral point of the aircraft is 31.0 in from the nose when three ounces of ballast are placed in the nose. Fully loaded, the center of gravity, at 29.4 in, provides a 13% static margin. However, when the aircraft is empty, the center of gravity travels to 32.8 in, for a static margin of 15%. This static margin indicates that the aircraft is unstable when empty. In order to improve the stability characteristics it is necessary to move the center of gravity forward until the static margin lies in the ideal 10-20% range.

Two methods of improving the static margin and providing stability exist. The first is to alter the distribution of payload so that the center of gravity of the payload is farther forward, thereby increasing the payload center of gravity distance from the neutral point, providing a longer moment arm about the aircraft's center of gravity, and thus pulling the overall center of gravity forward. However, this may not always be possible due to the amount, size, and weight of the payload for any given flight. Also, this process would require excess calculations at the time of the flight in order to determine the optimum payload center of gravity location and proper payload distribution.

The second alternative is to add some ballast to the nose of the aircraft while maintaining the payload center of gravity at the center of the fuselage cargo hold. Ballast addition is a common practice in the construction of canard configured RPV's. Calculations made on an Excel spreadsheet show that the addition of as little as three extra ounces of ballast in the nose for the full payload condition can move the center of gravity far enough forward to ensure acceptable static margins, and hence the stability of the aircraft. As the payload weight decreases, however, even more ballast must be added in the nose for stability. As much as ten ounces may be needed to balance the aircraft at the empty payload condition.

The weight and balance diagram seen in Figure 7.8 gives the ballast requirements for aircraft stability at various payload weights. Stability is defined here as the condition for which the static margin ranges between 10% and 20%. The payload center of gravity is assumed to be 22 in from the nose of the aircraft. This location is at the center of the cargo hold and thus a symmetric cargo loading about this point has been assumed as well. For the zero ballast case, the center of gravity must be between 28.24 in and 29.44 in from the nose, allowing for a travel distance of only 1.2 in. Thus, when the aircraft is empty it is inherently unstable.

Figure 7.8
Weight and Balance Diagram for Jeff

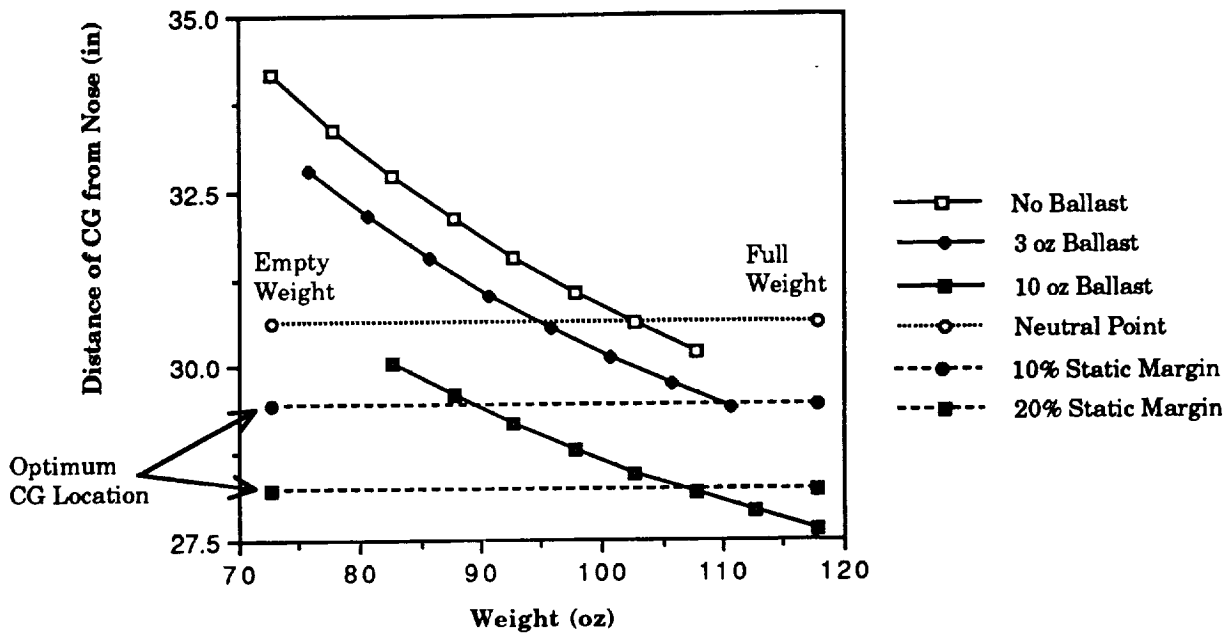

It can be seen from the figure that the center of gravity is behind the neutral point (located 30.64 in from the nose of the aircraft for the empty, no ballast condition). Even when full the aircraft cannot achieve an acceptable static margin without ballast addition. As ballast is added, however, the static margin moves into the acceptable range and the aircraft becomes statically stable. When enough ballast is added (10 oz) the center of gravity moves forward of the neutral point even when the aircraft is empty.

Because this analysis is based on preliminary weight estimations exact amount of ballast required must be determined after the technology demonstrator is constructed, as variations in weight and center of gravity of individual components will affect the neutral point location. However, Figure 7.8 is still a very useful assessment of the static pitch stability characteristics of our aircraft.

Roll stability is achieved by two vertical stabilizers, each 1.5 ft^2, incorporated into both sides of the wing. While these stabilizers do not provide directional control, they do serve to maintain the roll stability of the aircraft.

Control surfaces were sized so as to provide yaw, pitch, and roll control for the aircraft when the static margin ranges from 10-20%. A spreadsheet is available for calculation of proper payload center of gravity placement at all payload weight conditions so as to determine the optimum position for acceptable static margins. With a nearly full payload, as is expected for most flight cycles, Jeff will be statically stable, provided the payload is distributed correctly throughout the fuselage to provide an adequate static margin.

8. Performance Estimate

8.1 Takeoff and Landing

The takeoff phase of the flight is a critical time during the overall flight of the plane. It is especially important given the constraints that the plane must be able to become airborne within 60 feet, and that it must fly at a speed below 30 ft/s. Thus, the variables weight, propeller diameter, coefficient of friction, and coefficient of lift were varied to determine their affect on meeting the predefined constraints.

An analysis was done to determine a "heavy" weight range that can exist and still meet the aforementioned constraints. Thus a larger and therefore heavier plane that meets the takeoff constraints is desirable because it enables one to build a plane that can carry more cargo. This benefit results in the need to build fewer airplanes to complete the existing routes.

The fortran program *takeoff.f* written by Dr. Stephen Batill was used to analyze Jeff's performance. An iterative process was used to output the takeoff velocity and distance, where takeoff was assumed to occur when $V_{T.O.}=1.2V_{stall}$. In calculating the ground roll, it was assumed that the coefficient of friction was constant along the runway. Finally, the electric motor was modeled by a circuit with a battery voltage and resistances due to the armature and the battery.

Figure 8.1 plots wing area versus takeoff velocity for three different airplane weights. The results show that for our configuration (S=13 ft) acceptable takeoff velocities (<25 ft/s) can be achieved in the shown weight range. The wide weight range that is used is important because the weight estimation process appears to a tenuous one. It is apparent from looking at figure 8.1 that takeoff velocity decreases with increasing lifting surface area in a linear fashion. This result is in accordance with what would be expected since $V_{takeoff}=1.2C_{Lmax}\rho V^2 S$ where S is the total lifting surface area.

Figure 8.1
Plot of Takeoff Velovity Versus the Total Wing Area

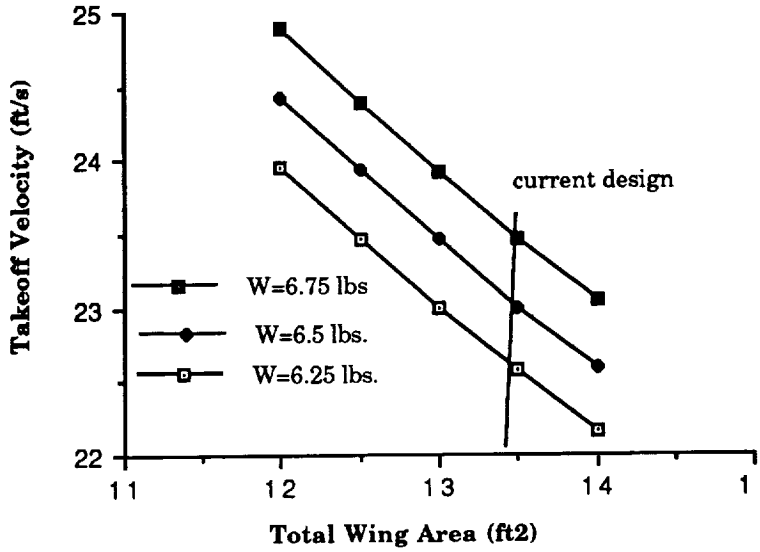

Figure 8.2 shows that propeller diameter has a significant effect on the distance covered in takeoff. The reason for this is that the thrust is proportional to the reciprocal of the diameter raised to the fourth power. Quantitatively, this results in a.thrust at takeoff going from 3.37 pounds with a 1 foot diameter prop to 2.41 pounds with a .9 foot diameter prop. Therefore, a small decrease in diameter corresponds to a large decrease in thrust which manifests itself into a large increase in takeoff distance. This result is valuable in case we find it difficult to meet the necessary clearance needed for a 1.0 foot propeller or if we think it is more beneficial to go with shorter landing gear. The plot shows that in this scenario we can go with a 11 inch propeller as opposed to the 12 inch and still fulfill our takeoff requirements. There is, however, a limit to how small a propeller we can use. Anything below 10.8 inches results in an exceeding of the minimum takeoff distance of 60 feet.

Figure 8.2
Takeoff Distance Versus Propeller Diameter

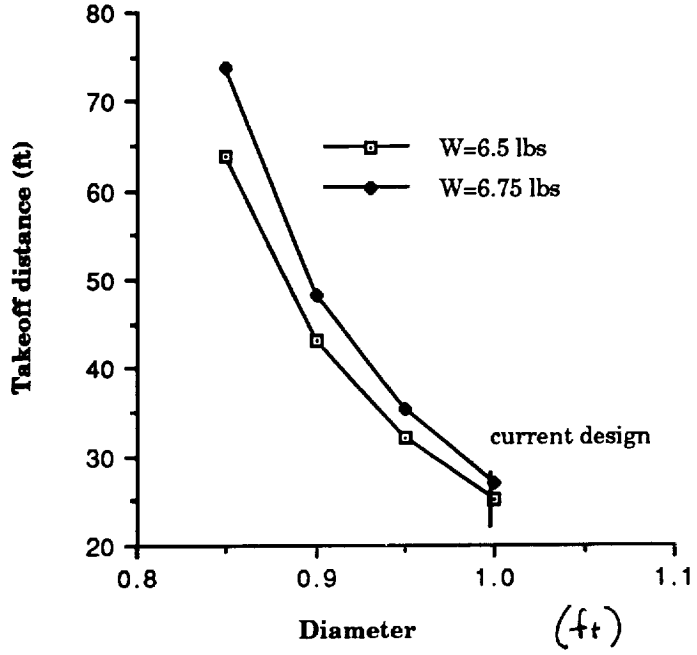

Figure 8.3 plots how coefficient of friction affects the takeoff distance. This was necessary because of the difficulty that exists in finding data on μ (coefficient of friction) for astro turf on small diameter wheels. The plot here shows that varying values of μ does not have a profound affect on takeoff Distance. It should be noted that the magnitudes of these takeoff distances in both figures 8.3 and 8.4 are low. This is because the propeller efficiencies used in inputing the C_T and C_P for a given advance ratio were assumed to be too high. This was not corrected due to the late time in the semester in which this error was found. However, the fact that the magnitudes of the takeoff distance were low by 20 to 30 percent is not critical given the low variation in takeoff distance that occurs for large changes in μ.

Figure 8.3
Plot of Coefficient of Friction Versus Takeoff Distance

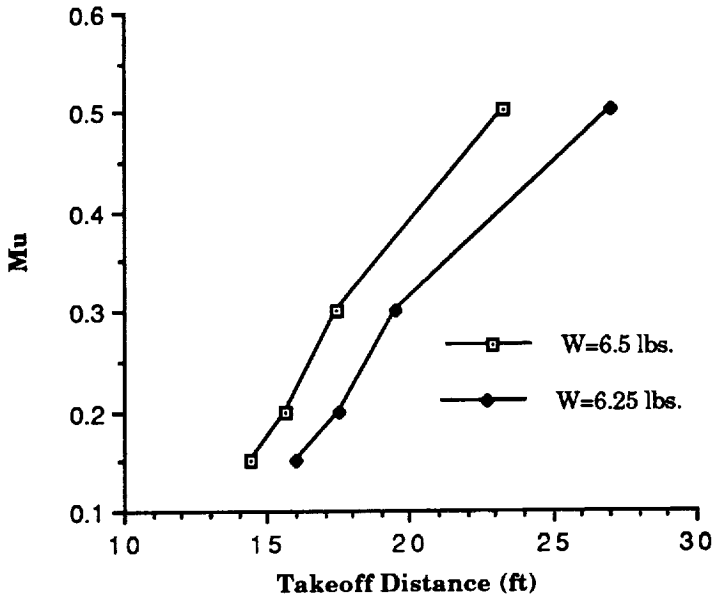

Finally, figure 8.4 shows that takeoff distance varies only slightly with different values of C_L during horizontal takeoff. This makes sense given that takeoff velocity and distance are governed by the condition that takeoff occurs when 1.2 V_{stall} is reached and 1.2 V_{stall} is a function of C_{Lmax} not C_L during the horizontal takeoff roll. Interestingly, however, the magnitude of the change in C_L and its effect on takeoff distance seems to mirror that of μ. This makes sense when one considers that varying C_L affects the normal force of the plane on the runway. Thus it seems that the two are a measure of the effect of friction on takeoff distance.

Figure 8.4
Takeoff Distance Versus CL

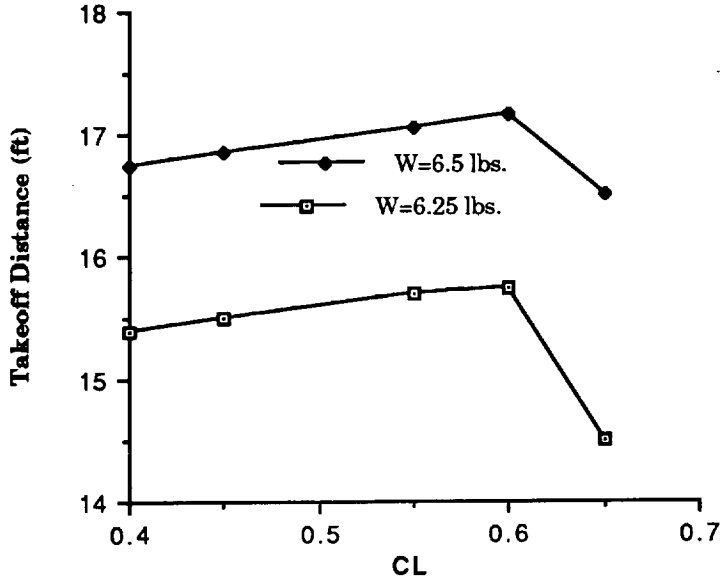

Validation of the results were difficult to do due to the fact that none of the planes in previous years were comparable in size to our design. However, one can notice trends that occur by looking at other designs. From this one can extrapolate as to whether the results produced by *Takeoff.f* were reasonable. Using this method the results appear to be validated. For Figure 8.1 a second means of validation was also used. As a double check, I calculated the maximum lift that our present design could generate and then calculated the lift it generated as it was rolling horizontally down the runaway at the takeoff velocity. It was then hoped that the computer program, takeoff.f, would output a takeoff lift (the weight of the airplane) in between these two extremes. The maximum lift was determined using the formula

$$L_{max}=.5C_{Lmax}\rho v^2 \qquad \text{where } C_{Lmax}=1.0.$$

Similarly the lift generated during horizontal roll was calculated using

$$L=.5C_L\rho v^2 \qquad \text{where } C_L=.6.$$

This indeed turned out to be the case with L_{max}=9 lbs. and L=5 lbs. and the airplane weight equal to 6.75 lbs.

The current status of the design has a total lifting surface area of 13.0 ft^2, a weight of around 6.75 lbs., a $C_{Lmax=1.0}$, a C_L=.6 when a=0, and a resulting takeoff velocity of around 25 ft/s (see graphs).

The takeoff phase of the flight is one of the most critical phases. The parameters of weight, friction coefficient, propeller diameter, and takeoff C_L have either an uncertainty associated with their estimation or one may find a need to "play" with these values if unsuspected problems arise during the construction of the plane. Thus, it was the aim of this section of the report to determine a margin for error or adjustment of certain key parameters and see how these would affect the takeoff phase of the flight.

8.2 Range and Endurance

The range constraint set on the Aeroworld mission is that Jeff should be able to fly to the city of furthest location plus the distance covered in loitering around this city for one minute to allow potential runway problems to clear up. Given this constraint it was calculated that Jeff must be able to fly at least 9800 feet. As can be seen on figure 8.6 Jeff meets this constraint easily even for the wide range of weights shown (4.5-6.9 lbs). The constraint on endurance is that *Jeff* should be able to stay in the air long enough to fly to the city furthest away on our Aero World route and loiter for one minute. This results in the constraint that Jeff must be able to fly for over 350 seconds. Again by looking at Figure 8.5 one can see that Jeff meets this for weights up to 6.9 pounds. Jeff is expected to have a range of 18,700 feet and an endurance of 670 seconds. The endurance was calculated based on the formula

E = battery capacity / current draw

where the battery capacity was taken as 1000 milliamp-hours and the range was calculated based on the formula

R=Endurance x Velocity.

Figure 8.5
Endurance Versus Payload

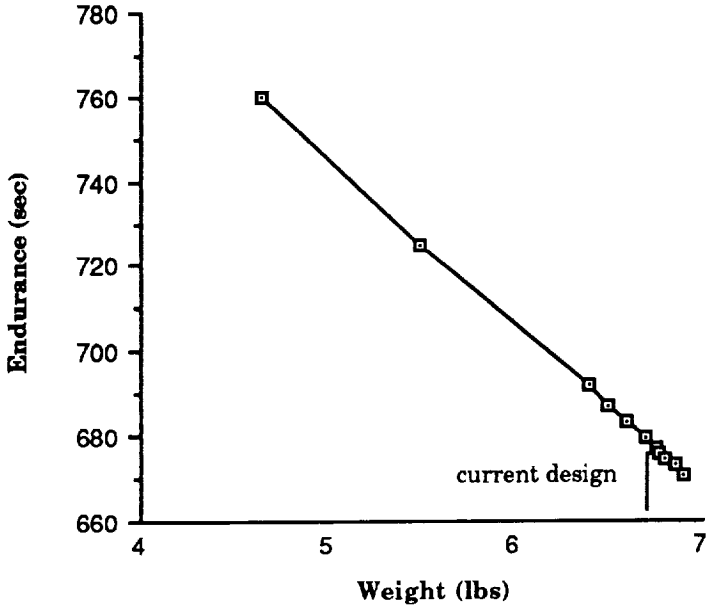

Figure 8.6
Range Versus Payload

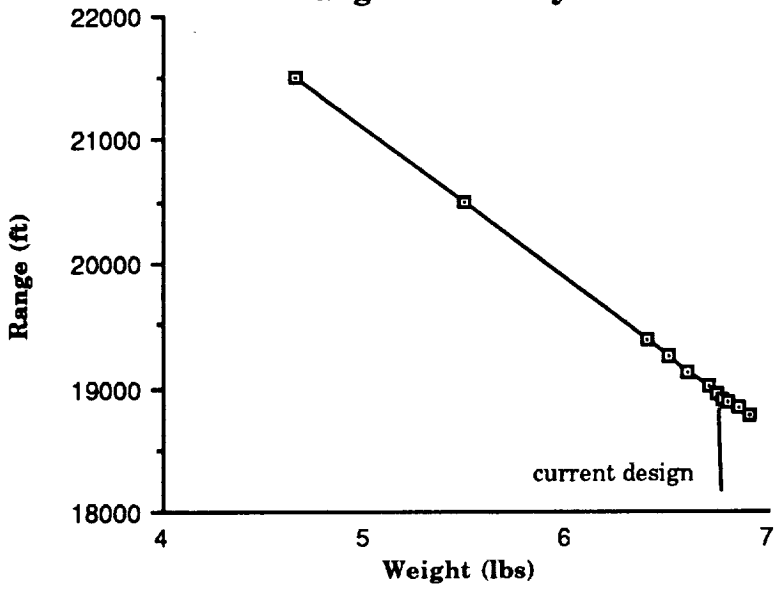

The current draw was taken from the fortran program *Takeoff.f*. It was noted that current draw varies strongly with propeller diameter. Unfortunately, in looking at the effects of propeller diameter and takeoff distance we realized that by going to an 11 inch prop we were cutting it close with respect to our takeoff distance constraint. Therefore a tradeoff between current draw and takeoff distance had to be chosen and as a result a 12 inch prop for Jeff was chosen. This choice is fixed unless upon construction of our plane we realize that we have underestimated the propeller clearance needed for takeoff. In this case we know that we can go with an 11 inch diameter propeller but that we will be pushing our takeoff distance constraint close to its limit.

8.3 Climbing and Glide performance

Climbing performance is characterized by rate of climb. A design goal of 5.5 ft/s was initially set for Jeff's rate of climb. This was based upon the desire to have Jeff at cruising altitude before entering the first turn of the Loftus course. By dividing our excess power (see figure 8.5) by the weight of our aircraft a rate of climb of 14.0 ft/s was achieved. Thus Jeff has the rate of climb performance to achieve the cruising altitude well before the first turn at Loftus is completed.

Glide performance is governed by the glide angle and the minimum turning radius. The glide angle was calculated by taking the inverse tangent of the drag divided by the lift. This yielded a minimum glide angle (at alpha=0) of 3.7 degrees.

The turning radius constraint that had to be met was 60 feet. The minimum turning radius for Jeff was 25 feet. The main difficulty with turning Jeff is the danger of stalling the inside wing due to the decreased velocity it sees in the turn and the decrease in force in the vertical direction that results when one turns the lift vector 29 degrees from the vertical. Using a maximum bank angle of

29 degrees it was calculated that our stall velocity was approximately 24 ft/s. This speed was calculated based on projecting the magnitude of the lift vector in the vertical direction such that the magnitude of this vector was equal to the weight of our plane.

8.4 Catapult Performance Estimate

Analysis for this section was begun but because of the crash that ocurred during the test flight it was decided that to do the catapult performance estimate would be of little value since our prototype was damaged. However, for future references there exists a program written by Kevin Costello which performs this estimate given an accurate description of your plane in the input file his catapult program uses.

8.5 Power Required and Available

Figure 8.7 shows the power available for different diameter propellers of the same pitch in comparison to the power required for cruise at various velocities. Of note, is the fact that the graph was constructed using a full throttle setting of 14.4 volts. This will not actually be the case, as the motor operates at higher efficiencies at lower voltage settings (as shown in section 5.4). Therefore, the power available, P_{av}, on Figure 8.7 is the maximum power obtainable for that diameter prop operating at full throttle with twelve batteries, 14.4 volts. As was already mentioned this is not the optimum situation based on efficiency, so the P_{av} shown is higher than the actual power available for a certain diameter prop over this range of velocities. Also of note is the fact that the C_T, C_P, and η data collected at various advance ratios from the Apple IIe were calculated using the Clark Y airfoil section. Data would be more realistic using the LOWRE NACA 44XX airfoil for the propellers which produces lower values for C_T, C_P, and η.

Figure 8.7

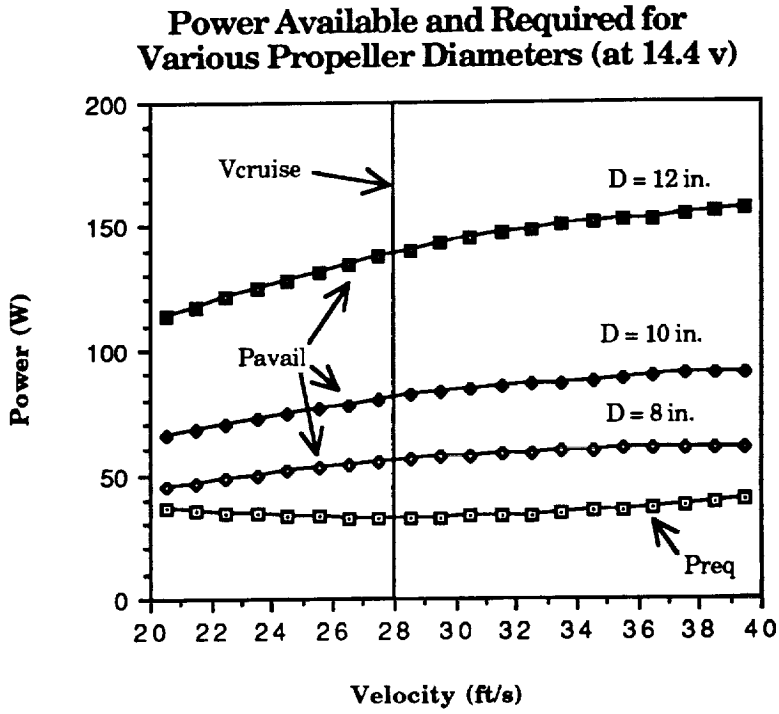

From Figure 8.7, keeping in mind that the Clark Y airfoil section and a full throttle setting were employed in the analysis, it seems that an 8 inch diameter propeller is not large enough to perform the desired task. In fact, because the power input to the motor will be considerably less than the maximum power input, which is shown on the graph, 9 and 10 inch diameter propellers were also eliminated from consideration. The 10 inch diameter propeller does produce enough power for flight at an acceptable efficiency and enough power for take-off. However, less than ten watts of excess power exist. If the aircraft, when constructed, turns out to be heavier than predicted, happens to be taking off on a rougher runway (with a higher friction factor) than expected, or has higher drag than approximated, take-off might prove to be difficult to achieve within the allotted 60 ft. For these reasons, and those mentioned in Chapter 5, a 12 in propeller will be employed. This results in quite a bit of excess power, over 80 watts as shown on Figure 8.7, when in cruise at 28 ft/s. However, when the

aircraft is flying at optimum propeller and motor efficiency, less than 35 watts of excess power result. This does seem like a great deal, but problems, such as those mentioned above, should be able to be overcome.

9. Structural Design Detail

9.1 Structural Design

The basic structure of Jeff is similar to those of previous RPV designs. The one characteristic, however, that stood out in all of the studied airframes was the inefficiency of the fuselage structure. Some estimations stated that the possibility existed for a 40% improvement in the weight of these structures.

These estimations were based upon finite element models that were set up on, SWIFTOS, a finite element program writtern by Richard Swift. This program utilizes a least-weight, fully-stressed member routine to optimize the structure. Unfortunately, SWIFTOS was intended for the development of wing structures. With the help of the developer, modifications were made to allow for the input of a fuselage structure. First, a file was created to model the cross section of the fuselage as an airfoil cross section. At this point the terminology applied to the members of a wing section needed to be translated into those associated with the development of a fuselage. Spar caps became main beams, ribs became bulkheads, etc, etc. Rib and spar membranes were removed from the inputs entirely as to end up with a true truss-like structure. Another major modification was made by changing the hard points, or fixed reference positions on the fuselage model. The wings are cantilevered in the original program, for the purposes of the development of the fuselage the reference points were place at the wing-fuselage junctions.

Structures similar to those of previous years were then inputed into SWIFTOS,. It was then noticed from SWIFTOS, least-weight, fully-stressed, optimization routine that in many of the members there was structural overkill. For example, the standard cross sectional area of the main beam supports in many previous designs were .25"x.25" and made of balsa. In Jeff's optimized

fuselage structure .125x.125 spruce supports were used. Based upon the model made in SWIFTOS this fuselage structure can handle load factors of up to 3.7 and still remain structurally intact. This results in a weight savings per cantilever beam of .15 ounces over 50 inches.

At first, there was surprise at these results. Upon further discussion with Dr. Batill, a specialist in structures, and the construction of cantilever beams that were constructed and loaded, the results using SWIFTOS appeared to be validated. What allows this decrease in cross sectional area to occur is the advantage of using a more efficient material like spruce.

A quick look at the optimization routine may be beneficial at this point. As stated earlier, SWIFTOS was given input data that defined an existing structure. For this case, all of the elements balsa and had a cross sectional area of .04 sq.in. Minimum gage specifications were set at .015625 sq.in., or the equivalent of a 1/8 by 1/8 inch square cross sectional beam. Those members which were pushed to minimum gage were left alone. Members that were increased in area, stayed the same, or were only reduced slightly, were replaced with a spruce member.

Rod Element 12

Original configuration	*Optimization*	*2nd Input*	*Final Opt.*
Area - 0.0400 sq in	0.0400 sq in	0.0400 sq in	0.015637 sq in
Material - Balsa	Balsa	Spruce	Spruce

This table illustrates the process used for optimization of the single elements. The finite element mesh was then taken and elements were combined in groups to represent long beams that would be used in the construction of the airframe. On example of this is the spar caps in the wing. The gages along these beams were compared and a gage that satisfied all of the area and stress

requirements was determined. These values were then used for the final construction dimensions.

The fuselage model was subjected to estimated Limit loadings, and Landing loads which were then superimposed to arrive at the final design. The structure was designed to withstand 2.5 G inertial loading with a factor of safety of 1.5. The landing load was simulated using a 4 G loading. The input files for the major components may be found in Appendix A.

The weight of the avionics, control mechanisms, and propulsion devices are absolutely fixed. Therefore, the weight savings must come from the efficient design of the airframe. For the large cargo capacity of Jeff, every ounce of weight savings in the airframe directly translates in to an ounce of cargo weight that may be sold.

The program was then used to develop models for the wing, and canard frames. Using the same developing tool for the entire structure also gives Jeff the benefit of design integrity: a consistent approach to the design of the entire airframe. The following plot illustrates the operation limits of Jeff in V-N diagram.

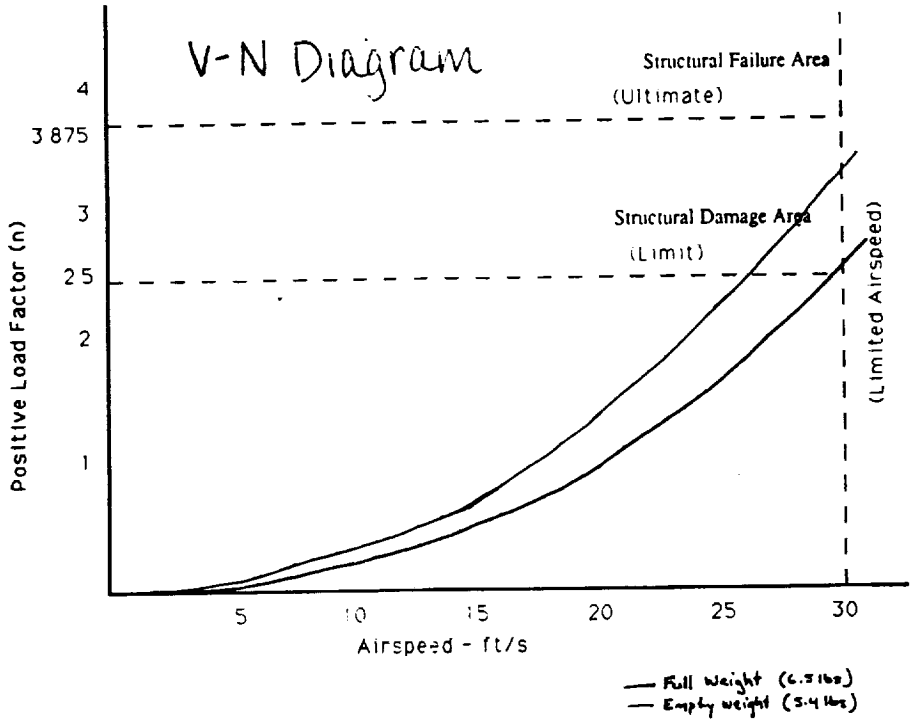

9.2 Basic Structural Components, Substructures and Assembly

The airframe consists of three major components; the fuselage, wing and canard. As mentioned much time was spent in the design of the fuselage to increase the overall weight efficiency of the aircraft. The fuselage is basically an 8" x 4" x 50" rectangular box. Spruce main beams and balsa supports define the configuration, and 1/16 inch balsa membranes are used to add torsional rigidity to the structure.

The wing was also developed using SWIFTOS, but this time without modification. Jeff's main wing is a 3 spar configuration; the leading edge spar at 5% chord, main spar at 33% chord, and the trailing edge spar is positioned at 66.6% chord length. The placement of the T.E. spar was dictated by the sizing of the control surfaces, and will be the hinge position for the elevators and ailerons. The hinge will be constructed out of overlapping monokote from the main wing and the control surface sections. The spar caps are 1/8" x 1/8" spruce beams that extend the length of the section. The main wing will have 3 modular sections in order to comply with the constrained size of its transportation box. The breaks in the wing will be reinforced with double rib bulkheads and reinforced spar caps.

The canard will be a single section similar to the wing. The only difference will be the 85% chord placement of the trailing edge spar. Neither the wing or the canard will be hard pointed to the fuselage, they will be attached with a lightweight rubber lashing. This is also a result of assembly time and maintenance constraints.

9.3 Material Selection

The materials used in the airframe construction are exclusively balsa wood and spruce. research of previous RPV designs overwhelmingly pointed to these materials as the best suited for this type of aircraft. Availability, cost, and ease of

manufacturing were also taken into consideration when choosing these materials. The materials selected for specific load carrying members was based upon optimization iterations in the FEM development program, and material weight trade-off analysis for each member.

Monokote, a heat shrink film, will be used for the skin of the aircraft. This material was chosen for its extremely high strength to weight ratio, availability, and its proven effusiveness in previous designs.

The material properties listed below are the same that were used in the input files for the structural modeling of the airframe, as used in SWIFTOS.

Material Properties			
	Balsa	Spruce	Monokote
Youngs Modulus	6.50E+03	1.30E+06	7700
Poisson's Ratio	0.08	0.08	0.2
Mass Density	0.0058	0.016	0.00349
Stress Direction and Limit			
XX (psi)	400	6.20E+03	2.40E+04
YY (psi)	600	4.00E+03	2.40E+04
XY (psi)	200	7.50E+02	2.40E+04

9.4 Landing Gear Design

The landing gear for Jeff consists of a steerable nosewheel and a main gear under the main wing. This tricycle configuration will be constructed of thin gage music wire and independently purchased wheel trucks. This type of wire is extremely resilient under buckling loads, and is intended to dissipate some of the energy upon landing impact as well as ease the translation of the landing loads across the lower portion of the fuselage. As stated previously, landing loads of up to 4 Gs are expected. The least-weight construction of the fuselage demands that the landing gear dissipate as much energy as possible so as not to overload the lower structure.

The secondary function of the landing gear will be to keep the pusher-propeller from striking the ground upon take-off rotation. For this reason the landing gear has been designed to keep the bottom of the fuselage 7 inches, and the tip of the propeller 3 inches from the runway. This long landing gear will also help facilitate dissipation of the landing loads.

10. Construction Plans

10.1 Major Assemblies

Construction of Jeff is set to begin immediately upon completion of the Draft Proposal and delivery of the airframe materials. The construction philosophy will one of parallel progression of the major airframe components. The wing, canard and fuselage will be constructed at the same time, all with a final deadline of 2 days before the Roll-Out date. Manufacture and assembly procedures will be directed by one supervisor to reduce tolerance discrepancies.

Mass production techniques will be employed (specifically jigging) in the manufacture of the wing and canard rib membranes as well as for the connecting posts and bulkhead caps of the fuselage. From the initial conception of this aircraft measures have been taken to insure that the manufacturing and assembly are simple. Measures such as the design of a rectangular fuselage, wing, and canard make jigging possible as well as reduce the assembly complications. The end result of this approach will be savings for the customer by reducing manufacturing costs.

After the construction of the airframe has been completed, the internal components such as motor, servos, and control actuation devices will be placed. Any structural reinforcement above and beyond the planned design will be instituted at this point. After the final approval of the airframe the monokote skin will be applied to all of the major assemblies. The deadline for this operation will be two days before Roll-Out. Cargo and maintenance access ports will be completed in the remaining days as well avionics and control systems ground tests will be performed in preparation of Taxi tests.

10.2 Complete Parts Count

The following tables are a complete parts listing of the airframe members.

Fuselage Parts List			
	Dimensions	Material	Number and Notes
Main Beam	1/8 x 1/8 x 50	Spruce	4
Beam Reinforcements	1/8 x1/8 x 15. 1/4	Spruce	2
Bulkhead Caps	1/8 x 1/8 x 8	Balsa	28 (14 top and 14 bottom)
Connecting Posts	1/8 x 1/8 x 4	Balsa	6
Connecting Posts	1/8 x 1/8 x 4	Spruce	14
Connecting Posts	1/8 x 1/8 x 3. 7/8	Spruce	6 between reinforced Main Beams
End Posts	1/8 x 1/8 x 4	Spruce	2
Angled Supports	1/8 x 1/8 x 5. 3/4	Balsa	6
Angled Supports	1/8 x 1/8 x 5. 3/4	Spruce	20
Torsional Supports	1/8 x 1/8 x 9. 1/4	Spruce	2
Bulkhead Membranes	1/16 x 8 x 4	Balsa	3 membranes
			Total Number of Members = 93

Main Wing Section			
	Dimensions (inches)	Material	Number and Notes
L.E. Spar Membrane	1/16 x 1/3 x 6	Balsa	8
Main Spar Membrane	1/16 x 1. 2/5 x 6	Balsa	8
T.E. Spar Membrane	1/16 x 1/2 x 6	Balsa	8
L.E. , Main ,T.E Spar Caps	1/8 x 1/8 x 48	Spruce	6
Main Spar Cap Reinforce	1/8 x 1/8 x 60	Spruce	1 (top)
	1/8 x 1/8 x 48	Spruce	1 (bottom)
L.E. Spar Reinforce	1/8 x 1/8 x 24	Balsa	1 (top)
Rib Membranes	1/16 x 2 x 12	Balsa	7 (size before contour)
Modular Wing Sections			
L.E. Spar Membrane	1/16 x 1/3 x 6	Balsa	12
Main Spar Membrane	1/16 x 1. 2/5 x 6	Balsa	12
T.E. Spar Membrane	1/16 x 1/2 x 6	Balsa	12
L.E. , Main ,T.E Spar Caps	1/8 x 1/8 x 36	Spruce	12
Modular Joint Rods	1/8 x 1/8 x 8	Spruce	8
Rib Membranes	1/16 x 2 x 12	Balsa	14
			Total Number of Members = 110

Canard Parts Count			
	Dimensions (inches)	Material	Number and Notes
L.E. Spar Membrane	1/16 x 1/4 x 6	Balsa	9
Main Spar Membrane	1/16 x 5/8 x 6	Balsa	9
T.E. Spar Membrane	1/16 x 1/4 x 6	Balsa	9
L.E. , Main ,T.E Spar Caps	1/8 x 1/8 x 54	Spruce	6
Main Spar Cap Reinforce	1/8 x 1/8 x 54	Balsa	1 (top)
	1/8 x 1/8 x 24	Balsa	1 (bottom)
L.E. Spar Reinforce	1/8 x 1/8 x 16	Balsa	1 (top)
Rib Membranes	1/16 x 1 x 6	Balsa	10 (size before contour cut)
			Total number of Members = 46

11. Environmental Impact and Safety Issues

11.1 Disposal Costs for Each Component

Increasing demand for environmental responsibility on the part of manufacturers dictates the presence of impact and disposal contingencies in this proposal. The major concerns, from an environmental aspect, are the disposal of old airframes, skins, and avionics within the aircraft.

The canard, wing and fuselage all contain certain avionics packages. Batteries, servos, actuation rods, etc. The working lifetime of all of the avionics packages range far beyond the structural life time of Jeff. Therefore, the disposal concerns for these components are limited by their frequency of occurrence. In most cases the avionics packages will be transferred between new and old aircraft until this is deemed a risk. At that point the salvageable parts of the avionics will be cannibalized and used for replacement and maintenance pieces. The remaining parts will be sold to recycling centers for further disassembly. The disposal of the batteries also poses a special problem due to the fact the they contain potentiality dangerous amounts of heavy metals. The only responsible disposal practice in this case is the contracting of a battery disposal group to take over the disposal of the batteries.

The Canard, wing, and fuselage structures are are constructed of wood, monokote and a CA adhesive. These should pose the least difficulty in disposal. The monokote skin may be stripped off the frame, collected and integrated in to a comprehensive plastics recycling program. These programs typically use the waste plastics in the production of permanent community enhancing items, such as park benches or outdoor park equipment. This practice could also be applied to the construction of hangers or storage facilities for the overnight packages. Beams and stringers from the aircraft can be reinvested into the company in this fashion. Inspection of the individual beams should insure the use of sound

members in this construction. Those beams which are determined unable to handle further loading can be incinerated in a community plant. Special attention should be paid to the temperatures of the furnace so that the CA adhesives used in the joints are completely disassociated.

The landing gear for Jeff may also be recycled responsibly. The music wire used can be included in the used avionics packages and sold to an electronics recycling group as stated above. There are a multitude of possible recycling uses for the used aircraft tires. The is even a process available today that can separate the petroleum byproducts used in the production of the tires and reuse them in further production. The recycling program entered into in this case is purely a matter of preference.

The main philosophy behind the disposal of the aircraft is the avoidance of land filling. The exorbitant costs of land fill disposal as well as its negative public response and environmental impact, point to a solid recycling policy for disposal. Manufacturing wastes may also be disposed of in this same program. Those corporations that are able to develop a comprehensive recycling policy now will not be susceptible to the growing power of the environmental platform down the road.

11.2 Noise Characteristics

One topic of frequent discussion in aircraft design is that of noise reduction. The reduction of mechanical noise (vibration) translation from the motor to the airframe will be addressed using foam rubber washers in on the motor mount itself. These measures should be sufficient to inhibit and mechanical failures do to excessive vibration in an aircraft of this size.

Audible noise reduction is also a concern in the aircraft design and has been responded to by placing the motor mount in the fuselage directly. By

isolating the motor in the rear compartment of the fuselage, the audible noise pollution will be reduced by using the frame and skin itself as a buffer. This is somewhat of a modified cowling, except that in this case the cowling is an integral part of the fuselage structure. Depending upon the sensitivity of the flight areas, an actual cowling may be applied as a modification in further models.

12. Economic Analysis

12.1 Production Costs

The production costs for the construction of Jeff were minimized in order to maximize the end of year profit. Table 12.1 displays the planned cost break down for each major component of the plane excluding production time.

COMPONENT	COST ($)
Materials (wood, glue, monokote)	135
Propulsion (batteries, motor)	134
Controls (servos, radio, elevons)	200

Table 12.1 Plane Cost Per Component

The production of the plane will be planned out very carefully in order to minimize the production cost and time. The number of man hours planned to produce Jeff is 100 hours. Therefore the total unit production cost will be $287,600. This value will be further minimized upon completion of construction. The technology demonstrator is the first prototype built. Thus upon further production models, the process and materials needed to build the plane will become more efficiently used to lower the cost per plane. Figure 12.1 shows the cost breakdown relative to the total cost of the plane. As can be seen, the production cost accounts 34% of our cost. Thus, it is important to minimize the time needed to produce the plane. This will require a detailed and efficient production outline before construction begins.

FIGURE 12.1
PRODUCTION COST BREAKDOWN

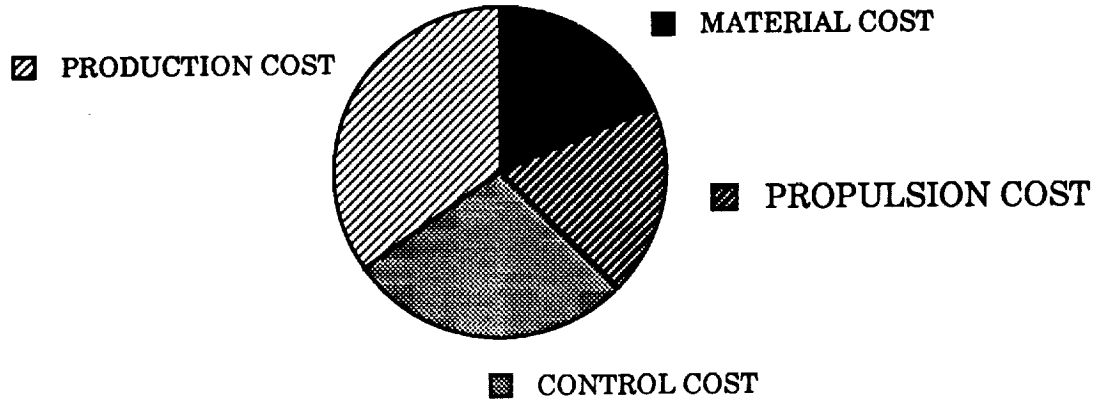

12.2 Maintenance Costs

Jeff's ability to compete with other transports will require the plane to be both economical to fly and to service. The maintenance cost per flight is relatively small compared to the total cost per flight. However, the ability to perform the maintenance efficiently and effectively will increase profit. Table 12.2 examines the average maintenance cost in refueling and serviceably. Furthermore it details the time when certain aircraft will need to be checked for fatigue. From the fatigue diagram, 700 cycles was chosen to be the limit were the structure would be considered unsafe to fly. Thus, due to a planes specific route structure, it will need structural repairs at an earlier time than the rest of the fleet

Maintenance			Planes	Days Fatigue
Service Time	2 minute		2	200
Men needed	1 man		4	280
MCPF	$100		13	350

Table 12.2 Maintenance Cost

12.3 Operation Costs

The operation costs of Jeff in Aero World are governed by the cost of fuel. Figure 12.2 shows the percent breakdown of the cost per flight of Jeff.

Figure 12.2
Cost Per Flight Breakdown

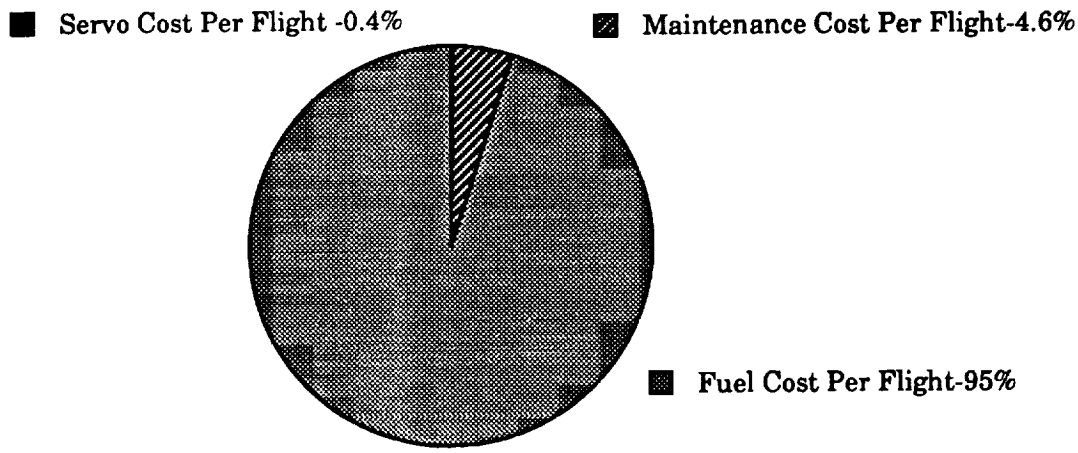

The variation in the price of fuel from $5 - $20 a milli-amp hour will have a significant impact in to the operation of the fleet and price charged per cu. in. Figure 12.3 shows the sensitivity to fuel price to the total cost of the fleet. This graph will help investors plan their ability to purchase a fleet if the projected cost of fuel is $X.

This high cost of fuel per flight necessitates that the current draw be as low as possible. Unfortunately our 12" diameter prop is needed for takeoff and thus our current draw is high at 5.2 amps. The higher the current draw, the more fuel burned and the lower the profit. Since the cost of fuel can fluctuate by such a large margin, an average value of 12.5 $/milli-amp hr. was used in forecasting the profit margins and cost of the fleet.

Figure 12.3
The Fleet Cost Per Fuel Rate

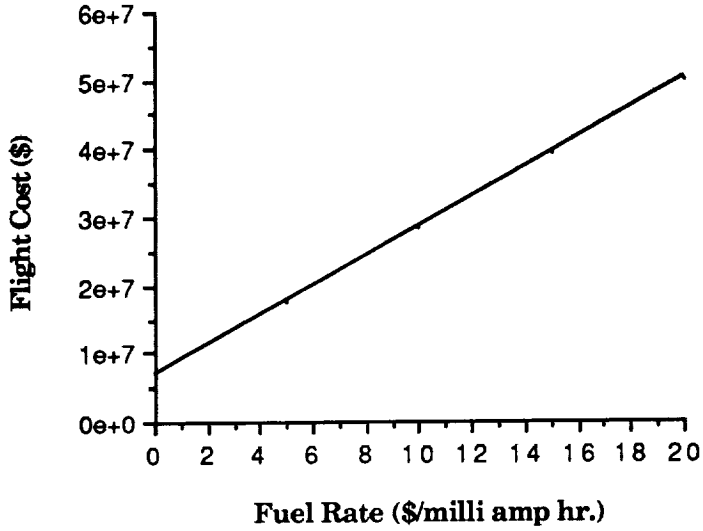

In determining the price that will be needed to charge costumers in order to make a profit, a detailed economic analysis was performed on the operation costs of flying the fleet for its whole life span. The cost per cubic inch needed to break even is $3.72. This computation was calculated by finding the average time for a typical flight. The average time is dependent upon the route system that was chosen in Section 2. Thus, the average fuel cost per flight was calculated. A different way to base the cost per cu. in. was to use the maximum design range and the time it takes to accomplish the task. The differences are staggering. The Maximum range method requires a price of $9.95 just to break even. In order to realistically determine the total profits at the end of the year, the Maximum range method was neglected. Table 12.3 lists several important profit analyses data for the operation of Jeff. The data source spreadsheet can be found in Appendix B.

The return on investment by charging $4 per cu. in. is 26.59%. This value, as well as the profit, can change depending on what the competition charges.

Cargo Cost ($ / cu. in.)	$3.72
Charge Price for Cargo ($ / cu. in.)	$4.00
Single Flight Gross Income	$5,600
Single Flight Operating Cost	$2133
Single Flight Profit	$3466
Number Flights to Break Even	9762
Number of Days to Break Even	227
End of Year Profit	$12,261,388
Return on Investment	26.59%

Table 12.3 Economics of Jeff

Figure 12.4 plots the return on investment with the price of cargo. The graph is non-linear and as the price of cargo is increases, the percent increase on the return of investment decreases.

FIGURE 12.4
THE SENSITIVITY OF THE RETURN ON INVESTMENT DUE TO CARGO PRICE

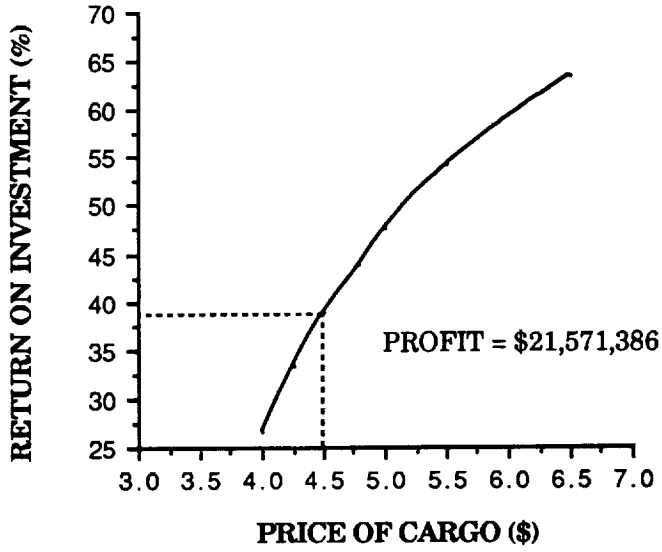

In order to keep competitive the range of cargo pricing will be between $4.00 and $5.00. This will allow for a very lucrative return on investment between 25%-

45%. Furthermore, since the cost of cargo depends the most on how far it travels a price scale can be developed for the Northern Hemisphere. This scale be derived by taking the average time to fly to one island, find the fuel used, and take into account how many planes fly to the island and how many cycles are flown each day. Once this has been done, the rate will just be determined by finding at what price the return on investment is 20% or greater. Table 12.4 gives the current price list the would be charged for the Aero World Northern Hemisphere. This idea could be used for expansion purposes to the lower hemisphere as well.

Area	Avg. Time	Fuel Used	Cargo Price	Profit	Inv. Return
City A,B	3.36 min	290 mA	$6.25	$2,458,145	17.49%
Main Land	1.29 min	111 mA	$3.00	$5,058326	29.66%
City L, M, N	1.74 min	150 mA	$4.00	$5,157,217	33.92%

Table 12.4 Price Rate Per City

The coat breakdown for each component as well as the time needed to build the technology demonstrator can be seen in Table 12.5.

Part	Cost ($)	Time (Hr.)
Fuselage	32	17
Canard	19	10
Wing	52	60
Vertical Stabilizer	7	2
Landing Gear	25	5
Elevons	10	10
Miscellaneous	8	0

Table 12.5 Price and Time Per Part

13. Results of Technology Demonstrator Development

13.1 Complete Configurational Data

The construction of the technology demonstrator was completed, for the most part, according to the original design. The various components were sized as follows:

Wing:	airfoil	Wortman FX63-137
	chord	12.0 in
	span	
	main section	48.0 in
	outboard sections	36.0 in (each)
	total	120.0 in
Canard:	airfoil	Wortman FX63-137
	chord	6.6 in
	span	
	main section	60.0 in
	outboard sections	3.0 in (each)
	total	66.0 in
Fuselage:	width	
	inner	8.0 in
	outer	8.25 in
	height	
	inner	4.0 in
	outer	4.25 in
	length	
	main body	46 in
	tail section	4.0 in
	nose	1.5 in
	total	51.5 in
	cargo hold	1408 in^3
Vertical Tails		
	height	12.0 in
	width	8.0 in
Landing Gear:		
	nose wheel	
	diameter	3.5 in
	height	7.0 in
	main gear	
	diameter	3.5 in
	height	7.0 in
	spacing	12.0 in

Propulsion System		
	propeller	Top Flight 12-6
	engine	Astro 15
Avionics	batteries	12 @1200mA-hr each
	3 servos, system battery, receiver, speed controller	

For the actual flight test we chose to fly the technology demonstrator at its lightest possible weight, and thus no payload was carried in the aircraft. However, the final weight of the empty technology demonstrator was considerably higher (approximately 35 %) than the original estimated weight. This difference was due in part to the addition of monokote to all of the structural components, as the monokote provided a greater contribution to the overall weight than originally estimated. Also, many of the avionics weighed more than the weights given in for the preliminary estimation. The batteries, in particular, weighed 22% more than expected due to the change from 1000 to 1200mA-hr batteries. (This change was due only to the result of a technician error.) The final weights of the various components are given in Table 13.1.

Determination of the center of gravity of the technology demonstrator was extremely important, as an adequate static margin was required for good flight performance. Initially the center of gravity was determined to be 29.6 in from the nose of the aircraft without the addition of ballast (27.6 in from the nose wall of the fuselage). With the neutral point located at 31.4 in the static margin was acceptable at 15.08%. However, when the plane was taxied and actually lifted off, its performance indicated that these calculations were not accurate and that the static margin was not acceptable. Later testing showed the actual center of gravity to be 30 in from the front of the fuselage. Thus, the center of gravity needed to be pulled forward considerably. To accomplish this task, the battery pack was moved as far forward as possible and ballast was added to the nose of the aircraft. The actual center of gravity was then determined by balancing the

technology demonstrator on a metal rod. With approximately 4.25 oz of ballast in the front of the fuselage the center of gravity did appear to be at the required 27.5 in from the front of the fuselage. Thus 5 oz of ballast in the form of a lead plate were secured to the nose wall for a center of gravity at 26.5 in.

Component	Weight (oz)	Weight Percentage	CG Location (in from nose wall)
Fuselage	23.63	24.03	32.0
Wing	14.18	14.42	39.5
Canard	6.17	6.28	7.0
Vertical Tails	0.74 (each)	0.76 (each)	40.0
Batteries	17.60	17.90	6.5
Servo #1	0.76	0.77	6.0
Servo #2	0.76	0.77	39.25
Servo #3	0.76	0.77	41.7
Receiver	0.99	1.00	39.25
System Battery	2.15	2.19	39.25
Speed Controller	1.76	1.79	44.0
Nose Wheel	1.50	3.66	0.0
Main Gear	6.14	6.24	42.0
Engine and Mount	10.67	10.85	47.0
Propeller	0.71	0.72	50.5
Ballast	7.00	7.12	0.25
Payload	0.00	0.00	0.0
Total	98.40	100	26.0

Table 13.1 Technology Demonstrator Component Weights and CG Locations

After one flight test, however, even more ballast was added for a total of 7 oz of ballast. Center of gravity was thus moved to approximately 26 in from the nose board. According to the neutral point calculations, the neutral point was located at approximately 31.4 in from the nose (29.9 in from the nose board) for a large static margin of 32.5%. However, this calculation may not be exact due to difficulties in determining the true neutral point. Final component center of gravity locations are given in Table 13.1.

13.2 Flight Test Plan and Test Safety Considerations:

The flight test plan for this RPV basically was determined by the design requirements. The aircraft had must be able to take off in less than 60 ft, complete a figure 8 on the length of a football field, maneuver a turn in less than a 60 ft radius, and then land. The flight tests are to be held in the Loftus Sports Center on the University of Notre Dame campus. This is an indoor track and practice football field. Indoor flight was specified so that all of the competing design teams could fly under the same environmental conditions.

Jeff's three components fuselage,wing and canard, were transported from the construction area to the test are in a medium sized truck. There the Demonstrator was assembled, and checked for any last minute problems. In any maiden flight situation safety of the aircraft and spectators was of utmost importance. the demonstrator was subjected to a number of pre-flight criteria before being allowed to taxi. Avionics, landing gear, control surfaces, and wing-fuselage junctions were all checked prior to takeoff. A drop test of the flight ready aircraft was done to insure structural integrity. Spectators were also required to stand behind a large net at the end of the field incase the were in-flight control problems. Only upon satisfactory adherence to all of these requirements were the aircraft allowed to attempt flight.

13.3 Manufacturing Details

The manufacturing and construction of the Technology Demonstrator was approached utilizing a plan for the parallel production of the major components. The design team was broken down into groups responsible for the construction of the fuselage, main wing, and canard airframes. Each of these groups were then to be supervised by a Construction Manager in order to affect continuity of design and adherence to the proposed structural designs.

In theory, this procedure would seem to provide for all considerations in the limited production time allowed. In reality, a number of problems arose which severely limited the application of the construction plan, and disrupted the organization of the groups. What resulted was many extra man-hours expended in duplication of tasks, and useable time wasted in on the spot organization. The largest problem that arose from the disintegration of the original plan was the lack of a universally understood picture of the design of the airframe and the order in which the construction tasks needed to be completed.

In this format it would be impossible to discuss all of the minute details which contributed to the manufacturing headaches that occurred along the way. But, one factor is noteworthy in this regard. Perhaps the most important factor which dissolved the original plan of action was the availability of construction supplies. It was assumed that the local craft store would be able to accommodate all of the material needs at any given moment. This was not the case. The relative uniqueness of the dimensions of wood beams specified in the design created problems with the supply. This immediately interrupted the parallel production of the airframe components by actually causing some competition between the build groups as to who would use the available material. In any case there were a number of times where production was completely halted due to the lack of proper materials. This problem may have been avoided by formulating a

pre-production estimate of needed materials a number of weeks in advance of the final design. At that point, stocks could have been checked and rough advance orders placed if inadequacies were found.

The interruptions in the material supply broke the continuity of the construction plan and had some serious side effects. Individual build groups had to work on different schedules than other groups and therefore lost contact with the progress of the aircraft as a whole. In this case some of the subtleties of the design were lost due to the closed view each group had on the overall design.

Valuable information was also gained in the physical arena of the construction process as well as the organizational. The tools that were on hand were very adequate for the job. Complete construction of the airframe was afforded by access to a belt sander, reciprocating table saw, drill and hobby craft kit. It was also determined through trial and error that the very thin CA glue used in conjunction with baking soda for joint filler worked much better than the Ca glues advertised for gap filling properties. The watery nature of the CA glue used allowed for faster drying times (almost instantaneous) and better penetration into the joints. Splices in the beams used to extend their lengths using this glue also held up well. In the test cases under load, the spliced joints never failed.

Specifically in the fuselage structure, bulkheads used for torsional stiffness were modeled in balsa. However, in the actual case, due to the fact that extra mountings for servos and landing gear assemblies were attached at these bulkheads. Plywood was used, instead of balsa, in all but one of these cases because of the softness of the balsa and the danger of pull-through of screws and bolts. This design change added considerable weight to the fuselage but was absolutely needed to insure the integrity of the attached subsystems.

In both the main wing and canard designs a solid trailing edge was needed to support the monokote skin. The TE spar was placed at 66% chord and a traditional TE spar was left out for weight reduction. The inclusion of a solid TE could not be avoided do to the constraints of monokote application but also because of the fragility of the ribs. The application of the monokote also necessitated some innovation on the leading edge also. With the LE spar at 10% chord, there was no support structure for the skin to follow the airfoil contour. Instead of placing another beam at the chord tip, paper cut outs were taped to the LE and the skin was applied over the top. This gave the leading edge the correct shape as well as adequate stiffness (do to the laminate properties) without the weight of an extra beam running the entire span.

For purposes of the flight tests, the modular wing sections were also modified. The mission had required that the entire aircraft fit in a 5ft x 2ft x 2ft box for transportation purposes. In the case of actual production aircraft this would be the case. Bu for the test case the modular wing sections were epoxied to the main section to reduce instability at the tip. There was some play in the joint just prior to the flight tests so in the interest of safety and controllability these sections were hard pointed to the rest of the wing.

13.4 Flight Test Results

Jeff crashed during the completion of the first turn in the flight test. Although the takeoff and the turn appeared to go well in terms of stability and control, as the pilot tried to regain the altitude that was lost during the turn, the plane nosed up causing the canard to stall. Once the canard stalled the nose-down moment produced by the wing lying behind the center of gravity resulted in a pitch-down that was unrecoverable given the low altitude that this occurred. This resulted in Jeff nose-diving into the ground.

After viewing the films of the flight test some important conclusions can be drawn to aid those interested in building canard configured planes in the future. First in trying to attain proper trim it is recommended the incidence angle difference between the wing and the canard not be too large. In our case this was a major problem. Jeff's canard was set at 4 degrees whereas the wing was set at -2 degrees. This situation leaves very little room for error with the pilot as he tries to regain altitude coming out of the turn. If the pilot tries to increase the angle of attack of the plane too much the canard will stall resulting in a npitch-down condition. If one ends up with a configuration as ours then it is recommended that the pilot at least be warned about this danger and that he be careful in the degree with which he pulls back on the throttle coming out of turns. In conclusion, it is recommended that future canard configured planes construct their planes such that the canard is not set at such a high incidence angle when compared to that of the wing.

Finally, another concern that was noticed in reviewing the films was the apparent high takeoff velocity during takeoff. Even though Jeff was flying fairly heavy (98 ounces) it seemed as if Jeff may have been in danger of exceeding acceptable flight speeds (V_{flight}>30 ft/s). Although we cannot be certain whether this is true it should have been checked so that we could investigate some of the reasons as to why this happened if this was indeed the case.

Appendix A

	A	B	C
1	Parameter	4/7/92	5/6/92
2	*[all distances relative		
3	to common reference		
4	and in common units]*		
5			
6	DESIGN GOALS:		
7	V cruise	28 ft/s	28 ft/s
8	Altitude cruise	25 ft	25 ft
9	Turn radius	60 ft	60 ft
10	Endurance	8 min	8 min
11	Max Payload Volume	1400 in^3	1400 in^3
12	Range-max payload	10,000 ft	10,000 ft
13	Payload at Max R (wgt)	35 oz	35 oz
14	Range-min payload	12,000 ft	12,000 ft
15	Weight (MTO)	< 7 lb (112 oz)	< 7 lb (112 oz)
16	Design life cycles	700	700
17	Aircraft sales price	$400,000	$400,000
18	Target cost per In3 payload	$5.00	$5.00
19	Target cost per oz payload	$5.00	$5.00
20			
21	BASIC CONFIG.		
22			
23	Wing Area	10 ft^2	10 ft^2
24	Weight(no payload)	73.1 oz	98.40 oz
25	Weight(maximum)	108.1 oz	126.40 oz
26	Wing loading(max Wgt)	.676 lb/ft^2	.79 lb/ft^2
27	Length	50 in	51.5 in
28	Span	60 in	60 in
29	Height	4 in	4.25 in
30	Width (fuselage)	8 in	8.25 in
31	Location of ref. axis origin	base of nose	nose wall base
32			
33	WING		
34	Aspect Ratio	10	10
35	Span	60 in	60 in
36	Area	1440 in^2	1440 in^2
37	Root Chord	12 in	12 in
38	Tip Chord	12 in	12 in
39	Taper Ratio	1	1
40	C mac - MAC	-0.175	
41	Leading edge sweep	0°	0°
42	1/4 chord Sweep *	0°	0°
43	Dihedral	0°	0°
44	Twist (washout)	0°	0°
45	Airfoil section	FX63-137B	FX63-137
46	Design Reynolds number	150000	150000
47	t/c		
48	Incidence angle (root)		neg 2°
49	Hor. pos of 1/4 MAC	39.7 in	39.5 in
50	Ver. pos of 1/4 MAC	4.25 in	4.5 in
51	e- Oswald efficiency	0.8	0.8
52	CDo -wing	0.007	0.007
53	CLo - wing	0.52	0.52
54	CLalpha -wing	0.09 deg^-1	0.09 deg^-1
55			
56	FUSELAGE		
57	Length	50 in	51.5 in
58	Diameter - max	8 in	8 in
59	Diameter - min	4 in	4 in
60	Diameter - avg	-	-
61	Finess ratio	0	0
62	Payload volume	1408 in^3	1408 in^3
63	Total volume	1600 in^3	1600 in^3
64	Planform area	400 in^2	425 in^2
65	Frontal area	32 in^2	35 in^2
66	CDo - fuselage	0.00242	0.00242
67	CLalpha - fuselage	0.09 deg^-1	0.09 deg^-1

	A	B	C
68			
69	EMPENNAGE		
70			
71	Canard		
72	Area	2.0 ft^2	3.0 ft^2
73	Span	53.67 in	66 in
74	Aspect ratio	10	10
75	Root chord	5.37 in	6.6 in
76	Tip chord	5.37 in	6.6 in
77	Taper ratio	1	1
78	L.E. sweep	0°	0°
79	1/4 chord sweep	0°	0°
80	Incidence angle	7	4°
81	Hor. pos. of 1/4 MAC	6 in	7 in
82	Ver. pos. of 1/4 MAC	.5 in	neg 0.25 in
83	Airfoil section	FX63-137B	FX63-137
84	e - Oswald efficiency	0.8	0.8
85	CDo -horizontal	0.0016	0.0016
86	CLo-horizontal	0.52	0.52
87	CLalpha - horizontal	0.09 deg^-1	0.09 deg^-1
88	CLde - horizontal	2.369	2.369
89	CM mac - horizontal	-0.175	-0.175
90			
91	Vertical Tail		
92	Area	1.5 ft^2	1.5 ft^2
93	Aspect ratio	0.75	0.75
94	Root chord	8 in	8 in
95	Tip chord	8 in	8 in
96	Taper ratio	1	1
97	L.E. sweep	45°	45°
98	1/4 chord sweep	45°	45°
99	Hor. pos. of 1/4 MAC	1.5 in	1.5 in
100	Vert. pos. of 1/4 MAC	1.5 in	1.5 in
101	Airfoil section	Flat Plate	Flat Plate
102			
103	SUMMARY AERODYNAMICS		
104			
105	Cl max (airfoil)	1.6	1.6
106	CL max (aircraft)	1.39	1.3
107	Lift curve slope (aircraft)	.08 deg^-1	.078 deg^-1
108	CDo (aircraft)	0.0185	0.0185
109	Efficiency - e (aircraft)	0.73	0.73
110	Alpha stall (aircraft)	8°	8°
111	Alpha zero lift (aircraft)	4 °	4°
112	L/D max (aircraft)	15.4	17.5
113	Alpha L/D max (aircraft)	0°	0°
114			
115	WEIGHTS		
116			
117	Weight total (empty)	73.10 oz	98.4 oz
118	C.G. most forward-x&y	31.24 in	26 in
119	C.G. most aft- x&y	34.23 in	26 in
120	Avionics	4.75 oz	24.78 oz
121	Payload (max)	35.00 oz	35.00 oz
122	Engine & Engine Controls	12.07 oz	14.58 oz
123	Propeller	2.00 oz	0.71 oz
124	Fuel (battery)	14.76 oz	17.60 oz
125	Structure	32.50 oz	45.46 oz
126	Wing	16.00 oz	14.18 oz
127	Fuselage/emp.	11.50 oz	23.63 oz
128	Landing gear	7.00 oz	7.64 oz
129	lcg - max weight	31.24 in	26 in
130	lcg - empty	34.23 in	26 in
131			
132	PROPULSION		
133	Type	Astro 15	Astro 15
134	Number	1	1

	A	B	C
135	Placement	48 in	47 in
136	Pavil max @engine	160 W	160 W
137	Preq cruise	32 W	30.5 W
138	Max. current draw	14 mA	14 mA
139	Ccruise current draw	5.2 mA	5.05 mA
140	Propeller diameter	12 in	12 in
141	Propeller pitch	6°	6°
142	Number of blades	2	2
143	Max. prop. rpm	10000	10000
144	Cruise prop. rpm	7200	7200
145	Max. thrust	6.8 lb	4.83 lb
146	Cruise thrust	1.2 lb	1.1 lb
147	Battery type	N100 SRC	N120 SRC
148	Number	12	12
149	Individual capacity	1000 mA	1200 mA
150	Individual voltage	1.2 V	1.2 V
151	Pack capacity	1000 mA	1200 mA
152	Pack voltage	14.4 V	14.4 V
153			
154	STAB AND CONTROL		
155	Neutral point	33.15 in	31.4 in
156	Static margin %MAC	15.91%	32.50%
157	Hor. canard volume ratio	0.421	0.421
158	Vert. tail volume ratio	0.143	0.143
159	Elevon area	3.00 ft^2	1.5 ft^2
160	Elevon max deflection	±10°	±10°
161	Rudder Area	-	-
162	Rudder max deflection	-	-
163	Aileron Area	-	-
164	Aileron max deflection	-	-
165	Cm alpha	5.765 deg^-1	5.765 deg^-1
166	Cn beta	-	-
167	Cl alpha canard	0.11 deg^-1	0.11 deg^-1
168	Cl delta e canard	2.369	2.369
169			
170	PERFORMANCE		
171			
172	Vmin	25 ft/s	20.8 ft/s
173	Vmax	30 ft/s	30 ft/s
174	Vstall	20.8 ft/s	20.8 ft/s
175	Range max - Rmax	21,492 ft	22,500 ft
176	Endurance @ Rmax	767 s	778 s
177	Endurance Max -Emax	767 s	778 s
178	Range at @Emax	21,492 ft	22,500 ft
179	ROC max	2.8 ft/s	2.9 ft/s
180	Min Glide angle	3.7°	3.7°
181	T/O distance	23 ft	20 ft
182	T/O rotation angle	-	0°
183	Landing Distance	-	30 ft
184	Catapult Range	-	-
185			
186	SYSTEMS		
187			
188	Landing gear type	Tricycle	Tricylce
189	Main gear position	42 in	42 in
190	Main gear length	7 in	7 in
191	Main gear tire size	3.25 in	3.5 in
192	Nose/tail gear position	2 in	0 in
193	N/t gear length	7 in	7 in
194	N/t gear tire size	3.25 in	3.5 in
195	Engine speed control	Futaba	Futaba
196	Control surfaces	elevons	elevons
197			
198	TECH DEMO		
199			
200	Payload volume		1408 in^3
201	Payload Weight		0.00 oz

	A	B	C
202	Gross Take-Off Weight		6.15 lb (98.4 oz)
203	Empty Operating Weight		6.15 lb
204	Zero Fuel Weight		80.8 oz
205	Wing Area		10 ft^2
206	Canard		3.03 ft^2
207	Vert Tail Area		1.5 ft^2
208	C.G. position		26 in
209	1/4 MAC position		39.5 in
210	Static margin %MAC		32.50%
211	V takeoff		24.6 ft
212	Range max		22,500 ft
213	Endurance max		778 s
214	V cruise		28 m/s
215	Turn radius		60 ft
216	Airframe struct. weight		45.46 oz
217	Propulsion sys. weight		11.38 oz
218	Avionics weight		24.78 oz
219	Landing gear weight		7.64 oz
220	Est. Catapult range		-
221			
222	ECONOMICS:		
223			
224	unit materials cost	$135	$175
225	unit propulsion system cos	$134	$134
226	unit control system cost	$200	$200
227	unit total cost	$469	$509
228	scaled unit total cost	$187,600	$203,600
229	unit production manhours	100	160
230	scaled production costs	$100,000	$160,000
231	total unit cost	287600	$363,600
232	cargo cost ($/in3)	$3.72	$3.88
233	single flight gross income	$5,600	$5,600
234	single flight op. costs	$2,133	$2,133
235	single flight profit	$3,466	$3,466
236	#flights for break even	9762	10179

Range Versus Payload

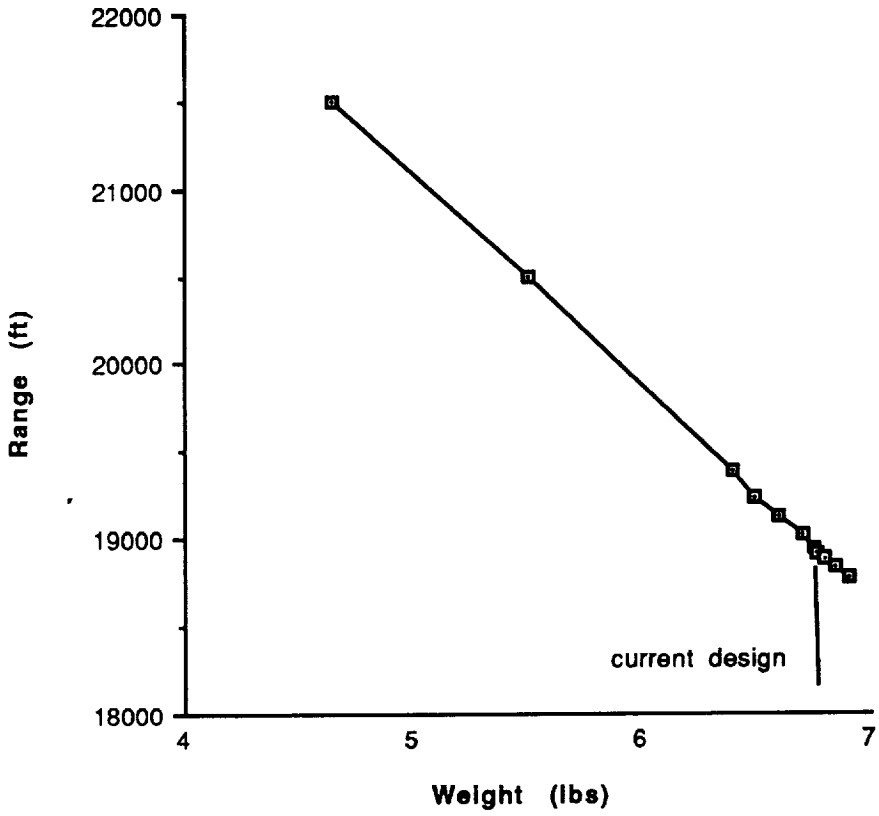

Airfoil Data

FX 63-137

Reynolds Number		Test Conditions	
6.0×10^4	———	Tunnel:	IAG Stuttgart #2
8.3×10^4	.....	Date:	1980
8.8×10^4	.....	Test:	2-D
1.0×10^5	.....	Turbulence:	0.08%
2.0×10^5	.....	Surface:	Smooth

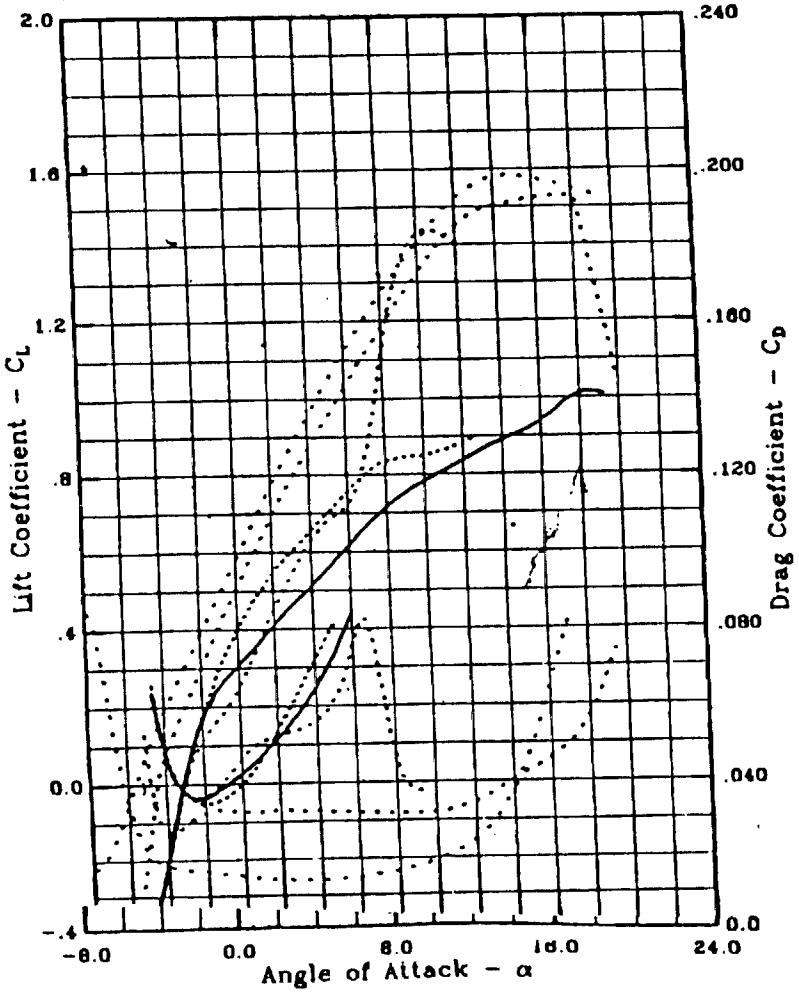

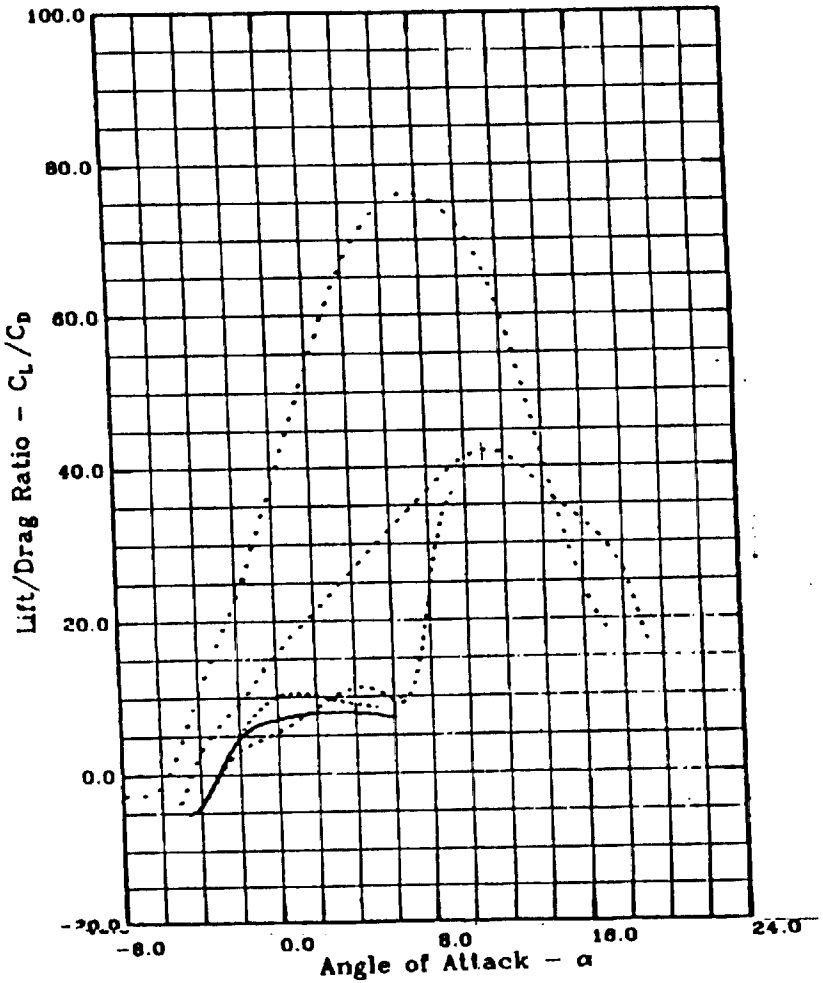

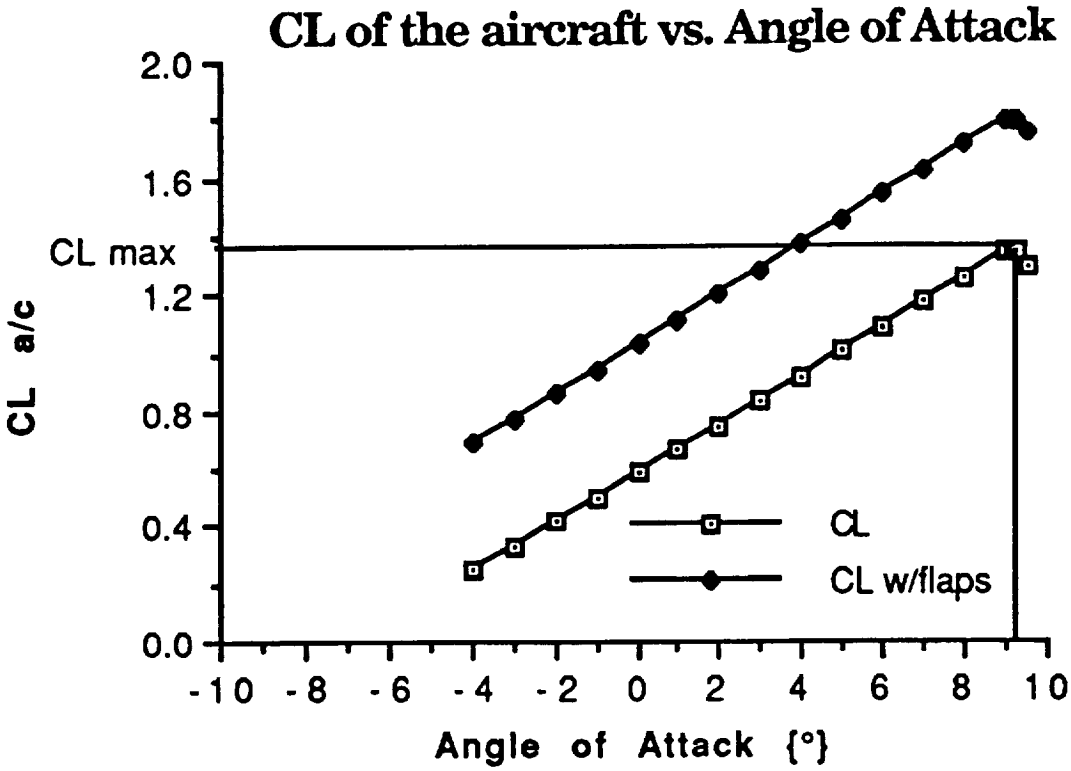
CL of the aircraft vs. Angle of Attack
2.0
1.6
CL max
1.2
0.8
0.4
0.0
CL a/c
-10 -8 -6 -4 -2 0 2 4 6 8 10
Angle of Attack {°}
CL
CL w/flaps

Drag Polar

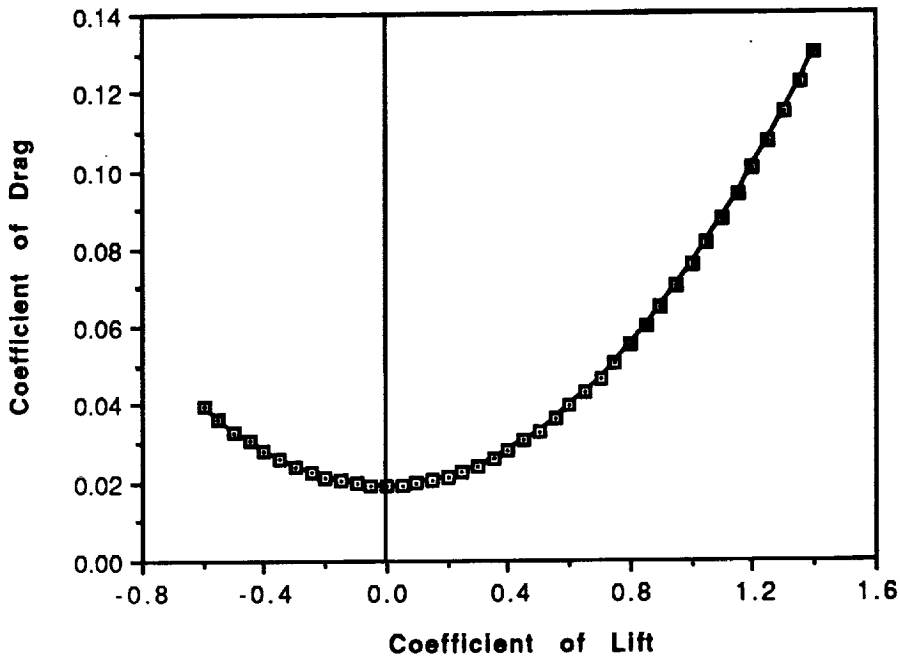

Component	$C_{D\pi}$	A_{π} (ft^2)	% of Total Drag
Fuselage	.110	0.22	14.26
Wing	.007	10.0	40.93
Landing Gear	.017	0.06	5.96
Canard	.008	2.00	10.52
Vertical Tail	.008	1.50	7.01
Elevons (deflected)	.03	1.50	26.31

Component Drag Breakdown

L/D for the Aircraft vs. Angle of Attack

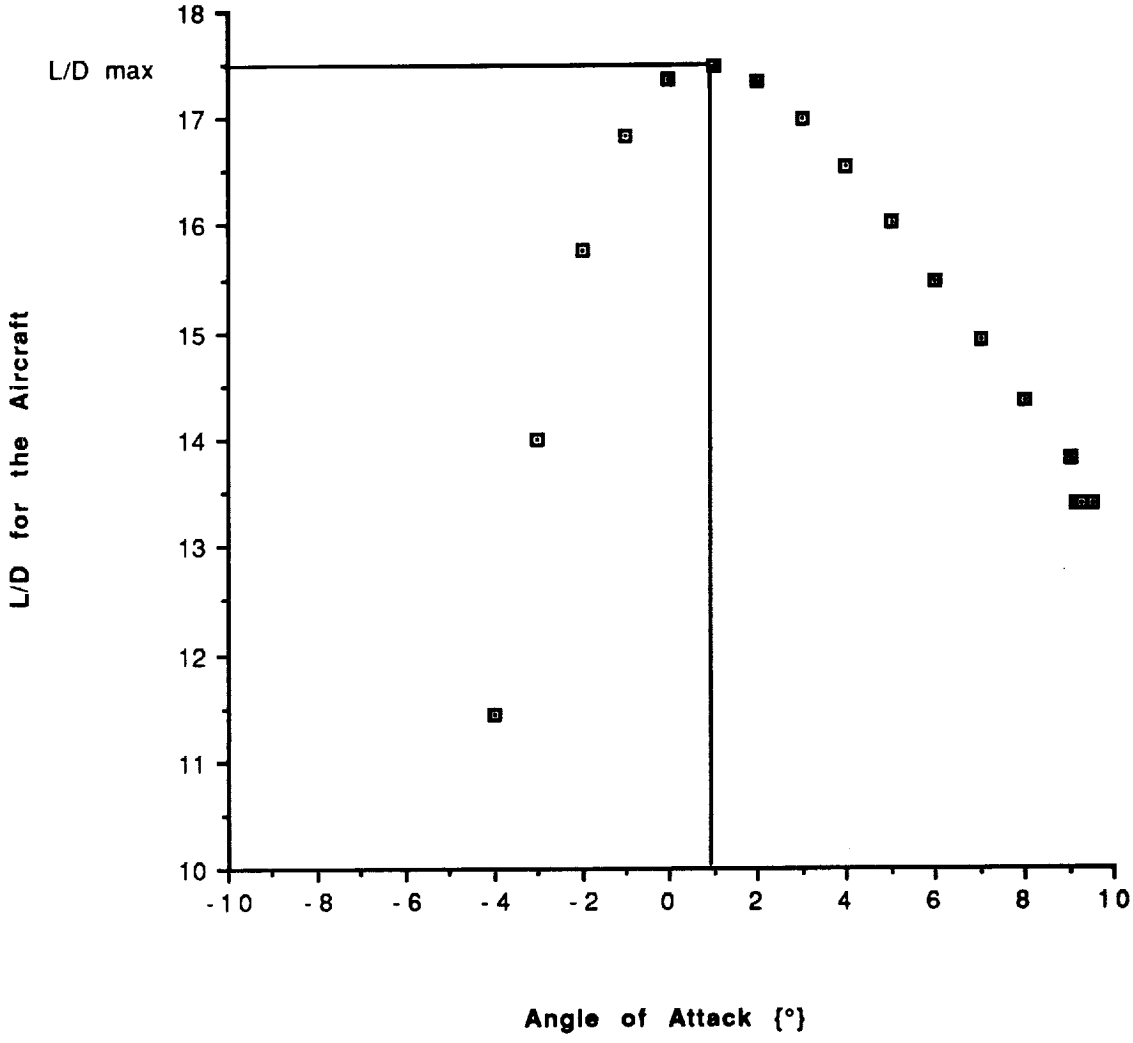

Effect Of Cargo Loading Condition On Moment Coefficient

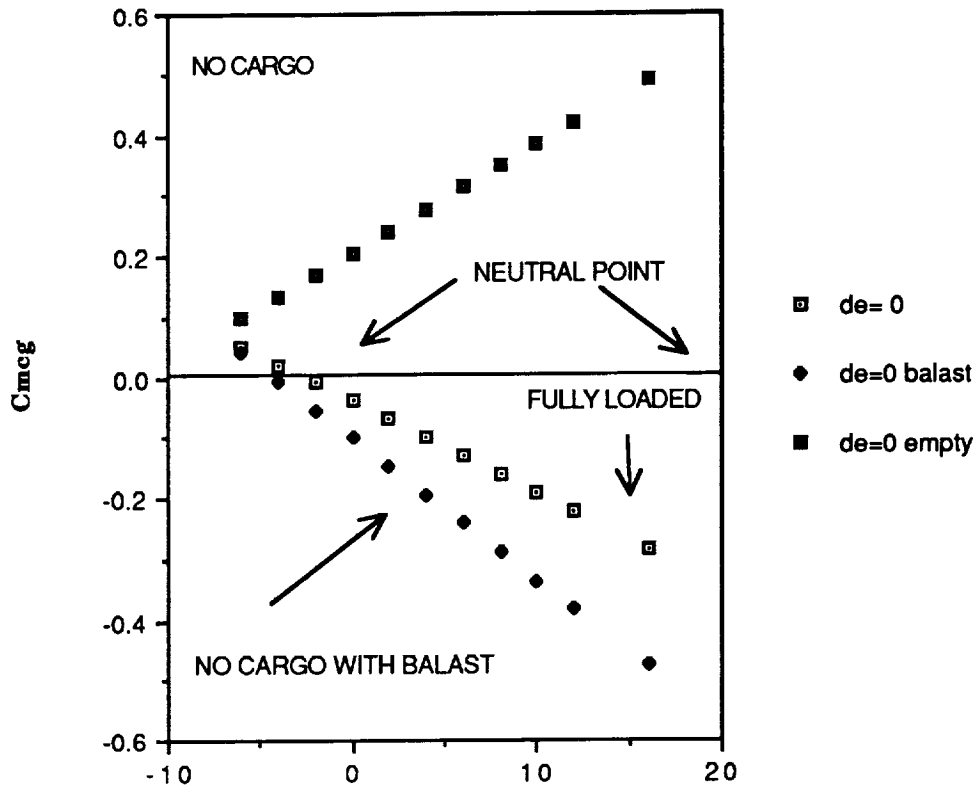

ALPHA (DEG)

Power Available and Required for Various Voltage Settings for the Top Flight 12-6

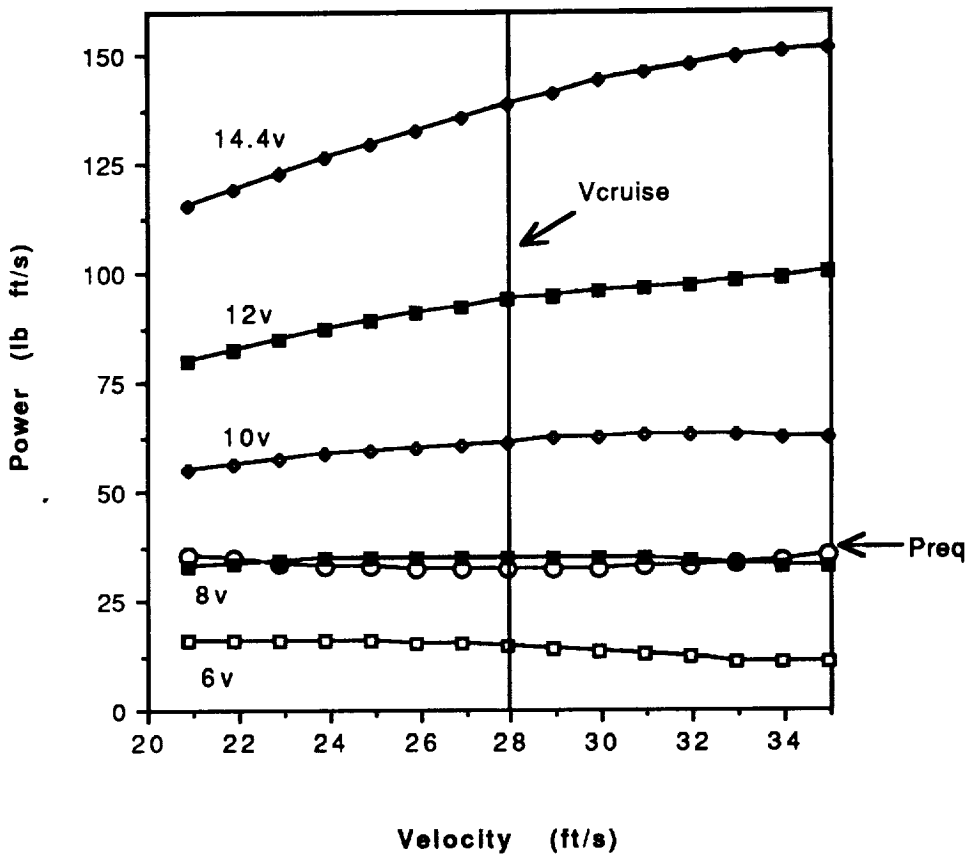

Efficiencies of Various Propellers versus Advance Ratio

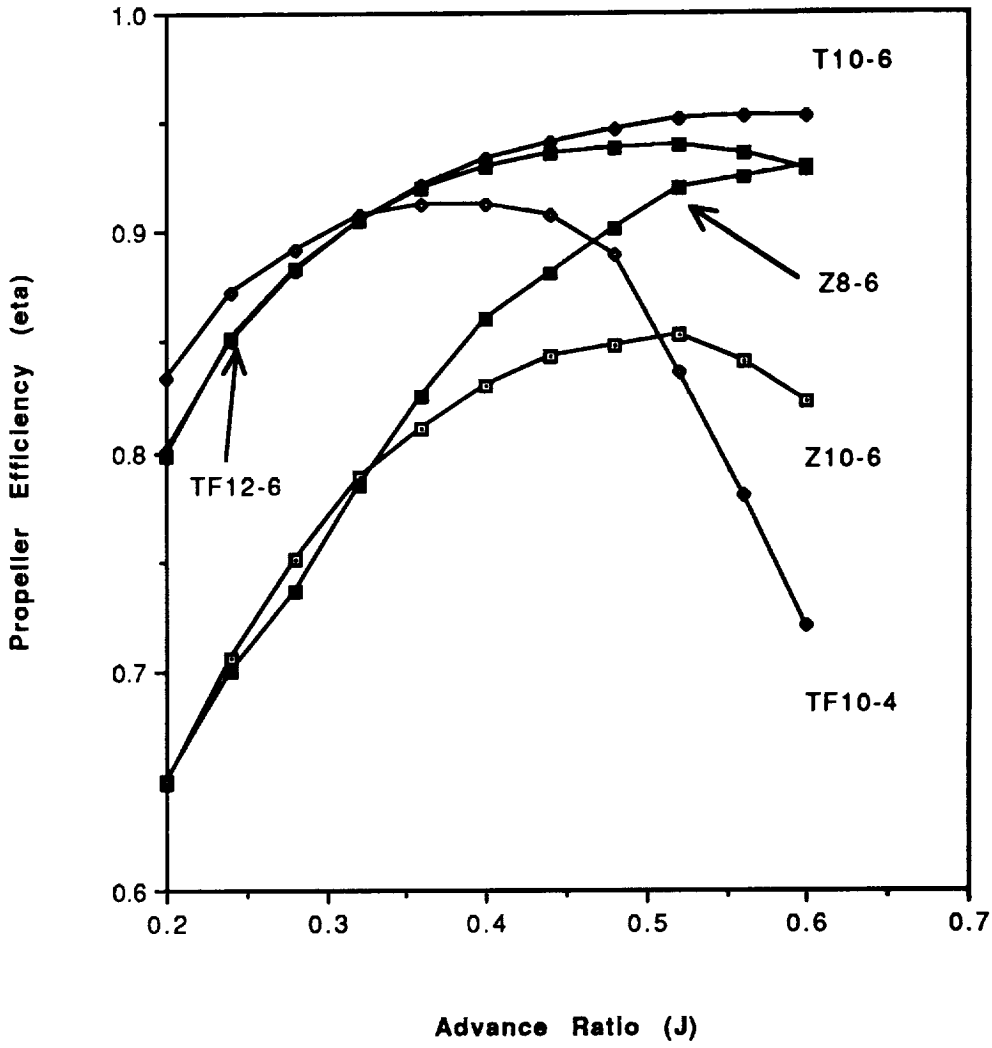

Weight and Balance Diagram for Jeff

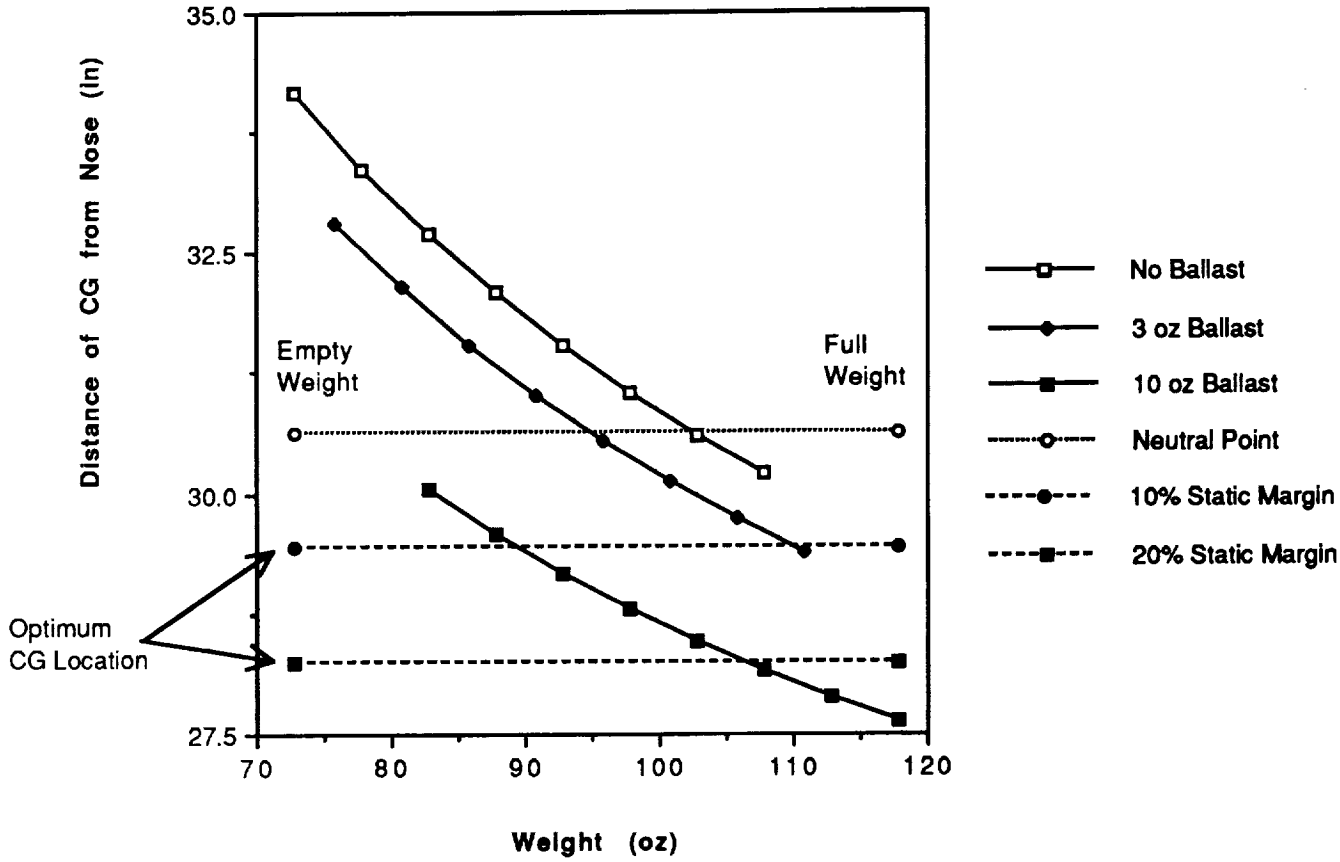

V-n diagram - JEFF

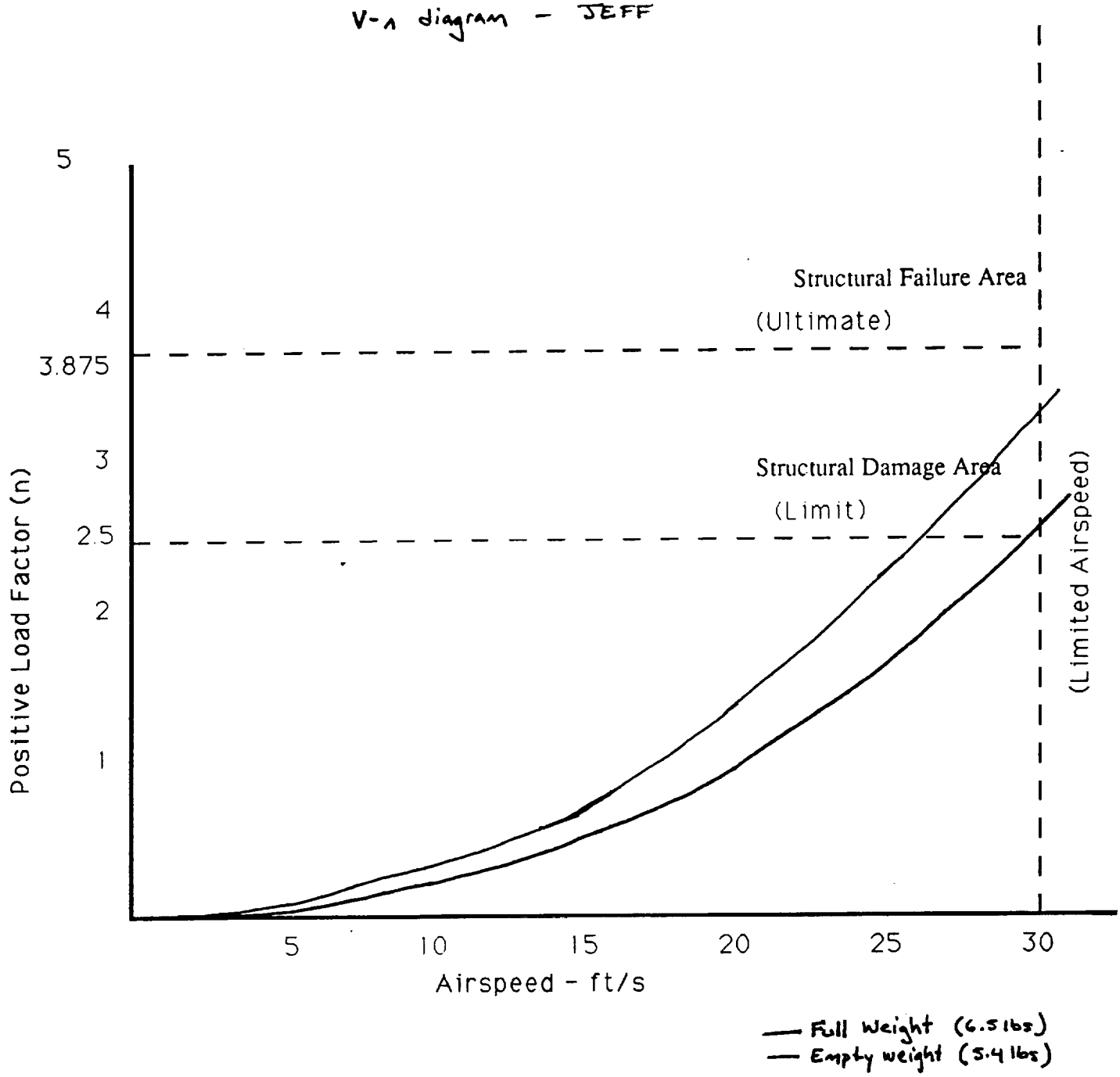

Technology Demonstrator

Component Weights

Component	Weight (oz)	Weight Percentage
Fuselage	23.63	24.03
Wing	14.18	14.42
Canard	6.17	6.28
Vertical Tails	0.74 (each)	0.76 (each)
Batteries	17.60	17.90
Servo #1	0.76	0.77
Servo #2	0.76	0.77
Servo #3	0.76	0.77
Receiver	0.99	1.00
System Battery	2.15	2.19
Speed Controller	1.76	1.79
Nose Wheel	1.50	3.66
Main Gear	6.14	6.24
Engine and Mount	10.67	10.85
Propeller	0.71	0.72
Ballast	7.00	7.12
Payload	0.00	0.00
Total	98.40	100

Part	Cost ($)	Time (Hr.)
Fuselage	32	17
Canard	19	10
Wing	52	60
Vertical Stabilizer	7	2
Landing Gear	25	5
Elevons	10	10
Miscellaneous	8	0

Price and Time Per Part

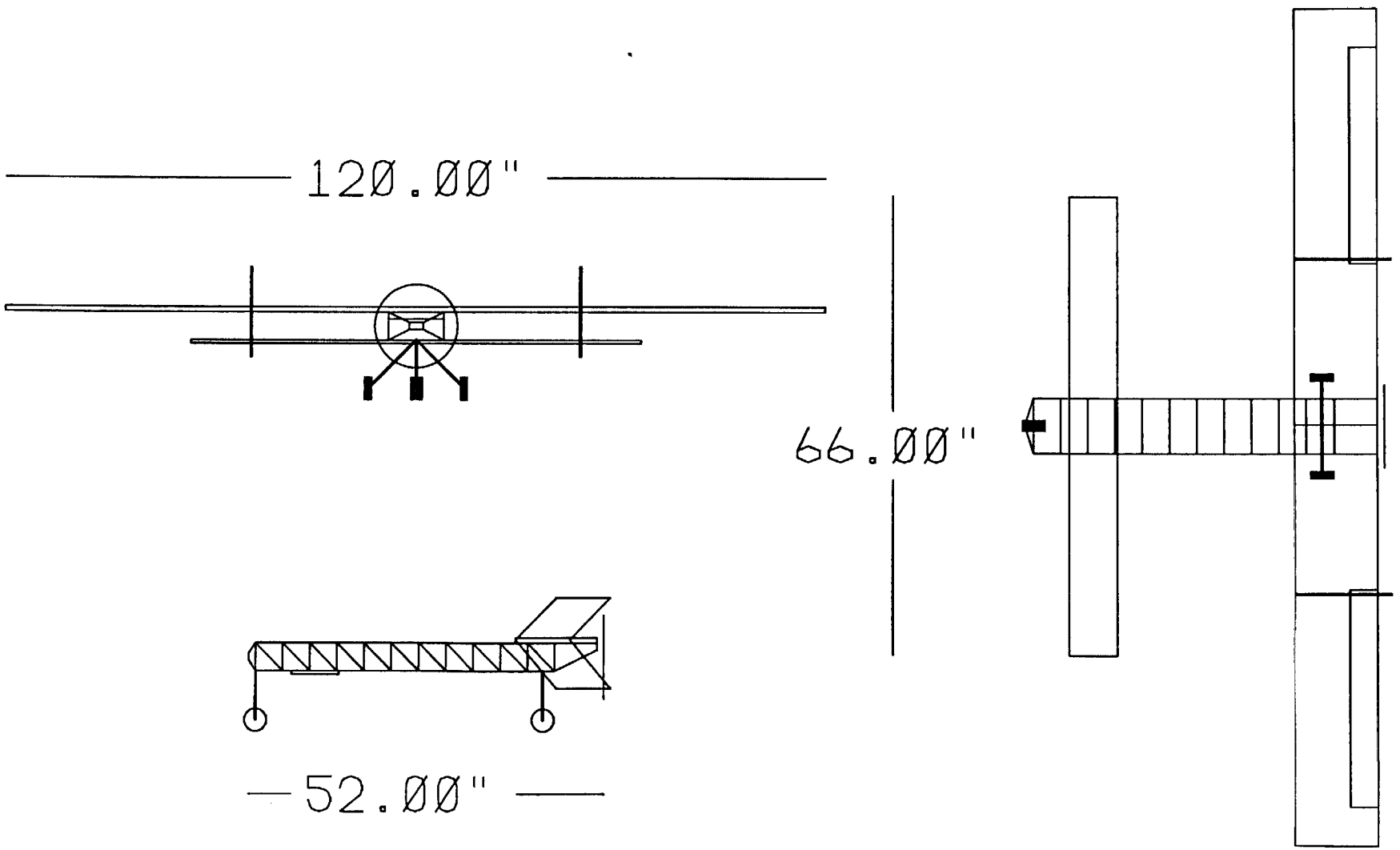
120.00"
66.00"
52.00"

Appendix B

	A	B	C	D	E	F
1	**BASIC COSTS**			**Operations**		
2						
3	materials	175		# servos	3	
4	propulsion	134		avg flight tim	1.87232393	
5	control	200		**OCPF**	**5.6169718**	
6	man hours	160				
7				maint. time	2	
8				maint. men	1	
9				**MCPF**	**100**	
10	UTC	509				
11	Scale UTC	203600		fuel rate	12.5	
12				fuel mili amp	162.24	
13	scaled UPC	160000		**FCPF**	**2028**	
14						
15	**U.P.C.**	**363600**		**O.C.P.S**	**4267.2339**	
16				O.C.P.F	2133.61697	
17						
18	**P.C.P.S**	**22335.429**		**V cruise**	**28**	
19	P.C.P.F	11167.7143		DESVOL	1400	
20				% CAPACITY	0.955	
21	**Planes**	**Days Fatigue**		NFLEET	19	**TOTAL**
22	2	200		Battery Cap.	1000	
23	4	280		i cruise	5.2	
24	13	350		**Endurance**	**11.538462**	
25				**Range**	**3145**	Tavg=5.81
26	**FLVPD**	**29400**		NCYC	700	
27				DESWGT	35	
28	**FLVPDF**	**25450**		FFPD	43	
29						
30	**UVCPF**	**0.0006026**		**FCPO**	**75.801301**	
31	**UWCPF**	**0.0241022**		**FCPCI**	**1.8950325**	
32	**FLC**	**35285506**		**FLIFE**	**309.30233**	
33	**FLV**	**18620000**		**FCPVOL**	**3.8803047**	
34	**FLW**	**465500**				
35						
36	**PROFIT**					
37	**CARGO COST**		**3.8803047**			
38	**CARGO CHARGE**		**4**			
39	**single flight gross income**		**5600**			
40	**single flight op. cost**		**2133.617**			
41	**single flight profit**		**3466.383**			
42	**#flights to break even**		**10179.344**			
43	**#days to break even**		**236.72893**			
44	**EOY CASH FLOW**		**10817389**			
45	**RETURN ON INVESTMENT**		**23.463578**			

	A	B	C	D	E	F
44	EOY CASH FLOW		12261388.6			
45	RETURN ON INVESTMENT		26.5957024			

```
final.wort

     wortmanfx_63

    12.00000    12.00000    60.00000     0.00000     0.00000     0.03000     0.000

    3    5   33   66

10 10.00 20.00 30.00 40.00 50.00 60.00 70.00 80.00 90.00100.00

    y    y    n

   33   60    0   30   20   40    3    0

  3  1  2  3

 3

balsa           6500.000000          0.080000          0.005800
0.4000E+030.6000E+030.2000E+03

monocote        7700.000000          0.200000          0.003490
0.2400E+050.2400E+050.2400E+05

spruce       1300000.000000          0.080000          0.016000
0.6200E+040.4000E+040.7500E+03
   66   93   90
  1   -5.4000    0.0000    0.4434    0.0000    0.0000    0.0929 0 0 0
  2   -5.4000    0.0000   -0.1163    0.0000    0.0000    0.0929 0 0 0
  3   -2.0400    0.0000    1.4469    0.0000    0.0000    0.1083 0 0 0
  4   -2.0400    0.0000   -0.1723    0.0000    0.0000    0.1083 0 0 0
  5    1.9200    0.0000    1.1144    0.0000    0.0000    0.0689 0 0 0
  6    1.9200    0.0000    0.2395    0.0000    0.0000    0.0689 0 0 0
  7   -5.4000    6.0000    0.4434    0.0000    0.0000    0.1857 1 1 1
  8   -5.4000    6.0000   -0.1163    0.0000    0.0000    0.1857 1 1 1
  9   -2.0400    6.0000    1.4469    0.0000    0.0000    0.2166 1 1 1
 10   -2.0400    6.0000   -0.1723    0.0000    0.0000    0.2166 1 1 1
 11    1.9200    6.0000    1.1144    0.0000    0.0000    0.1377 1 1 1
 12    1.9200    6.0000    0.2395    0.0000    0.0000    0.1377 1 1 1
 13   -5.4000   12.0000    0.4434    0.0000    0.0000    0.1857 1 1 1
 14   -5.4000   12.0000   -0.1163    0.0000    0.0000    0.1857 1 1 1
 15   -2.0400   12.0000    1.4469    0.0000    0.0000    0.2166 1 1 1
 16   -2.0400   12.0000   -0.1723    0.0000    0.0000    0.2166 1 1 1
 17    1.9200   12.0000    1.1144    0.0000    0.0000    0.1377 1 1 1
 18    1.9200   12.0000    0.2395    0.0000    0.0000    0.1377 1 1 1
 19   -5.4000   18.0000    0.4434    0.0000    0.0000    0.1857 1 1 1
 20   -5.4000   18.0000   -0.1163    0.0000    0.0000    0.1857 1 1 1
 21   -2.0400   18.0000    1.4469    0.0000    0.0000    0.2166 1 1 1
 22   -2.0400   18.0000   -0.1723    0.0000    0.0000    0.2166 1 1 1
 23    1.9200   18.0000    1.1144    0.0000    0.0000    0.1377 1 1 1
 24    1.9200   18.0000    0.2395    0.0000    0.0000    0.1377 1 1 1
 25   -5.4000   24.0000    0.4434    0.0000    0.0000    0.1857 1 1 1
 26   -5.4000   24.0000   -0.1163    0.0000    0.0000    0.1857 1 1 1
 27   -2.0400   24.0000    1.4469    0.0000    0.0000    0.2166 1 1 1
 28   -2.0400   24.0000   -0.1723    0.0000    0.0000    0.2166 1 1 1
 29    1.9200   24.0000    1.1144    0.0000    0.0000    0.1377 1 1 1
 30    1.9200   24.0000    0.2395    0.0000    0.0000    0.1377 1 1 1
 31   -5.4000   30.0000    0.4434    0.0000    0.0000    0.1857 1 1 1
 32   -5.4000   30.0000   -0.1163    0.0000    0.0000    0.1857 1 1 1
 33   -2.0400   30.0000    1.4469    0.0000    0.0000    0.2166 1 1 1
 34   -2.0400   30.0000   -0.1723    0.0000    0.0000    0.2166 1 1 1
 35    1.9200   30.0000    1.1144    0.0000    0.0000    0.1377 1 1 1
 36    1.9200   30.0000    0.2395    0.0000    0.0000    0.1377 1 1 1
 37   -5.4000   36.0000    0.4434    0.0000    0.0000    0.1857 1 1 1
 38   -5.4000   36.0000   -0.1163    0.0000    0.0000    0.1857 1 1 1
```

39	-2.0400	36.0000	1.4469	0.0000	0.0000	0.2166 1 1 1
40	-2.0400	36.0000	-0.1723	0.0000	0.0000	0.2166 1 1 1
41	1.9200	36.0000	1.1144	0.0000	0.0000	0.1377 1 1 1
42	1.9200	36.0000	0.2395	0.0000	0.0000	0.1377 1 1 1
43	-5.4000	42.0000	0.4434	0.0000	0.0000	0.1857 1 1 1
44	-5.4000	42.0000	-0.1163	0.0000	0.0000	0.1857 1 1 1
45	-2.0400	42.0000	1.4469	0.0000	0.0000	0.2166 1 1 1
46	-2.0400	42.0000	-0.1723	0.0000	0.0000	0.2166 1 1 1
47	1.9200	42.0000	1.1144	0.0000	0.0000	0.1377 1 1 1
48	1.9200	42.0000	0.2395	0.0000	0.0000	0.1377 1 1 1
49	-5.4000	48.0000	0.4434	0.0000	0.0000	0.1857 1 1 1
50	-5.4000	48.0000	-0.1163	0.0000	0.0000	0.1857 1 1 1
51	-2.0400	48.0000	1.4469	0.0000	0.0000	0.2166 1 1 1
52	-2.0400	48.0000	-0.1723	0.0000	0.0000	0.2166 1 1 1
53	1.9200	48.0000	1.1144	0.0000	0.0000	0.1377 1 1 1
54	1.9200	48.0000	0.2395	0.0000	0.0000	0.1377 1 1 1
55	-5.4000	54.0000	0.4434	0.0000	0.0000	0.1857 1 1 1
56	-5.4000	54.0000	-0.1163	0.0000	0.0000	0.1857 1 1 1
57	-2.0400	54.0000	1.4469	0.0000	0.0000	0.2166 1 1 1
58	-2.0400	54.0000	-0.1723	0.0000	0.0000	0.2166 1 1 1
59	1.9200	54.0000	1.1144	0.0000	0.0000	0.1377 1 1 1
60	1.9200	54.0000	0.2395	0.0000	0.0000	0.1377 1 1 1
61	-5.4000	60.0000	0.4434	0.0000	0.0000	0.0929 1 1 1
62	-5.4000	60.0000	-0.1163	0.0000	0.0000	0.0929 1 1 1
63	-2.0400	60.0000	1.4469	0.0000	0.0000	0.1083 1 1 1
64	-2.0400	60.0000	-0.1723	0.0000	0.0000	0.1083 1 1 1
65	1.9200	60.0000	1.1144	0.0000	0.0000	0.0689 1 1 1
66	1.9200	60.0000	0.2395	0.0000	0.0000	0.0689 1 1 1

1	1	20.4000E-01	1
2	7	80.4000E-01	1
3	13	140.4000E-01	1
4	19	200.4000E-01	1
5	25	260.4000E-01	1
6	31	320.4000E-01	1
7	37	380.4000E-01	1
8	43	440.4000E-01	1
9	49	500.4000E-01	1
10	55	560.4000E-01	1
11	61	620.4000E-01	1
12	3	40.4000E-01	1
13	9	100.4000E-01	1
14	15	160.4000E-01	1
15	21	220.4000E-01	1
16	27	280.4000E-01	1
17	33	340.4000E-01	1
18	39	400.4000E-01	1
19	45	460.4000E-01	1

```
c15edit.ed

     blue2.2

     8.00000      4.00000     50.00000      0.00000      0.00000      0.00000      0.000

    2    1   99

13  7.69 15.38 23.08 30.77 38.46 46.15 53.85 61.54 69.23 76.92 84.62 92.31100.00

    y    y    y

   28   55   56   26   00   26    2   13

  2  1  2

 13  1  2  3  4  5  6  7  8  9 10 11 12 13

 3

balsa          65000.000000          0.080000          0.005800
0.4000E+030.6000E+030.2000E+03

monocote        7700.000000          0.200000          0.003490
0.2400E+050.2400E+050.2400E+05

spruce       1300000.000000          0.080000          0.016000
0.6200E+040.4000E+040.7500E+03
   56  136   55
  1   -3.9200    0.0000    2.0000    0.0000    0.0000    0.0000 1 1 1
  2   -3.9200    0.0000   -2.0000    0.0000    0.0000    0.0000 1 1 1
  3    4.0000    0.0000    2.0000    0.0000    0.0000    0.0000 1 1 1
  4    4.0000    0.0000   -2.0000    0.0000    0.0000    0.0000 1 1 1
  5   -3.7692    3.8462    1.9231    0.0000    0.0000    0.0000 1 1 1
  6   -3.7692    3.8462   -1.9231    0.0000    0.0000   -0.9125 1 1 1
  7    3.8462    3.8462    1.9231    0.0000    0.0000    0.0000 1 1 1
  8    3.8462    3.8462   -1.9231    0.0000    0.0000   -0.9135 1 1 1
  9   -3.6185    7.6923    1.8462    0.0000    0.0000    0.0000 1 1 1
 10   -3.6185    7.6923   -1.8462    0.0000    0.0000   -0.3417 1 1 1
 11    3.6923    7.6923    1.8462    0.0000    0.0000    0.0000 1 1 1
 12    3.6923    7.6923   -1.8462    0.0000    0.0000   -0.3417 1 1 1
 13   -3.4677   11.5385    1.7692    0.0000    0.0000    0.0000 1 1 1
 14   -3.4677   11.5385   -1.7692    0.0000    0.0000   -2.7170 1 1 1
 15    3.5385   11.5385    1.7692    0.0000    0.0000    0.0000 1 1 1
 16    3.5385   11.5385   -1.7692    0.0000    0.0000   -2.7170 1 1 1
 17   -3.3169   15.3846    1.6923    0.0000    0.0000    0.0000 1 1 1
 18   -3.3169   15.3846   -1.6923    0.0000    0.0000   -2.7170 1 1 1
 19    3.3846   15.3846    1.6923    0.0000    0.0000    0.0000 1 1 1
 20    3.3846   15.3846   -1.6923    0.0000    0.0000   -2.7170 1 1 1
 21   -3.1662   19.2308    1.6154    0.0000    0.0000    0.0000 1 1 1
 22   -3.1662   19.2308   -1.6154    0.0000    0.0000   -0.3417 1 1 1
 23    3.2308   19.2308    1.6154    0.0000    0.0000    0.0000 1 1 1
 24    3.2308   19.2308   -1.6154    0.0000    0.0000   -0.3417 1 1 1
 25   -3.0154   23.0769    1.5385    0.0000    0.0000    0.0000 1 1 1
 26   -3.0154   23.0769   -1.5385    0.0000    0.0000   -0.3417 1 1 1
 27    3.0769   23.0769    1.5385    0.0000    0.0000    0.0000 1 1 1
 28    3.0769   23.0769   -1.5385    0.0000    0.0000   -0.3417 1 1 1
 29   -2.8646   26.9231    1.4615    0.0000    0.0000    0.0000 1 1 1
 30   -2.8646   26.9231   -1.4615    0.0000    0.0000   -0.3417 1 1 1
 31    2.9231   26.9231    1.4615    0.0000    0.0000    0.0000 1 1 1
 32    2.9231   26.9231   -1.4615    0.0000    0.0000   -0.3417 1 1 1
 33   -2.7138   30.7692    1.3846    0.0000    0.0000    0.0000 1 1 1
 34   -2.7138   30.7692   -1.3846    0.0000    0.0000   -0.3417 1 1 1
 35    2.7692   30.7692    1.3846    0.0000    0.0000    0.0000 1 1 1
 36    2.7692   30.7692   -1.3846    0.0000    0.0000   -0.3417 1 1 1
```

37	-2.5631	34.6154	1.3077	0.0000	0.0000	0.0000	1	1	1
38	-2.5631	34.6154	-1.3077	0.0000	0.0000	-0.3417	1	1	1
39	2.6154	34.6154	1.3077	0.0000	0.0000	0.0000	1	1	1
40	2.6154	34.6154	-1.3077	0.0000	0.0000	-0.3417	1	1	1
41	-2.4123	38.4615	1.2308	0.0000	0.0000	-2.6563	0	0	0
42	-2.4123	38.4615	-1.2308	0.0000	0.0000	-0.3417	1	1	1
43	2.4615	38.4615	1.2308	0.0000	0.0000	-2.6563	0	0	0
44	2.4615	38.4615	-1.2308	0.0000	0.0000	-0.3417	1	1	1
45	-2.2615	42.3077	1.1538	0.0000	0.0000	-2.6563	0	0	0
46	-2.2615	42.3077	-1.1538	0.0000	0.0000	-0.3417	1	1	1
47	2.3077	42.3077	1.1538	0.0000	0.0000	-2.6563	0	0	0
48	2.3077	42.3077	-1.1538	0.0000	0.0000	-0.3417	1	1	1
49	-2.1108	46.1538	1.0769	0.0000	-1.5000	-2.6563	0	0	0
50	-2.1108	46.1538	-1.0769	0.0000	-1.5000	-1.1621	1	1	1
51	2.1538	46.1538	1.0769	0.0000	-1.5000	-2.6563	0	0	0
52	2.1538	46.1538	-1.0769	0.0000	-1.5000	-1.1621	1	1	1
53	-1.9600	50.0000	1.0000	0.0000	0.0000	0.0000	1	1	1
54	-1.9600	50.0000	-1.0000	0.0000	0.0000	-0.8203	1	1	1
55	2.0000	50.0000	1.0000	0.0000	0.0000	0.0000	1	1	1
56	2.0000	50.0000	-1.0000	0.0000	0.0000	-0.8203	1	1	1

1	1	20.4000E-01	3
2	5	60.4000E-01	1
3	9	100.4000E-01	1
4	13	140.4000E-01	1
5	17	180.4000E-01	3
6	21	220.4000E-01	3
7	25	260.4000E-01	3
8	29	300.4000E-01	3
9	33	340.4000E-01	3
10	37	380.4000E-01	3
11	41	420.4000E-01	3
12	45	460.4000E-01	3
13	49	500.4000E-01	3
14	53	540.4000E-01	3
15	3	40.4000E-01	3
16	7	80.4000E-01	1
17	11	120.4000E-01	1
18	15	160.4000E-01	1
19	19	200.4000E-01	3
20	23	240.4000E-01	3
21	27	280.4000E-01	3
22	31	320.4000E-01	3
23	35	360.4000E-01	3